UNIVERSIDADE FEDERAL DO CEARÁ
CENTRO DE CIÊNCIAS
DEPARTAMENTO DE BIOQUÍMICA E BIOLOGIA MOLECULAR
PROGRAMA DE PÓS-GRADUAÇÃO EM BIOQUÍMICA

PAULO VINICIUS LEITE DE SOUZA

METABOLIC REGULATION MEDIATED BY THIOREDOXINS AND NADPH-DEPENDENT THIOREDOXIN REDUCTASES IN *ARABIDOPSIS THALIANA L.*

FORTALEZA
2023

PAULO VINICIUS LEITE DE SOUZA

METABOLIC REGULATION MEDIATED BY THIOREDOXINS AND NADPH-DEPENDENT THIOREDOXIN REDUCTASES IN *ARABIDOPSIS THALIANA L.*

Tese apresentada ao Programa de Pós-Graduação em Bioquímica da Universidade Federal do Ceará, como requisito parcial para a obtenção do título de Doutor em Bioquímica. Área de concentração: Bioquímica Vegetal

Orientador: Prof. Dr. Danilo de Menezes Daloso

FORTALEZA

2023

Dados Internacionais de Catalogação na Publicação
Universidade Federal do Ceará
Sistema de Bibliotecas
Gerada automaticamente pelo módulo Catalog, mediante os dados fornecidos pelo(a) autor(a)

S234m Souza, Paulo Vinicius Leite de.
Metabolic regulation mediated by thioredoxins and NADPH-dependent thioredoxin reductases in Arabidopsis thaliana.L / Paulo Vinicius Leite de Souza. – 2023.
153 f. : il. color.

Tese (doutorado) – Universidade Federal do Ceará, Centro de Ciências, Programa de Pós-Graduação em Bioquímica , Fortaleza, 2023.
Orientação: Prof. Dr. Danilo de Menezes Daloso.

1. Thioredoxins. 2. Metabolic regulation. 3. NADPH-dependent thioredoxin reductases. 4. Primary metabolism. 5. Nitrogen metabolism. I. Título.

CDD 572

PAULO VINICIUS LEITE DE SOUZA

METABOLIC REGULATION MEDIATED BY THIOREDOXINS AND NADPH-DEPENDENT THIOREDOXIN REDUCTASES IN *ARABIDOPSIS THALIANA L.*

Tese apresentada ao Programa de Pós-Graduação em Bioquímica da Universidade Federal do Ceará, como requisito parcial para a obtenção do título de Doutor em Bioquímica. Área de concentração: Bioquímica Vegetal

Aprovada em: 20/04/2023

BANCA EXAMINADORA

_____

Prof. Dr Danilo de Menezes Daloso (Orientador)

Universidade Federal do Ceará (UFC)

_____

Prof. Dr Joaquim Albenísio Gomes da Silveira

Universidade Federal do Ceará (UFC)

_____

Prof. Dr Humberto Henrique de Carvalho

Universidade Federal do Ceará (UFC)

_____

Dra. Rachel Hellen Vieira de Sousa Lima

Universidade Federal do Ceará (UFC)

_____

Dra. Ana Luiza Sobral Paiva

Universidade Federal do Ceará (UFC)

AGRADECIMENTOS

O presente trabalho foi realizado com apoio da Coordenação de Aperfeiçoamento de Pessoal de Nível Superior – Brasil (CAPES) - Código de financiamento 001.

Agradeço primeiramente a Deus, que permitiu que todas as conquistas em minha vida se concretizassem. Agradeço à Universidade, que me deu o conhecimento necessário para concluir este trabalho.

Dedico esta tese de pesquisa à minha esposa Kássia Lia Costa Fernandes cuja presença foi essencial para a conclusão deste trabalho. Grato pela sua compreensão com as minhas horas de ausência e pelo apoio incondicional oferecido em todos os aspectos. Muito obrigado pela sua presença em minha vida. Te amo.

Ao meu filho, Miguel Fernandes Souza, por seu amor e carinho que me deram força para continuar e nunca desistir de terminar este trabalho. Te amo meu filho.

Aos meus pais, Julio Paiva de Souza e Lauriane Leite de Souza, pelo carinho, afeto, dedicação e cuidado que meus pais me deram durante toda a minha existência, dedico esta tese a eles. Com muita gratidão.

Gostaria de agradecer ao meu orientador Dr. Danilo de Menezes Daloso cuja dedicação, conhecimento, ensinamentos e paciência serviram como pilares de sustentação para a conclusão deste trabalho. Grato por tudo.

Aos professores participantes da Banca examinadora, Joaquim Albenísio Gomes da Silveira, Humberto Henrique de Carvalho, Rachel Hellen Vieira de Sousa Lima, Ana Luiza Sobral Paiva, pelo tempo e pelas valiosas colaborações.

Aos colegas do Labplant, pelas reflexões, críticas e sugestões recebidas aos longos dos anos.

Por fim, agradeço a meus amigos e familiares, pelas suas presenças em todos os momentos difíceis.

ABSTRACT

Thioredoxins (TRXs) consist of a family of oxi-redox proteins capable of (de)activating enzymes, being an important post-translational mechanism for metabolic regulation. Plant TRXs are found in different cell compartments, such as chloroplast, mitochondria, and cytosol. TRXs are activated by specific TRX reductases (TRs), according to their subcellular location. For instance, chloroplasts contain two TRs, named FTR (ferredoxin-dependent TR) and NTRC (NADPH-dependent TR C), which receives reducing power from ferredoxin and NADPH, respectivelly. On the other hand, plant cells contain two other NTRs (NTRA and NTRB) that are mainly located in cytosol and mitochondria. NTRA/B are thus the main TRs responsible for reducing the non-chloroplastic TRXs. Previous works showed that the single *ntrc* mutant and the double *ntrab* mutant have reduced growth, but are still viable, i.e. they can complete the full life cycle and produce viable seeds. However, plants lacking all NTRs remained to be investigated, raising the question on whether the plant NTR system is essential for plant growth and development. In paralell, previous works suggested that the mitocondrial NTR/TRX system can regulate the interplay between carbon and nitrogen metabolisms, but how redox-mediated mechanisms regulate these metabolisms remained to be deeply investigated. Aiming to address these questions, this thesis was divided into three parts. We first reviewed how TRX-mediated mechanisms regulate the primary metabolism, especially the (photo)respiratory metabolism. The second and third chapters involve the characterization of *Arabidopsis thaliana* L mutants lacking different NTRs and TRXs. The second chapter describes the unprecedented characterization of the triple *ntrabc* mutant, which lacks all NTRs (NTR A, B and C), whilst the third involves experiments using mutants lacking TRX *h2*, TRX *o1* or NTRA/B aiming to investigate how the NTR/TRX system regulates glutamine synthetase (GS) and the fluxes throughout the GS/GOGAT (glutamate synthase) cycle. Our results showed that the triple *ntrabc* mutant showed a leaf pale green phenotype with strong reduction in growth and substantial metabolic changes. Despite this, the *ntrabc* remained viable and was able to complete the full developmental cycle, including the production of viable seeds. These results suggest that the NTR system is highly important for plant growth, but not essential for plant development. Furthermore, our results indicate that the mitochondrial NTR/TRX system is key for the regulation of the redox status of GS and the metabolic fluxes thorughout the GS/GOGAT cycle, which is important for plant high light stress acclimation. Thus, our works provide important and

unprecendented informations regarding the regulation of primary metabolism mediated by NTRs and TRXs.

Keywords: thioredoxins; metabolic regulation; NADPH-dependent thioredoxin reductases; primary metabolism; nitrogen metabolism; light stress.

RESUMO

As tioredoxinas (TRXs) constituem uma família de proteínas oxi-redox capazes de (des)ativar enzimas, sendo um importante mecanismo pós-traducional para a regulação do fluxo metabólico. As TRXs vegetais estão espalhados em diferentes compartimentos celulares, como cloroplastos, mitocôndrias e citosol. As TRXs são ativadas por TRX redutases (TRs). Os cloroplastos possuem dois TRs, a saber, FTR (TR dependente de ferredoxina) e NTRC (TR dependente de NADPH), que recebe poder redutor da ferredoxina e/ou NADPH. Por outro lado, as células vegetais contêm duas outras NTRs fora do cloroplasto, ou seja, as isoformas NTRA e NTRB que estão localizadas principalmente no citosol e nas mitocôndrias. As NTRA/B são, portanto, as principais TRs responsáveis pela redução dos TRXs não plastidiais. Trabalhos anteriores mostraram que o mutante nocaute para *ntrc* e *ntrab* apresentam forte decréscimo no crescimento, mas ainda são viáveis, ou seja, podem completar o ciclo de vida completo e produzir sementes viáveis. No entanto, as plantas que carecem de todos as NTRs ainda precisam serem investigadas, abrindo a questão sobre se o sistema NTR de plantas é essencial para o crescimento e desenvolvimento destes organismos. Paralelamente, trabalhos anteriores sugeriram que o sistema mitocondrial NTR/TRX pode regular a interação entre os metabolismos de carbono e nitrogênio, mas como os mecanismos mediados por redox regulam esses metabolismos ainda precisam ser profundamente investigados. Com o objetivo de responder a essas questões, esta tese foi dividida em três partes. Primeiro revisamos como os mecanismos mediados por TRX regulam o metabolismo primário, especialmente o metabolismo (foto)respiratório. O segundo e o terceiro capítulos envolvem a caracterização de mutantes da planta modelo *Arabidopsis thaliana L*. O segundo capítulo descreve a caracterização inédita do mutante triplo *ntrabc*, que carece de todos os NTRs (NTR A, B e C), enquanto o terceiro envolve experimentos usando mutantes sem TRX h2, TRX o1 ou NTRA/B com o objetivo de investigar como o sistema NTR/TRX regula a glutamina sintetase (GS) e os fluxos ao longo do ciclo GS/GOGAT (glutamato sintase). Nossos resultados mostraram que o mutante triplo *ntrabc* apresentou um fenótipo de folha verde pálida com forte redução no crescimento e alterações metabólicas substanciais. Apesar disso, o *ntrabc* manteve-se viável e conseguiu completar todo o ciclo de desenvolvimento, incluindo a produção de sementes viáveis. Nossos resultados sugerem que o sistema NTR é altamente importante para o crescimento da planta, mas não essencial para o desenvolvimento da planta. Além disso, nossos resultados indicam ainda que o sistema NTR/TRX mitocondrial é a chave para a regulação do status redox de GS e os fluxos metabólicos ao longo do

ciclo GS/GOGAT, o que é importante para a aclimatação da planta ao estresse de alta luz. Assim, nossos trabalhos fornecem informações importantes e inéditas sobre a regulação do metabolismo primário mediado por NTRs e TRXs.

Palavras-chave: tiorredoxinas; regulação metabólica; NADPH- Tiorredoxina redutase; metabolismo primário; metabolismo do nitrogênio; estresse de alta luz**.**

FIGURE LIST

TABLE LIST

SUMMARY

1 GENERAL INTRODUCTION

Plants have a sessile lifestyle, which makes them susceptible from undesired changes in the environment, raising great concerns on how plants will respond to the impacts generated by the climate change scenario (Cernusak *et al.*, 2019; Leakey *et al.*, 2009). The comprehension of intrinsic regulatory mechanisms that aid plants to respond to different environmental conditions has never been so necessary, given the predictions of a future with increased CO_2 concentration, accompanied by extreme temperature and drought periods (Ainsworth e Rogers, 2007). In this context, plants have an unprecedented redox system orchestrated by oxi-redox reactions, which allow them to measure the length of the light period and to rapidly respond to changes in environmental cues (Geigenberger, Thormählen, Daloso, Danilo M., *et al.*, 2017; Hotta, 2021). Light absorption rapidly alters the redox state of the chloroplasts by increasing the level of redox-active molecules such as NADPH, reduced ferredoxin (Fdx), and H_2O_2 (Meyer *et al.*, 2021a). H_2O_2 is a powerful oxidant, acting as an important regulator of plant metabolism by modulating gene expression and altering enzyme activity through the oxidation of Cys residues in redox-sensitive proteins (Foyer e Noctor, 2005, 2013; Kolla, Vavasseur e Raghavendra, 2007). H_2O_2 is counter-balanced by thioredoxins (TRXs), ubiquitous proteins involved in redox regulation of plant metabolism by modulating Cys thiol-disulfide exchange in targeted proteins (Fonseca-Pereira, da *et al.*, 2021).

TRXs receive reducing power derived from TRX reductases, which use either photosynthetically reduced Fdx or NADPH as electron donors in the chloroplasts and out of the plastids, respectively (Buchanan e Balmer, 2005; Busch e Hippler, 2011; Marty, Laurent *et al.*, 2009). Chloroplasts further contain the NADPH-dependent TRX reductase C (NTRC), which also harbours a TRX domain in its structure, allowing NTRC to (in)directly reduce TRXs and TRX targets (Cejudo, González e Pérez-Ruiz, 2021; Serrato *et al.*, 2004). Although NTRC and Fdx-dependent TRX reductase (FTR) are activated by distinct pathways, they cooperatively regulate chloroplastic metabolism (Yoshida e Hisabori, 2016a). On the other hand, NTRA and NTRB are the main responsible to reduce the TRXs in non-plastidial cellular compartments, especially cytosol and mitochondria (Daloso, Danilo M. *et al.*, 2015; Marchal *et al.*, 2014; Reichheld *et al.*, 2007). NTR proteins are thus highly important for plant growth. However, NTRC and the non-chloroplastic NTRAB systems are safeguarded by FTRs and glutathione reductases (GR),

respectively, which may act as compensatory systems and guarantee the viability of *ntrc* and *ntrab* mutants (Reichheld *et al.*, 2007; Yoshida e Hisabori, 2016a). Indeed, it has been shown that glutathione (GSH) can reduce plant TRXs *in vitro* and that NTRA/NTRB and GR act in cooperation (Marty, Bausewein, Müller, Bangash, Moseler, Schwarzländer, Müller-Schüssele, *et al.*, 2019; Marty, L. *et al.*, 2009; Reichheld *et al.*, 2007, 2005). This indicates that the plant NTR/TRX system is highly connected to other redox players, including glutathione and ascorbate metabolisms (Calderón *et al.*, 2018a).

Since their discovery, the search for TRX targets has been the main aim of TRX studies, given that the TRX-mediated enzyme regulation can presumably directly regulate the activity of the enzyme and consequently the metabolic fluxes through the associated metabolic pathway (Buchanan, 2014). In this context, *in vitro* TRX affinity chromatography assays were essential in electing possible TRX targets (Balmer *et al.*, 2004; Motohashi *et al.*, 2001; Yoshida *et al.*, 2014). However, these assays are carried out *in vitro* and their results cannot be extrapolated to *in vivo* conclusions, remaining open several questions on whether the TRX targets suffer redox regulation *in vivo* and what is the impact of this mechanism for the regulation of plant metabolism. Notwithstanding, an extensive effort has been recently made aiming to identify the role of TRXs in the regulation of mitochondrial and cytosolic metabolisms (Daloso, Danilo M. *et al.*, 2015; Fonseca-Pereira *et al.*, 2019; Geigenberger, Thormählen, Daloso, Danilo M, *et al.*, 2017; Yoshida *et al.*, 2013, 2014).For instance, both TRX *o1* and TRX *h2* has been shown to be important in the redox regulation of enzymes involved in (photo)respiration (Fonseca-Pereira, da *et al.*, 2021; Fonseca-Pereira *et al.*, 2019; Reinholdt, Schwab, Zhang, Reichheld, J., *et al.*, 2019).

It is already well-established that the TRX *o* (TRX *o1* and *o2*) family is located in mitochondria, while the exact location of TRX *h2* is still unclear. Previous studies suggested that TRX *h2* would be located at the mitochondria in Arabidopsis and *Populus trichocarpa* (Gelhaye et al., 2004; Meng et al., 2010), and associated with the endoplasmic reticulum (ER)-Golgi membrane system in Arabidopsis (Traverso et al., 2013). However, recent cell fractionation and immunoblot analyses demonstrated that TRX *h2* is found at the microsomal fraction (Hou et al., 2021). This suggests that TRX *h2* is found in the endomembrane system rather than mitochondria or cytosol (Daloso, Danilo M *et al.*, 2015; Fonseca-Pereira, da *et al.*, 2021; Reinholdt, Bauwe, *et al.*, 2019). Despite likely found in different location, recent results highlight that they parallel regulates plant metabolism through changes in NAD(P)(H) and other redox molecules, suggesting

a convergent role of these proteins for plant metabolism regulation (Hou, Lehmann e Geigenberger, 2021). Among the pathways regulated by them, although early evidence suggests that the enzyme glutamine synthetase (GS) is sensitive to DDT (Choi, Kim e Kwon, 1999), little attention has been given to confirm this hypothesis and whether/how this and other enzymes of the nitrogen metabolism are regulated by the NTR/TRX system.

Nitrogen is an essential element for plant growth and development (Liu, Hu e Chu, 2022; Oliveira e Coruzzi, 1999). Thus, the comprehension of the regulatory mechanisms of this metabolism can provide important information to inform plant breeding programs toward yield and/or stress resistance improvement according to the climate change scenario (Sweetlove, Nielsen e Fernie, 2017). Here, we aim to unveil the role of NTRs and TRXs in the regulation of the primary metabolism. For this, we characterized the triple NTR mutant (*ntrabc*) and provided compelling evidence indicating that GS is redox regulated by TRXs. The first chapter of this thesis is composed of a review already published in *Journal of Experimental Botany* (Fonseca-Pereira, da *et al.*, 2021). In the second chapter, we characterized the triple *ntrabc* mutant, in collaboration with several international institutions, but coordinated by our group. It is important to emphasize that the experiments described here refer only to those performed by our group, and that several other have been carried out in different laboratories. The manuscript of this work has been resubmitted to *Plant, Cell and Environment*. Finally, the third chapter is currently being finalized to be submitted.

2 HYPOTHESES

The NTR system is important, but not essential, for plant development, which are compensated by other redox players. In addition, the hypothesis of the third chapter is; the mitochondrial NTR/TRX system modulates the carbon flux from the TCA cycle to glutamate metabolism via redox regulation of glutamine synthetase.

3 OBJECTIVES

Main:

To investigate the role of the NTR/TRX system in the regulation of primary metabolism of *Arabidopsis thaliana.*

i. Specific;

- To characterize the triple mutant *ntrabc*;
- To determine the impact of the lack of all NTRs on the accumulation of primary metabolites and redox molecules such as H_2O_2, glutathione and ascorbate;
- To investigate the impact of the lack of all NTRs on the activity of antioxidant enzymes;
- To explore whether and how the enzymes glutamine synthetase (GS), glutamate synthase (GOGAT), and glutamate dehydrogenase (GDH) can form disulphide bonds, using different bioinformatics approaches;
- To examine the redox status of GS is altered in leaf samples from plants lacking TRX *h2*, TRX *o1* or NTRA/B;
- To investigate how the NTR/TRX-mediated mechanisms of regulation of the nitrogen metabolism influences plant high light stress acclimation.

4 CHAPTER 1: THIOREDOXIN-MEDIATED REGULATION OF CENTRAL METABOLISM

Article published in *Journal of Experimental Botany*, volume 72, issue 17, pages 5987-6002.

Paula da Fonseca-Pereira[1#]; Paulo V.L. Souza[2#]; Alisdair R. Fernie[3]; Stefan Timm[4]; Danilo M. Daloso[2]*; Wagner L. Araújo[1]*

[1]Departamento de Biologia Vegetal, Universidade Federal de Viçosa, 36570-900, Viçosa, Minas Gerais, Brasil

[2]Departamento de Bioquímica e Biologia Molecular, Universidade Federal do Ceará, 60451-970, Fortaleza, Ceará, Brasil

[3]Max-Planck-Institute of Molecular Plant Physiology, 14476 Potsdam-Golm, Germany

[4]University of Rostock, Plant Physiology Department, Albert- Einstein-Str. 3, D-18051 Rostock, Germany

[#]These authors contributed equally to this work

*Correspondence: daloso@ufc.br (D.M. Daloso) and wlaraujo@ufv.br (W.L. Araújo)

Running Title: Redox regulation of (photo)respiration

Abstract

Thioredoxins (TRXs) are ubiquitous proteins engaged in the redox regulation of plant metabolism. Whilst the light-dependent TRX-mediated activation of Calvin-Benson cycle enzymes is well-documented, the role of extraplastidial TRXs in the control of the mitochondrial (photo)respiratory metabolism has been revealed relatively recently. Mitochondrially located TRX *o1* has been identified as regulator of alternative oxidase, enzymes of, or associated to, the tricarboxylic acid (TCA) cycle and the mitochondrial dihydrolipoamide dehydrogenase (mtLPD) involved in photorespiration, the TCA cycle and the degradation of branched chain amino acids. TRXs are seemingly a major point of metabolic regulation responsible to activate photosynthesis and adjust mitochondrial photorespiratory metabolism according to the prevailing cellular redox status. Furthermore, TRX-mediated (de)activation of TCA cycle enzymes contributes to explain the non-cyclic flux mode of operation of this cycle in illuminated leaves. Here we provide an overview on the decisive role of TRXs in the coordination of mitochondrial metabolism in the light and provide *in silico* evidence for other redox-regulated photorespiratory enzymes. We further discuss the consequences of mtLPD regulation beyond photorespiration and provide outstanding questions that should be addressed in future studies to improve our understanding concerning the role of TRXs in the regulation of central metabolism.

Key words: metabolic control; metabolic regulation, redox metabolism; TCA cycle; mitochondrial thioredoxins, photorespiration.

Introduction

Thioredoxins (TRXs) are ubiquitous, redox-active proteins related to the regulation of plant metabolism by modulating Cys thiol-disulfide exchange in target proteins (Meyer *et al.*, 2009). Plant TRXs differ substantially in both amino acid sequence and subcellular location, being characterized by an unusually complex array of proteins (Belin *et al.*, 2015). In Arabidopsis, TRXs *m*, *f*, *x*, *y* and *z* isoforms are located in the chloroplast, TRXs *o1/2* are mitochondrial and nuclear, whereas eight TRX *h* proteins are found in diverse compartments, including cytosol, nucleus, endoplasmic reticulum (ER), and mitochondria (Buchanan, 2017a; Geigenberger, Thormählen, Daloso, Danilo M., *et al.*, 2017). In plastids, the TRXs are reduced by both the ferredoxin TRX reductase (FTR) and the NADPH-dependent TRX reductase C (NTRC) systems, whilst the extraplastidial TRX reductase system is composed by two highly similar NTR isoforms, namely NTRA and NTRB, which are responsible for reducing TRXs *h* in different subcellular compartments and *o1/2* in mitochondria (Reichheld *et al.*, 2005). TRXs play important roles in coordinating the metabolic fluxes through both the Calvin-Benson (CB) and the tricarboxylic acid (TCA) cycles (Buchanan *et al.*, 2012; Daloso, Danilo M *et al.*, 2015). However, whilst the operation of plastidial TRXs is well documented (Michelet *et al.*, 2013), considerably less is known concerning the extraplastidial TRXs.

Recent evidence has, however, shed considerably more light on the role of TRXs in the mitochondrial photorespiratory metabolism (Fonseca-Pereira, da *et al.*, 2020; Reinholdt, Schwab, Zhang, Reichheld, J., *et al.*, 2019). These studies demonstrated that the mitochondrial dihydrolipoamide dehydrogenase (mtLPD) is redox regulated by both TRX *o1* [9] and TRX *h2 in vitro* [10]. This is of particular interest, given that mtLPD is part of four multienzyme systems in mitochondria, namely as L-protein of photorespiratory glycine decarboxylase complex (GDC) and as an E3 subunit of the enzyme complexes branched-chain 2-oxoacid dehydrogenase (BCKDC), pyruvate dehydrogenase (PDH) and 2-oxoglutarate dehydrogenase (OGDH), respectively. In conjunction with the role of the mitochondrial TRX system in the control of alternative oxidase (AOX) (Florez-Sarasa, Obata, Del-Saz, Néstor Fernández, *et al.*, 2019; Gelhaye *et al.*, 2004; Umekawa e Ito, 2019) and TCA cycle enzymes (Daloso, Danilo M *et al.*, 2015; Schmidtmann *et al.*, 2014; Yoshida e Hisabori, 2014), it is thus suggested that, apart from their well-known role in plastids, the importance of TRXs regulation of plant metabolism is extended to the regulation of other major pathways of central carbon metabolism. In the next sections, we discuss the

consequences of the recent established role of TRXs in the control of photorespiratory metabolism for the overall regulation of plant cells. We will further discuss the presence of conserved Cys residues found in cyanobacteria and different plant species and the predicted formation of disulfide bond in several (photo)respiratory enzymes from Arabidopsis.

Behind the extraordinary complexity of plant redox metabolism

The cellular redox status is central for determining metabolic and developmental activities in biological systems (Foyer e Noctor, 2009; Geigenberger e Fernie, 2014). Overall, it results from the full inventory of redox reactions, distributed over all subcellular compartments and occurring in distinct metabolic pathways (Mock e Dietz, 2016). Amongst the redox network components, TRXs and glutaredoxins (GRXs) regulate several redox posttranslational modifications (PTMs), including disulfide bonds and de-glutathionylation (Gerna *et al.*, 2017; Zaffagnini *et al.*, 2019). These redoxins can modify the activity of target enzymes and thus adjust metabolic fluxes, especially in response to light/dark transitions (Mock e Dietz, 2016; Reinholdt, Bauwe, *et al.*, 2019). Beyond that, they are responsible for furnishing reducing power to peroxiredoxins (PRXs) and methionine sulfoxide reductases (MSRs) (Knuesting e Scheibe, 2018; Meyer *et al.*, 2012). Whilst NADPH is the main source of electron used by NTRs to reduce extraplastidial TRXs, GRXs use reduced glutathione (GSH) as an electron donor (Rouhier, Gelhaye e Jacquot, 2004). The oxidized glutathione (GSSG) formed after GRX reduction is itself reduced by the NADPH-dependent flavoprotein glutathione reductase (GR) (Reichheld *et al.*, 2007; Rouhier, Gelhaye e Jacquot, 2004). The complexity of the plant redox network is evidenced by the functional redundancy amongst the different thiol systems (Souza *et al.*, 2019a) and the wide spectrum of midpoint redox potential (E_m) of plant TRXs (Yoshida *et al.*, 2018). In chloroplasts, despite the substantial difference in E_m, FTRs and NTRC functionally overlap, their cooperative actions being critical for autotrophic growth (Cejudo, María-Cruz González e Pérez-Ruiz, 2020; Nikkanen, Toivola e Rintamäki, 2016; Thormählen *et al.*, 2015a; Yoshida e Hisabori, 2016a). Similarly, plant mitochondria have a well-orchestrated compensatory redox system (Geigenberger, Thormählen, Daloso, Danilo M., *et al.*, 2017). For instance, it seems likely that GR1 and GR2 proteins compensate for the absence of NTR proteins in the cytosol (Marty, L. *et al.*, 2009) and mitochondria (Marty, Bausewein, Müller, Bangash, Moseler, Schwarzländer, Müller-Schüssele, *et al.*, 2019), respectively. Notably, whilst the mitochondrial TRX/NTR system is seemingly essential

for animal cells (Conrad, Jakupoglu, Cemile, *et al.*, 2004; Holzerova *et al.*, 2016), plants lacking any of the mitochondrial redox components isolated are viable and fertile (Reichheld *et al.*, 2007). Furthermore, plant TRXs have high affinity to GPXs (Herbette *et al.*, 2002; Iqbal *et al.*, 2006; Jung *et al.*, 2002) and the NADPH/NTR/TRX system can reduce GSSG *in vitro* (Marty, Bausewein, Müller, Bangash, Moseler, Schwarzländer, Müller-Schüssele, *et al.*, 2019; Marty, L. *et al.*, 2009), although 200-fold higher activity is observed for GR1, revealing a low efficiency of the TRX-based reduction of GSSG (Marty, L. *et al.*, 2009). Moreover, the cytosolic TRX *h3* protein is alternatively reduced by the NADPH/GR/GSH/GRX pathway in plants (Reichheld *et al.*, 2007). Beyond that, glutathione peroxidases (GPX), sulfiredoxin and PRXIIF are other important elements of the plant mitochondrial redox network (see Table S1 for a list of mitochondrial redox proteins) (Max *et al.*, 2020). Collectively, these findings emphasize the redundancy and complementarity inherent to the plant cellular thiol-redox organization. The complexity of the plant redox system is probably important to finely adjust plant metabolism according to the prevailing environmental condition, especially the mitochondrial metabolism, which is regulated by different PTMs, including the NTR/TRX system, in a light-dependent manner (Nunes-Nesi *et al.*, 2013; Sweetlove *et al.*, 2010; Tcherkez *et al.*, 2012). Indeed, it has been shown that the mitochondrial NTR/TRX system is important for the light-induction of photosynthesis and to cope with drought stress cycles (Fonseca-Pereira, Da *et al.*, 2019).

Redox regulation of TCA cycle enzymes

The regulation of the TCA cycle in plants is mainly mediated by allosteric regulation and PTM of specific enzymes of the cycle (Max *et al.*, 2020; Nunes-Nesi *et al.*, 2013). Affinity chromatography studies have suggested several TCA cycle enzymes to be redox regulated (Balmer *et al.*, 2004; Yoshida *et al.*, 2013). Indeed, knockdown of the most abundant mitochondrial TRX (TRX *o1*) (Fuchs *et al.*, 2020a) increased the metabolic fluxes toward the TCA cycle (Daloso, Danilo M *et al.*, 2015; Florez-Sarasa, Obata, Del-Saz, Nï¿½stor Fernï¿½ndez, *et al.*, 2019). However, few putative mitochondrial TRX targets have been confirmed by site-directed mutagenesis of conserved Cys residues and/or using recombinant TRXs. It is currently known that citrate synthase 4 (CS4, AT2G44350) and a regulatory subunit of NAD^+-dependent isocitrate dehydrogenase (IDH-r, AT4G35260) are activated by TRX, whereas SDH and mitochondrial FUM

(FUM1, AT2G47510) have been shown to be deactivated by the TRX system (Fig. 1) (Daloso, Danilo M *et al.*, 2015; Schmidtmann *et al.*, 2014; Yoshida e Hisabori, 2014). Interestingly, aconitase (ACO) has been shown to be redox sensitive (Obata *et al.*, 2011), but its activity increased in *trxo1* mitochondrial extracts, with no effect of TRX *o1* recombinant addition in WT mitochondrial extracts. Similarly, the activity of both succinyl CoA Ligase (SCoAL) and OGDH is not altered by adding recombinant TRX *o1* to the assay. However, the knockdown of TRX *o1* substantially alters the activities of these enzymes, leading to changes in both metabolic fluxes and the accumulation of TCA cycle metabolites (Daloso, Danilo M *et al.*, 2015).

Redox regulation of cytosolic malate dehydrogenase (cytMDH1, AT1G04410) protected it against oxidative stress by TRX dependent homodimerization of Cys330 that avoid irreversible overoxidation of the enzyme (Huang *et al.*, 2018). However, whereas both plastidial (plMDH, AT3G47520) and cytMDH1 have been demonstrated to be activated by TRXs (Ashton e Hatch, 1983; Huang *et al.*, 2018; Thormählen *et al.*, 2015a, 2017), the mitochondrial (mtMDH, AT1G53240) and a plastidial NAD^+-dependent MDH are not redox-regulated (Berkemeyer, Scheibe e Ocheretina, 1998; Daloso, Danilo M *et al.*, 2015; Huang *et al.*, 2018; Yoshida e Hisabori, 2016b) (Fig. 1). MDH ($NADP^+$-dependent in chloroplasts and NAD^+-dependent all over the compartments) catalyses the reversible reaction between oxaloacetate (OAA) and malate using NAD(P)(H), and they are all involved in the malate valve that regulates both NAD(P)H homeostasis and the circulation of malate throughout the plant cycle (Selinski e Scheibe, 2019). Plant MDHs are thus important to regulate both NAD(P)(H) homeostasis and the circulation of malate throughout the plant cell (Hashida *et al.*, 2018; Zhao *et al.*, 2020). It has been demonstrated that the structure of the $NADP^+$-dependent plMDH facilitates its redox regulation by TRXs (Carr *et al.*, 1999). Conversely, there is no evidence that both mitochondrial MDHs (mtMDH1 and mtMDH2) are redox regulated. However, mtMDH activity has been shown to be modulated by light (Igamberdiev *et al.*, 2014; Tepperman *et al.*, 2004) and negatively regulated by adenine nucleotides, with ATP exerting the largest inhibitory effect (Yoshida e Hisabori, 2016b). Considering that, future studies are required to fully understand how active state of mtMDH respond to mitochondrial fluctuations in the adenine nucleotides pool, owing to photorespiration-dependent ATP production in illuminated leaves (Igamberdiev *et al.*, 2001) to allow rapidly re-oxidation of photorespiratory NADH.

Although the reasons behind the lack of redox regulation for mtMDHs are rather unclear, mtMDH activity was demonstrated to be important as a "buffer" capable of removing the excess of NADH that is known to allosterically inhibit mtPDH (Igamberdiev e Gardeström, 2014), several TCA cycle enzymes, and photorespiratory GDC (Bykova *et al.*, 2014; Lindén *et al.*, 2016; Nunes-Nesi *et al.*, 2013). In agreement with this hypothesis, double mutants for mtMDH displayed enhancement levels of glycine and, to a lesser extent, serine, clearly demonstrating the association of mtMDH with photorespiration, most likely as result of restriction on GDC mediated glycine oxidation (Tomaz *et al.*, 2010). Another possibility is that the reaction catalysed by mtMDH would sustain the synthesis of malate, which can be used for fumarate synthesis in either the mitochondria or the cytosol (Araújo, Nunes-Nesi e Fernie, 2011; Igamberdiev e Eprintsev, 2016; Zubimendi *et al.*, 2018), thus favouring the transport of fumarate to the vacuoles or to the apoplast, where it exerts considerable influence on the regulation of stomatal movements (Fig. 1) (Araújo *et al.*, 2011; Medeiros *et al.*, 2016, 2017; Nunes-Nesi *et al.*, 2007). Furthermore, fumarate can act as a backup pool for malate, establishing the equilibrium between NADH and $NADP^+$ which appears to stimulate mitochondrial enzyme complexes such as GDC (Bykova *et al.*, 2014) and PDH (Igamberdiev e Gardeström, 2014). It seems therefore that the maintenance of the concentration of TCA cycle intermediates in the light at levels enough for the activation of mitochondrial and cytosolic enzymes is controlled by complex and interconnected mechanisms. Additionally, mtMDHs are known to be part of a metabolite channel (metabolon) formed from FUM1 to IDH6, in which fumarate is channelled (Zhang *et al.*, 2017). Metabolite channels may improve the catalytic efficiency of the enzymes favouring metabolic flux toward the end of the channel (Graham *et al.*, 2007). Thus, the formation of this TCA cycle metabolon would improve the fluxes from fumarate to isocitrate and subsequently to 2-oxoglutarate to sustain the synthesis of amino acids such as proline, glutamate and glutamine in the light. This is particularly important given that the flux of the carbon derived from glycolysis and PDH activity toward glutamate synthesis is restricted in the light (Abadie *et al.*, 2017a). However, it remains unclear whether the redox regulation of FUM, CS and IDH would favour the formation of this metabolon or not. Further studies combining different approaches to investigate the formation and function of metabolite channels *in vivo* are, therefore, required to better understand the function of these channels for the overall regulation of the plant TCA cycle (Obata, 2020).

The recent established TCA cycle metabolon opens several possibilities for the regulation of metabolic fluxes throughout the TCA cycle (Sweetlove e Fernie, 2018; Zhang *et al.*, 2017, 2018). Given the high number of non-cyclic flux modes that has been observed in the leaf TCA cycle (Sweetlove *et al.*, 2010), it is reasonable to hypothesize that several PTMs would act in concert to regulate the fluxes through this pathway, depending on the prevailing environmental conditions. In this vein, it seems that TRXs contribute to maintain a non-cyclic flux mode of the TCA cycle by activating the C6-branch (from citrate to glutamate) and deactivating the C4-branch (from malate to succinate) of the TCA cycle in the light (Fig. 1). Beyond the evidence from the identification of TRX targets *in vitro*, this idea is further supported by genome scale metabolic modelling and *in vivo* ^{13}C-nuclear magnetic resonance-based metabolic flux analysis, in which the source of carbon for glutamate synthesis does not come from photosynthesis but rather from phospho*enol*pyruvate carboxylase-mediated CO_2 assimilation and from previously built up organic acid pools (Abadie *et al.*, 2017a; Abadie e Tcherkez, 2019; Maurice Cheung *et al.*, 2014) (Fig. 1). It remains unclear however if, and if so how, redox regulation combined with other PTMs (e.g., acetylation and (de)phosphorylation) integrate with the protein-protein interaction to regulate the activity of TCA cycle enzymes and thus the flux through this pathway *in vivo* under dark and light conditions (Nietzel *et al.*, 2017).

TRX-mediated regulation contributes to explain the inhibition of the metabolic fluxes toward the TCA cycle in illuminated leaves

Several enzymes of, or associated to, the TCA cycle are downregulated at transcriptional and/or posttranslational level in the light (Nunes-Nesi *et al.*, 2013), helping to explain why the TCA cycle does not operate in a circular fashion during the day. Overall, the restricted flux through the TCA cycle in illuminated leaves is explained by: firstly, the downregulation of mitochondrial PDH (mtPDH) complex in the light (discussed in details below); secondly, the feedback inhibition of TCA cycle dehydrogenases by NADH, NADPH and other effectors; thirdly, the export of 2-oxoglutarate for nitrogen assimilation in glutamate and fourthly, the operation of the citrate valve responsible for the distribution of NADPH to the cytosol and for directing carbon skeletons from stored citrate to amino acid biosynthesis and other metabolic purposes (Gauthier, Paul P.G. *et al.*, 2010; Igamberdiev, 2020; Igamberdiev e Gardeström, 2003; Tcherkez *et al.*, 2012). The inhibition

of NAD^+-dependent isocitrate dehydrogenase (IDH) by NADPH concurrent with the reversion of the reaction catalyzed by $NADP^+$-dependent IDH (Igamberdiev e Gardeström, 2003) are additional factors contributing to the significantly reduction of TCA flux in the light. Moreover, it is worth mentioning that, in addition to the regulation at the level of enzyme activity by TRX *o1* (Daloso, Danilo M *et al.*, 2015), both succinate dehydrogenase (SDH) and fumarase (FUM) are also regulated by modulation of gene expression mediated by phytochrome and cryptochrome (Eprintsev *et al.*, 2016, 2018; Eprintsev, Fedorin e Igamberdiev, 2013; Popov *et al.*, 2010).

According to the classical view, the start of the TCA cycle is the entrance of pyruvate within the mitochondrion, where it is decarboxylated by the mtPDH, yielding acetyl-CoA, thus connecting glycolysis to the TCA cycle (Fig. 1). However, mtPDH, a multi-complex protein composed by three subunits (E1, E2 and E3), is known to be light inhibited by phosphorylation of Ser residues on the E1 subunit by the action of a PDH kinase, whose activity is stimulated by conditions favoured by photorespiration, such as higher levels of ammonium ions (NH_4^+) and ATP (Tovar-Méndez, Miernyk e Randall, 2003). Also, photorespiratory metabolism increases mitochondrial NADH/NAD^+ ratio (Igamberdiev e Gardeström, 2003), further contributing to the light inhibition of PDH and of the other matrix dehydrogenases. Conversely, pyruvate allosterically inhibits the PDH kinase, thus stimulating PDH activity. The E3 subunit, a mtLPD, has recently been shown to be deactivated *in vitro* by both TRX *o1* and TRX *h2* (Fonseca-Pereira, da *et al.*, 2020; Reinholdt, Schwab, Zhang, Reichheld, J., *et al.*, 2019), in assays carried out in isolated mitochondria or using recombinant proteins. Therefore, TRX-mediated regulation of mtLPD appears as a second point which controls the entrance of carbon skeletons into the TCA cycle through redox regulation of the mtPDH (Fig. 1).

Out of the obvious - Redox regulation of alternative oxidase (AOX)

AOX works as an alternative pathway in the oxidative phosphorylation system, playing a crucial role in dissipating excess of energy, particularly under stress conditions (Selinski *et al.*, 2018). This mechanism is likely to avoid mitochondrial over-reduction due to enhanced formation of reactive oxygen and nitrogen species (ROS and RNS) (Del-Saz *et al.*, 2018). Arabidopsis possesses five genes encoding AOX proteins (AOX1A–AOX1D and AOX2) (Open *et al.*, 2017). All of them are found in a dimeric state that can be redox regulated through a disulfide/sulfhydryl-

system (Rhoads *et al.*, 1998; Siedow, 1993), although, at least in the case of AOX1A, 1C and 1D, a differential activation *in vivo* is observed, depending on the nature of the added effector and the amino acid composition around the conserved Cys residues of each isoform (Open *et al.*, 2017). Once its disulfide bond is reduced, the AOX activity can be stimulated through the formation of a thiohemiacetal with α-ketoacids, most notably pyruvate (Selinski *et al.*, 2017; Siedow e Umbach, 2000; Umbach, Joseph T. Wiskich e Siedow, 1994). Overall, AOX1A is the most abundant isoform, being highly expressed throughout all tissues and developmental stages in plants. Given that the expression of AOX members is regulated at both transcriptional and protein levels and is highly variable according to the tissue, developmental stage and stress conditions (Open *et al.*, 2017; Selinski *et al.*, 2018), it is rather difficult to individually ascertain the *in vivo* function of each isoform. Redox regulation of AOX has been postulated by TRX-affinity chromatography studies using isolated mitochondria (Balmer *et al.*, 2004; Yoshida *et al.*, 2013) and further confirmed by both *in vitro* and *in vivo* studies (Florez-Sarasa, Obata, Del-Saz, Néstor Fernández, *et al.*, 2019; Gelhaye *et al.*, 2004; Umekawa e Ito, 2019). The mitochondrial TRX system allows the reversible cleavage of disulfide bonds among AOX monomers *in vitro*. However, it was demonstrated only recently that the functional lack of TRX *o1* unexpectedly increases AOX activity *in vivo* under both moderate and high light conditions without changing its redox state (Florez-Sarasa, Obata, Del-Saz, Néstor Fernández, *et al.*, 2019). Furthermore, *trxo1* mutants were characterized by higher carbon fluxes toward the TCA cycle and photorespiration, especially under high light (Daloso, Danilo M *et al.*, 2015; Florez-Sarasa, Obata, Del-Saz, Néstor Fernández, *et al.*, 2019), as similarly observed in *trxh2* mutant (Fonseca-Pereira, da *et al.*, 2020; Reinholdt, Schwab, Zhang, Reichheld, J., *et al.*, 2019).

The fact that TRX *o1* is apparently not essential for AOX reduction *in vivo* (Florez-Sarasa, Obata, Del-Saz, Néstor Fernández, *et al.*, 2019) raises an important question: Could TRX *o2* compensate the lack of TRX *o1* in the regulation of AOX, GDC and TCA cycle enzymes ? To answer this question, one must consider the composition of the plant mitochondrial TRX system. TRX *o1* is seemingly by far the most abundant isoform of TRX in the mitochondrial matrix of Arabidopsis (Florez-Sarasa, Obata, Del-Saz, Nï¿½stor Fernï¿½ndez, *et al.*, 2019; Fuchs *et al.*, 2020a; Yoshida e Hisabori, 2016b). For instance, heterotrophically grown Arabidopsis cells indicated extremely low abundance of TRX *o2* (20 copies) compared to Trx *o1* (837 copies), whereas TRX *h2* was not detected (Fuchs *et al.*, 2020a). Albeit both TRX *h2* of poplar (Gelhaye *et*

al., 2004) and castor seed (Marcus *et al.*, 1991) were shown to be targeted to mitochondria, and heterologous expression of *At*TRX *h2*-GFP resulted in mitochondrial targeting in onion cells (Meng, Ling *et al.*, 2010), *At*TRX *h2* has not yet been found in mitochondrial proteomes. Further studies using stable Arabidopsis lines expressing TRX *h2* fused with redox-sensitive green fluorescent protein 2 (roGFP2) (Attacha *et al.*, 2017) should be carried out in order to clearly confirm TRX *h2* location in plants cells. Given that the redox state of AOX was unaltered in *trxo1* mutant and that the reduced state represented around 90% of the protein redox status (Florez-Sarasa, Obata, Del-Saz, Néstor Fernández, *et al.*, 2019), it is likely the existence of a compensatory system in mitochondria. However, whether TRX *o2* or other not yet identified mechanism could compensate, at least partially, the lack of TRX *o1* remain to be determined.

Regardless of the occurrence or not of functional compensatory roles between TRXs, the aforementioned observations suggest another important questioning that is: Does TRX *o1* have a role in the redox regulation of AOX activity *in vivo*? TRXs catalyse both reduction and oxidation of enzyme thiols. Accordingly, TRX *o1* also promotes oxidation of AOX (Florez-Sarasa *et al.*, 2019). In this connection, one possibility is that the lack of TRX *o1* would stabilize the reduced form of AOX by promoting its oxidation, which would demand the oxidation of the entire TRX system (Max *et al.*, 2020). This is a situation that can be observed during the mitochondrial isolation procedure (Max *et al.*, 2020) or possibly in the maturation drying period of orthodox seeds (Bailly, 2019; Gerna *et al.*, 2017). In these cases, the oxidation of existing thiols is favoured either by (i) the conditions of the isolation process or (ii) by the lower metabolic activity of dry seeds, in which internal tissues are exposed to oxidative environment conditions (Bailly, 2019; Gerna *et al.*, 2017).

The accumulated knowledge concerning AOX redox regulation suggests that the results observed *in vitro* are not strictly translated into *in vivo* physiological modifications. This idea is further supported by the fact that mitochondrial CS4 is activated by TRX *in vitro* (Schmidtmann *et al.*, 2014) but the total CS activity increased in both leaf and mitochondrial extracts of the *trxo1* mutant (Daloso, Danilo M *et al.*, 2015).The lack of correlation among *in vitro* and *in vivo* observations could be explained by the intrinsic complexity of the TRX system and/or of the cell environment, in which other PTMs and redundant/compensatory systems orchestrally act to regulate the activity of the enzymes. Furthermore, it is important to highlight that whilst TRXs evolved with particular dependency on their TRX reductase systems, a certain degree of promiscuity of TRXs in reducing target proteins is observed (Napolitano *et al.*, 2019). Given the

higher number of TRX isoforms found in each plant subcellular compartment, a higher degree of promiscuity (*in vitro*) and redundancy (*in vivo*) is expected to be observed in plants. Indeed, Arabidopsis cytMDH1 is activated by TRXs *h1-5 in vitro* (Huang *et al.*, 2018), suggesting either a redundant role of TRX *h* isoforms *in vivo* or a certain degree of promiscuity of these isoforms to reduce cytMDH1 *in vitro*. Considering the complexity of the mitochondrial redox system and the high number of putative TRX targets raised by different proteomic approaches, it is necessary to investigate whether the accumulated *in vitro* knowledge is translated to *in vivo* physiological responses. For this purpose, different genetic, biochemical and metabolomics approaches coupled to the characterization of mutants lacking different combinations of the mitochondrial redox proteins will be required.

TRX-mediated regulation of glycine decarboxylase (GDC)

In oxygenic phototrophs, GDC is the flux controlling enzyme of photorespiration and essential for the physiological interaction between photosynthesis and photorespiration (Timm *et al.*, 2012, 2015). Remarkably, GDC activity affects CO_2 concentration gradients within leaves and has further implications as an important link between photorespiration and other pathways such as C1 metabolism (Engel *et al.*, 2007), nitrate and ammonia assimilation and abiotic stress responses (Timm e Hagemann, [s.d.]). Furthermore, the remarkably high amounts of NADH produced under illumination, chiefly through photorespiratory flux over L-protein of GDC (Fig. 2), has important impacts on photosynthetic metabolism. For instance, a part of this NADH is exported to the cytosol via the malate valve, boosting hydroxypyruvate reduction in the peroxisome, further contributing to the maintenance of NADH levels in different compartments (Igamberdiev *et al.*, 2001; Igamberdiev e Gardeström, 2003).

In higher plants, GDC is located in mitochondria and is, in conjunction with serine hydroxymethyltransferase 1 (SHMT1), responsible for the decarboxylation of two glycine molecules yielding one molecule of each, serine, CO_2, NADH and ammonia, respectively (Oliver, 1994). It contains four subunits, namely P-, T-, H-, and L- protein (mtLPD) (Fig. 2), which are encoded by a total of eight genes in Arabidopsis: three encode for H protein, one for T protein and two genes each for the P protein and mtLPD (L-protein) (Bauwe e Kolukisaoglu, 2003; Engel *et al.*, 2007). It has been proposed that mtLPD1 gene expression is highly induced in response to light.

Furthermore, mtLDP1 is preferentially associated with GDC, while the second isoform, mtLPD2, is associated with PDH, OGDH and BCKDC (Lutziger e Oliver, 2001; Mooney, Miernyk e Randall, 2002). The role of GDC in the control of the flux through photorespiratory cycle and its importance for photosynthesis and plant growth has been revealed in terms of transcriptional regulation and by metabolomics and physiological analyses (Timm *et al.*, 2016). Additionally, it has been shown that the complete lack of GDC leads to lethality due to its role in C1 carbon metabolism (Engel *et al.*, 2007; Timm *et al.*, 2018). By contrast, enhanced GDC activity by overexpression of either GDC-H (López-Calcagno *et al.*, 2018) or mtLPD (Timm *et al.*, 2015) facilitates glycine-to-serine conversion through photorespiration and improves photosynthesis and growth in C_3 plants. These observations provide further evidence that GDC is a central step integrating photosynthetic and photorespiratory metabolism. Furthermore, GDC and SHMT1 have been demonstrated to be allosterically regulated by glycine and serine, as well as by the ratio of $NADH/NAD^+$ (Bourguignon, Neuburger e Douce, 1988) (Fig. 3). GDC is strongly regulated at the transcriptional level by light (Rasmusson e Escobar, 2007) and, at the posttranslational level, by glutathionylation, *S*-nitrosylation and some putative peptides sites of P- and H-protein are passive of phosphorylation (Hodges *et al.*, 2013; Max *et al.*, 2020; Oa *et al.*, 2010) (Fig. 3).

Despite the fact that GDC, and other photorespiratory enzymes, have been suggested as possible redox regulated enzymes (Balmer *et al.*, 2004; Keech *et al.*, 2017; Yoshida, Hara e Hisabori, 2015), experimental evidence supporting this idea was, until recently, still missing. Initial evidence from an affinity chromatography study suggested that SHMT and all GDC subunits are targets of mitochondrial TRX (Balmer *et al.*, 2004). Furthermore, reducing reagents such as DTT altered the redox state *in vitro* of GDC-P from *Synechocystis* and its crystal structure provided evidence for a redox regulation mechanism (Hasse *et al.*, 2013), most likely mediated by mitochondrial TRXs. In agreement with the high similarity between the protein sequences of mtLPD1 and mtLPD2 and the presence of Cys residues in both, *in silico* predictions of disulfide bond formation and protein structure modelling suggest that the two mtLPD isoforms of Arabidopsis can form disulfide bonds (Table S2 and Fig. S1). Taking this into account, two recent works have further confirmed that indeed mitochondrial TRXs *o1* and *h2* are able to redox regulate mtLPD (Fonseca-Pereira, da *et al.*, 2020; Reinholdt, Schwab, Zhang, Reichheld, J., *et al.*, 2019). By a combination of biochemical *in vitro* enzymatic activity and metabolomics approaches, it was demonstrated that mtLPD activity is decreased with the presence of DTT or by the addition of

NTRA plus TRXs *o1* or *h2* in the assay, indicating that these TRXs can regulate this GDC subunit *in vitro*. Additionally, gas exchange parameters in mutants of TRX *h2* (Fonseca-Pereira, da *et al.*, 2020) and TRX *o1* (Reinholdt, Schwab, Zhang, Reichheld, J., *et al.*, 2019) indicate an increase in the stoichiometry of the photorespiratory CO_2 release in these two mutants, as also previously found for intermediate photorespiratory mutants (Cousins *et al.*, 2011; Timm *et al.*, 2011). Beyond the expected effect that this regulation would have on photorespiration, it is worth to mention that the double mutant lacking TRX *o1* and up to 95% GDC-T protein has severe growth impairment compared to wild type (WT), whilst *gldt1*, a T-DNA insertion knockdown mutant, shows mild reduction in growth (Reinholdt, Schwab, Zhang, Reichheld, J., *et al.*, 2019), and the single *trxo1* has unaltered growth in normal air conditions (Reinholdt, Schwab, Zhang, Reichheld, J., *et al.*, 2019). This phenotype is most likely associated with glycine accumulation caused by impaired GDC functioning, given that glycine could become toxic by its capacity to chelate Mg^{2+}, which could potentially affect CB cycle activity, as suggested for *Synechocystis* (Eisenhut, Bauwe e Hagemann, 2007; Timm *et al.*, 2016). Similarly, Arabidopsis plants lacking the ER located ATP/ADP transporter 1 (ER-ANT1) show an unexpected photorespiratory phenotype, exhibiting 26-fold higher glycine content in leaves in a light-dependent manner (Hoffmann *et al.*, 2013) and a dwarf phenotype with a substantially decreased content of lipid and protein in seeds (Leroch *et al.*, 2008). The remarkable elevation in glycine levels is attributable to the inhibition of GDC activity caused by oxidative posttranslational protein modification induced by elevated ROS (H_2O_2 and superoxide) in the *er-ant1* mutants (Hoffmann *et al.*, 2013). These observations unveil a surprising and puzzling physiological connection between ER and mitochondrial photorespiration. The resultant ROS accumulating in *er-ant1* mutants are most likely a result of the disturbed mitochondrial metabolism, caused by ER stress (Hoffmann *et al.*, 2013). Therefore, the photorespiratory phenotype of *er-ant1* brings to light a further complexity of photorespiration and an unexpected and distinct communication between ER and mitochondria. Although the exact mechanism of ER/mitochondria communication in plants remains to be determined, it is possible that thiol switch-based sensing of H_2O_2 produced by the ER could serve as a potential mode to signal ER dysfunction to GDC in mitochondria, giving thus support to the concept of colocalization of ROS signal and ROS sensing (Huang *et al.*, 2016). Taking into account the wide distribution of TRXs in plants, and the suggestive role of TRXs in the intercellular communication in plants (Benitez-Alfonso *et al.*, 2009; Meng, Ling *et al.*, 2010), it seems possible that this interorganellar

communication between ER and mitochondria would require TRXs. However, which TRX modulates this interplay remain to be unveiled.

Consequences of the redox regulation of GDC beyond photorespiration

Posttranslational regulation is a fine and effective mechanism that fully depends on the cell microenvironment (Friso e Wijk, van, 2015). It also offers an important mechanism for rapid adjustment of plant metabolism according to the prevailing environmental conditions (Araújo *et al.*, 2012; Basler *et al.*, 2016; Plaxton e Podestá, 2006). Thus, given the role of the GDC as a central step for the control of photosynthesis and photorespiration, the recent discovery that GDC is redox regulated, together with the previously identified mitochondrial TRX-targets, several implications for the overall control of plant mitochondrial metabolism are evident. For instance, given that, in addition to GDC and BCKDC, mtLPD is also shared with the mtPDH complex, which is responsible for the carbon input to the TCA cycle, and OGDH, which exhibits a high flux control coefficient among the TCA cycle enzymes (Araújo *et al.*, 2012; Igamberdiev e Gardeström, 2014), it seems likely that the redox regulation of mtLPD represents a major control point in mitochondrial metabolism. Indeed, PDH redox-regulation was shown in *Escherichia coli* where mutation in mtLPD altered the NADH sensitivity of PDH complex (Kim, Ingram e Shanmugam, 2008). Moreover, Arabidopsis mtLPD overexpression lines have altered fluxes throughout TCA cycle enzymes and presented altered rates of photosynthesis, photorespiration and respiration (Timm *et al.*, 2015). Furthermore, plants lacking TRX *o1* have clearly increased carbon fluxes through the TCA cycle (Daloso, Danilo M *et al.*, 2015; Florez-Sarasa, Obata, Del-Saz, Néstor Fernández, *et al.*, 2019; Reinholdt, Schwab, Zhang, Reichheld, J., *et al.*, 2019). Thus, the TRX-mediated redox regulation of mtLPD coupled with the deactivation of PDH by phosphorylation (Budde e Randall, 1990; Tcherkez *et al.*, 2005; Tovar-Méndez, Miernyk e Randall, 2003) and the deactivation of SDH and FUM by TRX *o1* (Daloso, Danilo M *et al.*, 2015) contribute to explain the light-inhibition of respiration (Fig. 2) (Abadie *et al.*, 2017a; Gauthier, Paul P G *et al.*, 2010; Tcherkez *et al.*, 2005). However, it is interesting to note that whilst both TRXs *o1* and *h2* deactivate SDH and mtLPD *in vitro* (Daloso, Danilo M *et al.*, 2015; Fonseca-Pereira, da *et al.*, 2020; Reinholdt, Schwab, Zhang, Reichheld, J., *et al.*, 2019), suggesting a redundant role among these TRXs, FUM is respectively activated and deactivated by TRX *h2* and TRX *o1 in vitro* (Daloso, Danilo M *et al.*, 2015).

Therefore, it remains unclear whether TRXs *o1* and *h2* have redundant, compensatory and/or antagonist roles in the coordination of the fluxes through the leaf TCA cycle. Although part of the flux through mitochondrial respiration is inhibited in the light with the aid of mitochondrial TRX system, cytosolic isoforms such as cytMDH1 and FUM2 can be activated to support organic acid biosynthesis during the day (Eprintsev *et al.*, 2020). In accordance, phytochrome affects the gene expression of the mitochondrial (*ACO1*) and cytosolic (*ACO2*) forms of aconitase in opposite ways in maize leaves (Eprintsev *et al.*, 2020). While *ACO1* expression is inhibited in the light, the expression of *ACO2*, which is important for the remobilisation of citrate exported from mitochondria to the synthesis of amino acids, is stimulated via the phytochrome system (Eprintsev *et al.*, 2020). Furthermore, the cytosolic citrate-metabolizing enzyme ATP-citrate lyase (ACL) was shown to be activated by TRX *o1* and TRX *h2 in vitro* in Arabidopsis (Daloso, Danilo M *et al.*, 2015) (Fig. 1). Given that, in contrast to TRX *o1*, which is apparently the dominant mitochondrial TRX and is specific of mitochondria (and also nucleus), TRX *h2* is found in the cytosol, it seems reasonable to suggest that TRX *h2* and TRX *o1* play different roles in activating cytosolic (in case of TRX *h2*) and deactivating mitochondrial FUM (in case of TRX *o1*) isoforms, in the light (Fig. 1). Given that Arabidopsis has an overaccumulation of fumarate in the light period and this is abolished in *fum2* mutant (Pracharoenwattana *et al.*, 2010), it is likely that cytosolic and mitochondrial MDHs as well as FUM2 are activated under this condition (Fig. 1). However, this hypothesis has yet to be better experimentally tested. Furthermore, it remains to be experimentally assessed whether and under which environmental conditions the redox regulation of mtLPD also affects the activity of PDH, OGDH and BCKDC and what is the significance of this regulation to the overall regulation of the mitochondrial metabolism in the light.

Are any other photorespiratory enzymes regulated by TRX?

TRX chromatography affinity and proteomic thiol labelling assays have provided several candidate enzymes for redox regulation via TRX and GRX (Balmer *et al.*, 2004; Nietzel *et al.*, 2017; Yoshida, Hara e Hisabori, 2015), while experimental confirmation is still required (Balmer *et al.*, 2004; Buchanan, 2017a; Nietzel *et al.*, 2017). The presence of Cys residues in the sequence of the candidate proteins is a prerequisite for TRX redox regulation (Cejudo *et al.*, 2014; Fonseca-Pereira, da *et al.*, 2020) (Fig. 4). Thus, the identification of conserved Cys residues and the

prediction of disulfide bonds *in silico* perhaps eliminate false-positive results from TRX chromatography assays which would have to be further confirmed experimentally (Fig. 4) (Souza *et al.*, 2019a). Therefore, we collected protein sequences from enzymes associated with photorespiration, TCA cycle and nitrogen metabolism to search for other possible TRX targets. The sequences were submitted to DiANNA 1.1 web server in order to predict disulfide bonds in the input sequences (Ferrè e Clote, 2005). The predictions suggest the presence of disulfide bonds within protein sequences of all subunits of GDC, phosphoglycolate phosphatase, plLPD2, mtLPDs, aconitase, NADH-isocitrate dehydrogenase, succinyl-CoA ligase, SDH and both FUM 1 and FUM2 (Table S2). Several of these enzymes were previously shown to be TRX targets (Balmer *et al.*, 2004; Daloso, Danilo M *et al.*, 2015; Yoshida, Hara e Hisabori, 2015). Furthermore, both mtMDH and CS5 have no predicted disulfide bond formation, in agreement with previous results showing that these isoforms are not redox regulated (Schmidtmann *et al.*, 2014; Yoshida e Hisabori, 2016b). Further enzymes of nitrogen metabolism previously captured in chromatography TRX affinity assays also formed disulfide bonds, included NADH-dependent glutamate synthase 1 (GLT1), glutamate synthase 1 and 2 (GLU1 and 2), α and β glutamate dehydrogenase (GDH1 and GDH2) and glutamine synthetase 2 (GS2) (Table S2)(Balmer *et al.*, 2004; Daloso, Danilo M *et al.*, 2015; Yoshida *et al.*, 2013). By contrast, SHMT1, a further enzyme suggested to be TRX target (Balmer *et al.*, 2004; Buchanan e Balmer, 2005; Yoshida *et al.*, 2013), was predicted to not harbour disulfide bonds, indicating relatively low probability of disulfide bond formation at SHMT. Additionally, DiANNA predictions failed to identify disulfide bond formation in previous established TRX targets such as mtCS4, cytMDH1 and AOX 1A. It is important to highlight that DiANNA predictions are restricted to intramolecular disulfide bond formation, meaning that this platform cannot predict disulfide bond formation among monomers. This likely explain the lack of disulfide bond formation in mtCS4, cytMDH1 and AOX, given that these enzymes have been shown to form intermolecular disulfide bonds between two monomers (Gelhaye *et al.*, 2004; Schmidtmann *et al.*, 2014). One way to solve this is by adding the input protein sequence twice. In this case, disulfide bond formation is observed when the sequences of mtCS4, cytMDH1 and AOX are included twice. This highlights a limitation of the simple strategy we used and illustrates the importance of additional research efforts to precisely elucidate the interplay between the different TRX proteins and their regulatory nodes of (photo)respiratory metabolism.

Concluding remarks and future perspectives

A complex network of interacting metabolic pathways requires a precisely coordinated regulation to maintain cellular homeostasis. The recent discovery that photorespiration is also regulated by TRXs indicate these redoxins as important regulators of energy metabolism. Given that NTR/TRX-mediated regulation is intricately connected with the NAD(P)(H) metabolism, which is in turn modified in response to both light and dark conditions, it seems reasonable to suggest that TRXs finely control metabolic fluxes throughout the cell by activating and deactivating key metabolic steps of pathways such as CB cycle, the cytosolic malate metabolism, the TCA cycle and GDC activity, according to the redox condition. We further postulate that minimal changes in the presence or intensity of light and/or in the levels of NAD(P)(H) and ROS would be anticipated by the TRX system to tightly regulate metabolic fluxes through photosynthesis and (photo)respiration. From a myriad of studies, it has become increasingly evident that TRXs-mediated redox regulation facilitates plant metabolic adjustments in response to the prevailing environment conditions. Considering the role of mitochondrial TRX system in regulating GDC (Fonseca-Pereira, da *et al.*, 2020; Reinholdt, Schwab, Zhang, Reichheld, J., *et al.*, 2019), and given the importance of photorespiration for photosynthesis and plant productivity (López-Calcagno *et al.*, 2018; Timm *et al.*, 2015; Timm e Hagemann, [s.d.]), it will be interesting to elucidate how, and to what extent, TRXs integrate responses among subcellular compartments to coordinate mitochondrial operation in the light, by adding flexibility to not fully abolish TCA cycle flux by highly demanding fluxes from photorespiratory pathway and photosynthesis (Igamberdiev, 2020). However, given the known redundancy and the complementarity of the plant redox system (Souza, Paulo V.L. *et al.*, 2018), several questions remain rather unclear, including: (*i*) how do TRXs interact with the other components of this system to coordinate plant cell homeostasis, especially under sub-optimal environmental or stress conditions? (*ii*) Is redox regulation via TRXs the major mechanism that control metabolic fluxes throughout central metabolism? (*iii*) Which protein or mechanism compensate the lack of TRX *o1* in AOX regulation? (*iv*) Can TRX specifically guide metabolic fluxes through different pathways in response to environmental changes? (*v*) What is the implication of the redox regulation of photorespiration for plant stress acclimation? What is clear from the recent studies highlighted here is that redox regulation undoubtedly remains a potential target in which an inhibition or activation could

synergize with the metabolic response to sustain plant growth and development, particularly in response to environmental fluctuations such as light conditions (Souza, Paulo V.L. *et al.*, 2018). Given the multiplicity of targets that TRXs can reduce, much of which still deserve validation by different approaches, we posit that determining the precise subcellular location of TRXs, including TRX *h2*, and the specific targets of the mitochondrially located TRXs will likely be of paramount importance in providing useful information for improving metabolic engineering in land plants.

Acknowledgments

This work was made possible through financial support from the Max Planck Society, the National Council for Scientific and Technological Development (CNPq-Brazil, Grants 402511/2016-6 and 428192/2018-1), and the FAPEMIG (Foundation for Research Assistance of the Minas Gerais State, Brazil, Grant RED-00053-16). We also thank the scholarships granted by the Brazilian Federal Agency for Support and Evaluation of Graduate Education (CAPES-Brazil) to PFP and PVLS. Research fellowships granted by CNPq-Brazil to WLA and DMD are also gratefully acknowledged. ST gratefully acknowledges Hermann Bauwe for previous and Martin Hagemann for current support.

Conflict of interest: The authors declare that they have no conflict of interest.

Author contribution

P.F-P., P.V.L.S., D.M.D. and W.L.A. developed the concept of this review; P.F-P., and P.V.L.S. prepared the figures and wrote the first draft of the manuscript; D.M.D. and W.L.A. coordinated the writing process. All authors contributed to the writing and revision of the manuscript

Figure Chapter 1:

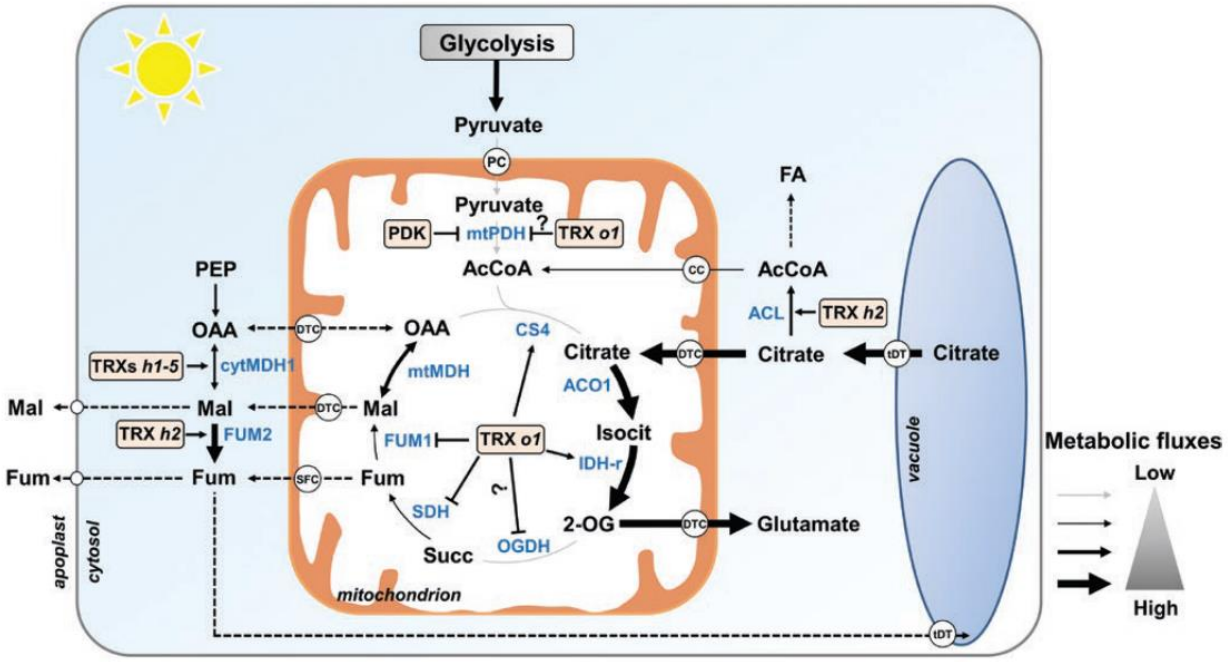

Fig. 1. Schematic representation of the proposed metabolic fluxes through the TCA cycle and associated pathways in the light. Compelling evidence indicate that TRXs contribute to stimulate the fluxes through the C6 branch of the TCA cycle by activating CS4 and a regulatory subunit of NAD^+-dependent isocitrate dehydrogenase (IDH-r) (Schmidtmann *et al.*, 2014; Yoshida e Hisabori, 2014). Given that PDH is inhibited by phosphorylation and possibly by TRX *o1* in the light (Fonseca-Pereira, da *et al.*, 2020; Tovar-Méndez, Miernyk e Randall, 2003), the activation of the C6 branch of the TCA cycle assumes a pivotal importance to increase the flux from citrate stored in the vacuole toward glutamate biosynthesis (Abadie *et al.*, 2017a; Maurice Cheung *et al.*, 2014). By contrast, the C4 branch of the TCA cycle seems to be downregulated through deactivation of both SDH and FUM1 by TRX *o1* (Daloso, Danilo M *et al.*, 2015). It seems likely that both malate and fumarate synthesized in the mitochondria are used to sustain the massive fumarate accumulation in the light (Pracharoenwattana *et al.*, 2010). This idea is supported by the fact that both cytMDH and FUM2 have been shown to be activated by TRX *h1-5* and TRX *h2*, respectively (Daloso, Danilo M *et al.*, 2015; Huang *et al.*, 2018). Alternatively, organic acids can be transported out of the cell to the apoplastic space, where it can reach guard cells and regulate stomatal movements (Araújo *et al.*, 2011). Collectively, the TRX-mediated regulation of TCA cycle enzymes contributes to explain why respiration is inhibit in the light (Tcherkez *et al.*, 2009) and why the TCA cycle operates in a non-cyclic mode under this condition (Sweetlove *et al.*, 2010). It remains unclear whether the TRX-mediated mtLPD regulation inhibits the activity of both mtPDH and OGDH *in vivo* (see question markers). Thicker arrows correspond to metabolic reactions carrying higher metabolic fluxes. Dashed lines represent possible fate of organic acids produced in mitochondria in the light. White spheres represent organic acid carriers. Abbreviations: Carriers: CC, mitochondrial acetyl-CoA carrier; DTC, dicarboxylate/tricarboxylate carriers; PC, pyruvate carrier; SFC, mitochondrial succinate/fumarate carrier; tDT, tonoplast dicarboxylate transporter. Metabolites: 2-OG, 2-oxoglutarate; AcCoA, acetil-CoA; Fum, fumarate; Isocit, isocitrate; Mal, malate; OAA, oxaloacetate; PEP, phospho*enol*pyruvate; Succ, succinate; TCA,

tricarboxylic acid. Enzymes: ACL, ATP citrate lyase; ACO1, aconitase 1; CS4, citrate synthase 4; cytMDH1, cytosolic malate dehydrogenase1; IDH-r, regulatory subunit of NAD^+-dependent isocitrate dehydrogenase; FUM1 and 2, fumarase 1 and 2; mtMDH, mitochondrial malate dehydrogenase; OGDH, oxoglutarate dehydrogenase; PDH, pyruvate dehydrogenase; PDK, pyruvate dehydrogenase kinase; SDH, succinate dehydrogenase; TRX *h2*, thioredoxin *h2*; TRX *o1*, thioredoxin *o1*. The scheme shown is mostly based on data from (Daloso, Danilo M *et al.*, 2015).

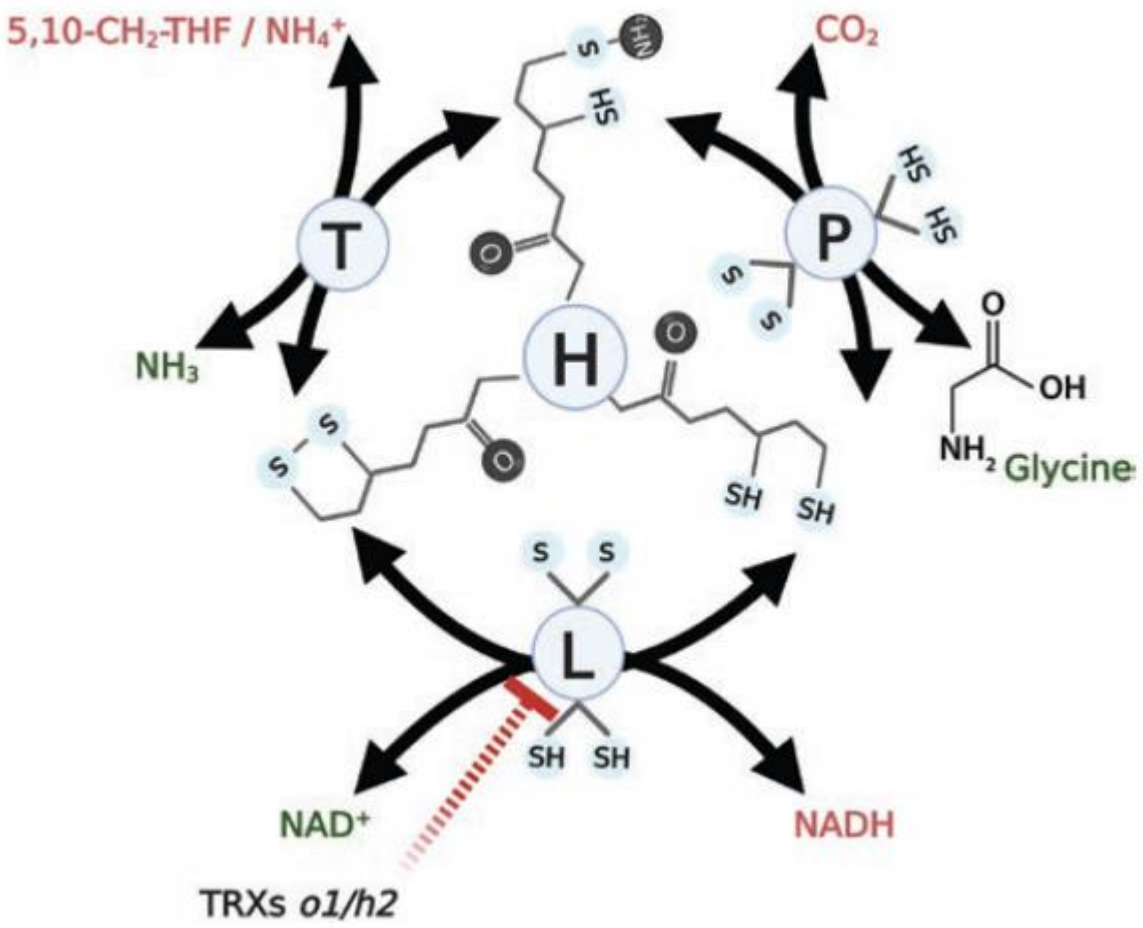

Fig. 2. Structure of plant glycine decarboxylase (GDC). Schematic representation of the four subunits H, L, P and T that compose GDC, highlighting the presence of Cys residues and the role of both TRXs *o1* and *h2* in deactivating the L subunit. GDC regulation via substrate, products and cofactors is also highlighted. Compounds in green and red colours indicate positive and negative regulators of GDC activity, respectively. Abbreviations: GDC, glycine decarboxylase; TRX *h2*, thioredoxin *h2*; TRX *o1*, thioredoxin *o1*. The scheme shown is mostly based on data from (Douce *et al.*, 2001).

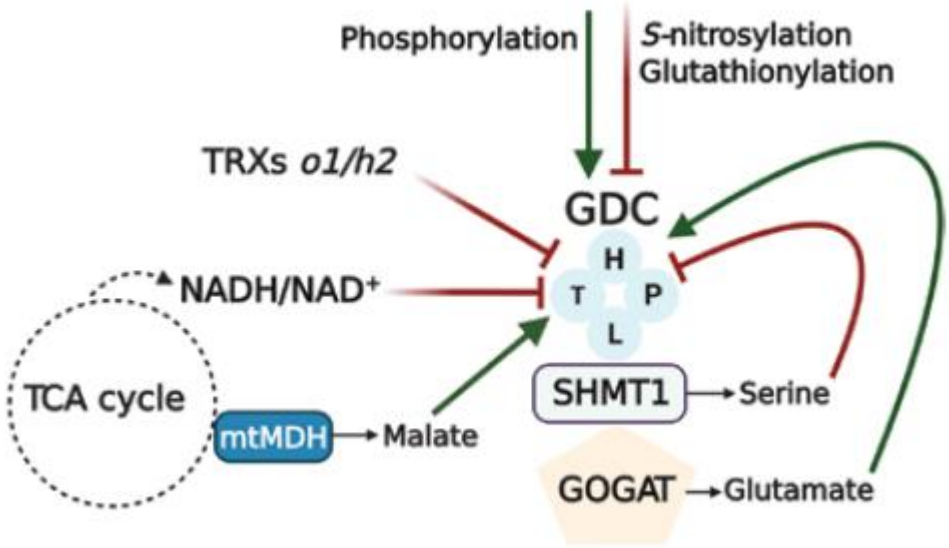

Fig. 3. Allosteric and posttranslational mechanisms that regulate glycine decarboxylase (GDC) activity. GDC is a key enzyme that integrates photorespiration, the tricarboxylic acid (TCA) cycle and nitrogen metabolism. Glutamate synthesized by GOGAT and malate formed by mtMDH contribute to the activation of GDC in mitochondria. SHMT1 and MDH are represented by rectangles, whilst GDC subunits (H, L, P and T) and GOGAT are represented by light blue spheres and by a hexagon, respectively. Green and red arrows indicate mechanisms and compounds that activate or deactivate GDC, respectively. Abbreviations: GDC, glycine decarboxylase; GOGAT, glutamine:2-oxoglutarate aminotransferase; mtMDH, mitochondrial malate dehydrogenase; SHMT1, serine hydroxymethyltransferase 1. The scheme shown is mostly based on data from (Bykova *et al.*, 2014; Eisenhut, Roell e Weber, 2019; Max *et al.*, 2020; Nietzel *et al.*, 2017).

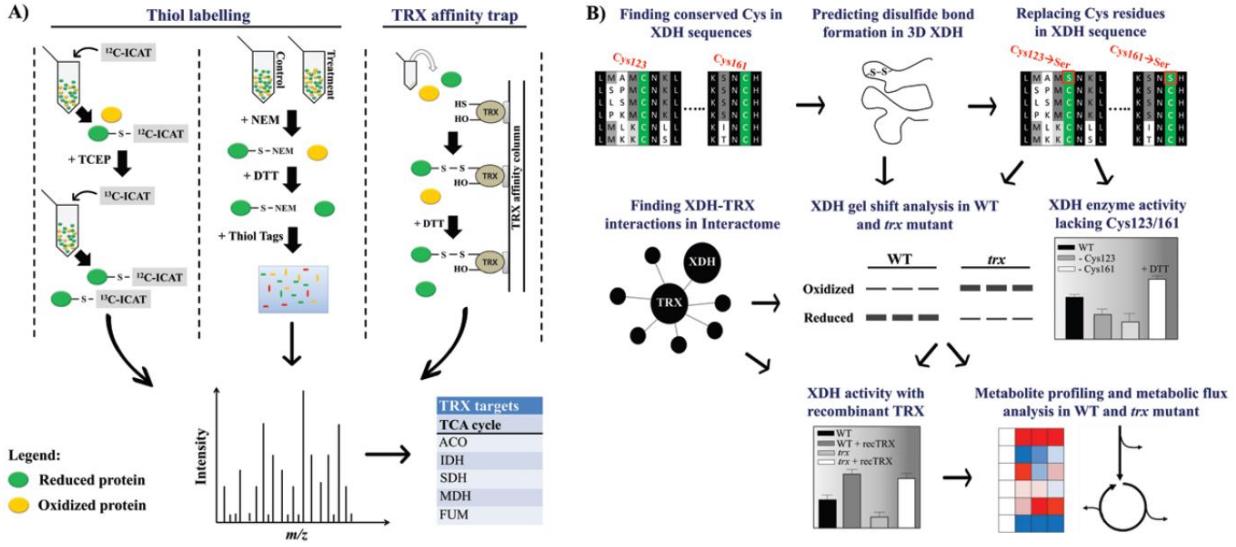

Fig. 4. Simplified representation of the main approaches used to identify potential thioredoxin (TRX) targets and to unveil the role of TRXs *in planta*. A) Approaches used to identify putative TRX targets based in labelling of thiol groups or trapping TRXs into a TRX affinity column with posterior mass spectrometry (MS) identification. The left side methodology allows the label of reduced thiols with different isotope-coded affinity tag (ICAT) reagents. First, all reduced Cys are labelled with ^{12}C-ICAT. After, Tris (2-carboxyethyl) phosphine (TCEP) is applied to reduce all remained oxidized Cys that are posteriorly labelled with ^{13}C-ICAT. After trypsination and purification, the proteins are identified by MS. In the middle panel, reduced thiol groups of control and treatment samples are separately marked and blocked with nethylmaleimide (NEM). After reduction of the remaining oxidized Cys with DTT, thiol-specific fluorescent tags are then applied. The samples are separately analysed in a 2-dimensional gel and the identification of protein spots are identified by MS. At the right panel, extracted proteins are applied into an affinity chromatography TRX column that contains a Cys residue modified to Ser. Stable hetero-disulfide complexes are formed with target proteins, whilst the non-TRX target proteins are eluted throughout the column. DTT is then applied to elute the TRX target proteins, being later identified by MS. B) There is evidence showing that TRX-target proteins have conserved Cys residues among different taxa. Thus, one way to identify possible TRX targets is by searching conserved Cys residues in putative TRX targets. However, the presence of conserved Cys residues does not unequivocally guarantee that those Cys residues are available for TRX reduction. Thus, it is important to verify the 3D position of the Cys residues. To do this, both DiANNA[2] and SWISS-MODEL[3] platforms are suggested for 3D visualization and to predict disulfide bond formation[4]. Another possibility to raise putative TRX targets is by interrogating interactome database. After obtaining putative TRX targets (exemplified here as XDH, a putative X dehydrogenase), several biochemical assays can be carried out in WT and a specific *trx* mutant that is located to the same subcellular localization of XDH. For instance, to identify which Cys residues are mostly contributing to the redox regulation of XDH activity, one way to investigate this is by replacing Cys to Ser residues. After that, XDH activity is analysed containing or lacking mutated Cys residues. In parallel, the redox status of XDH can be verified by gel shift analysis. XDH activity can also be investigated under the presence of recombinant TRX in WT and *trx* protein samples. Lastly, metabolite profiling and metabolic flux analysis can be performed using WT and *trx* mutant

to investigate the effect of the lack of the TRX on the metabolic reaction and pathway in which XDH is inserted.

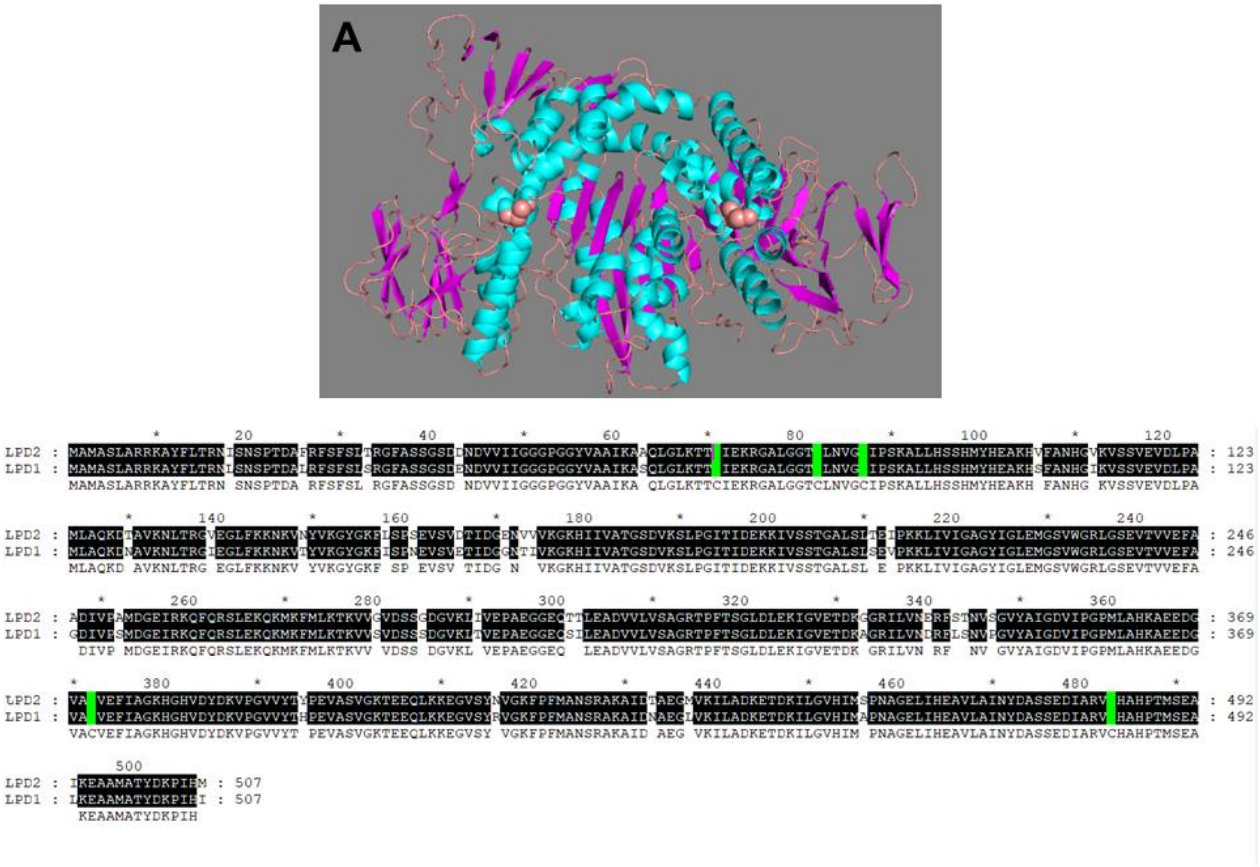

Fig. 5. Structure and amino acid alignment of mitochondrial dihydrolipoamide dehydrogenase (LPD) 1 (AT1G48030) and LPD2 (AT3G17240). A) The 3D model of the LPD1 and LPD2 was built using SWISS-MODEL program. The template used to generate both LPD1 and LDP2 models was 1dxl.2.A from *Pisum Sativum*. LPD1 and LPD2 have 88.6 % and 87.8 % of similarity with the template amino acid sequence, respectively. Spheres represent disulfide bonds. B) Amino acid alignment between Arabidopsis mitochondrial LPDs 1 and LPD2. Amino acid sequences were collected at the National Center for Biotechnology Information (NCBI) and analysed by using ClustalW and Genedoc platforms. These proteins share 92% of conserved domains. Cys residues are highlighted in green.

Table S1. List of mitochondrial redox proteins. * Despite evidence demonstrating that AtTRX *h2* is locate in both the cytosol and mitochondria in *Populus trichocarpa* [S13], and onion epidermal cell assays[S1], there is no other evidence that corroborate this result. In addition, TRX *h2* has not been found in a recent large-scale proteomic study [S2]. For further putative mitochondrial TRX redox-regulated proteins, please see [S2].

Arabidopsis gene ID	Abbreviation	Protein name	Location	References
AT5G39950	TRX *h2**	Thioredoxin *h2*	Cyt/Mitoc	(Meng, L. *et al.*, 2010; Traverso *et al.*, 2013)
AT2G35010	TRX *o1*	Thioredoxin *o1*	Mitoc	(Laloi *et al.*, 2001) (Finkemeier *et al.*, 2020)
AT1G31020	TRX *o2*	Thioredoxin *o2*	Mitoc	(Finkemeier *et al.*, 2020)
AT2G17420	NTRA	NADPH-dependent thioredoxin reductase A	Cyt/mitoc	(Reichheld *et al.*, 2007)
AT4G35460	NTRB	NADPH-dependent thioredoxin Reductase rB	Cyt/mitoc	(Reichheld *et al.*, 2007)
AT3G06050	PRX II F	Peroxiredoxin-2F	Mitoc	(Finkemeier *et al.*, 2005)
AT2G31570	GPX 2	Glutathione peroxidase 2	Cyt/ Chlorop	(Demircan, Cucun e Uzilday, 2020)(Mittler *et al.*, 2004)
AT2G43350	GPX 3	Glutathione peroxidase 3	Mitoc/Chlorop	(Demircan, Cucun e Uzilday,

AT4G11600	GPX 6	Glutathione peroxidase 6	Mitoc/Chlorop	2020)(Ozyigit *et al.*, 2016) (Demircan, Cucun e Uzilday, 2020)(Ozyigit *et al.*, 2016)
AT3G54660	GR2	Glutathione reductase 2	Mitoc/Chlorop	(Chew, Whelan e Millar, 2003)
AT3G15660	GRXs 15	Glutaredoxin	Mitoc	(Finkemeier *et al.*, 2020) (Moseler *et al.*, 2015)
AT1G31170	SRX	Sulfiredoxin	Mitoc/Chlorop	(Hyun *et al.*, 2005)
AT5G42150	mPGES-2	Microsomal prostaglandin E synthase type 2	Mitoc	(Finkemeier *et al.*, 2020)
AT3G10920.1	MnSOD(MDS1)	Manganese superoxide dismutase	Mitoc	(Finkemeier *et al.*, 2020)

Table S2. Putative thioredoxin (TRX)-mediated redox regulated enzymes related to photorespiration and associated pathways. The amino acid sequences from *Arabidopsis thaliana* L. were collected at the National Center for Biotechnology Information (NCBI) and the prediction of the disulfide bond formation was obtained using DiANNA web server program. We used the sequence of the major isoforms of each enzyme. Abbreviation: TCA cycle, tricarboxylic acid cycle.

Enzymes	**Tair**	**Disulfide bridge prediction**	**Score**	**Regulate via TRX *in vitro* or *in vivo***	
Photorespiration					
Glycine decarboxylase H	AT2G35370	33-47//43-70//45-57//45-70	0.995//0.998//0.995		
Glycine decarboxylase L (mtLPD1)	AT1G48030	71 – 483// 82 – 483	All above 0,98	TRX *o1* TRX *h2*	TRX *o1* TRX *h2*
Glycine decarboxylase P1	AT4G33010	98 - 245//228 - 280//253 - 463//402 - 777//569 - 768	All above 0.99		
Glycine decarboxylase P2	AT2G26080	103 - 251//234 - 286//259 - 670//408 - 783//575 - 774	All above 0.99		
Glycine decarboxylase T	AT1G11860	221 – 276	0.991		
Serine hydroxymethyl transferase	AT4G37930	-----	Lower than 0.03		
Glycolate oxidase (GO1)	AT3G14420	---	---		
Alanine Glyoxylate Aminotransferase	AT2G13360	66-382	0.678		
Hydroxypyruvate reductase 1	AT1G68010	----	Lower than 0.02		
Phosphoglycolate phosphatase 1	AT5G36700	27-232//43-86//43-239//43-302/43-320	All above 0,97		
TCA Cycle					
Citrate synthase 5 (mtCSY5)	AT3G60100	----	Lower than 0.02		
Citrate synthase (mtCSY4)	AT2G44350	-----	Lower than 0.02	TRX *o1*	

Aconitase	AT4G35830	338-368//338-407//338-766	0.999//0.999/0.999	TRX *o1*	
NADH-isocitrate dehydrogenase IV	AT3G09810.1	275 – 371	0.667	TRX *o1* TRX *h2*	
Succinyl-CoA ligase	AT5G08300	19-220//26-236//57-178//139-169	Higher than 0,7	TRX *o1*	
Succinate dehydrogenase	AT1G08480	179 - 261//261 – 433	0.997	TRX *o1* TRX *h2*	TRX *o1*
Cytosolic Fumarase (FUM 2)	AT5G50950	252-339//309-339//309-422//309-468	All above 0,95	TRX *o1* TRX *h2*	TRX *o1*
Mitochondrial Fumarase (FUM 1)	AT2G47510	302-415//302-461	Above 0,98		
Mitochondrial malate dehydrogenase	AT1G53240	----	Lower than 0.02		
Nitrogen metabolism					
Glutamine 2-oxoglutarete aminotransferase (NADH) GLT	AT5G53460.	132-168//132-1490//282-479	0.987//0986//0.988	PsTRX *m*	
Glutamate synthase 1 (GLU1)	AT5G04140	132-165//158-162//158-302//282-998//1400-1490	Higher than 0,97		
Glutamate synthase 2 (GLU2)	AT2G41220	255-455// 455-839//455-1510//759-785	Higher than 0,97		
Glutamate dehydrogenase α	AT5G18170	39-282//107-282	Higher than 0,97		
Glutamate dehydrogenases β	AT5G07440	107-282//107-288	Higher than 0,97		
Glutamine syntheses 2	AT5G35630	11-306// 150-306	Higher than 0,97		
Others					
mtLPD2	AT3G17240	71-82//82-483	0,99		
Cytosolic malate dehydrogenase	AT1G04410	----	Lower than 0.02	TRX *h1*	

Alternative oxidase	AT3G22370	----	Lower than 0.02	PtTRX*m* OsTRX *h* TRX *o1*	TRX *o1*
plLPD1	AT3G16950	----	Lower than 0.02		
plLPD2	AT4G16155	22-37// 22-55// 22-127// 37-127// 45-122// 55-122	Above 0.99		

5 CHAPTER 2: THE NADPH-DEPENDENT THIOREDOXIN REDUCTASE SYSTEM IS AN IMPORTANT HUB FOR THE REGULATION OF BOTH PRIMARY AND REDOX METABOLISMS, BUT IS NOT ESSENTIAL FOR ARABIDOPSIS DEVELOPMENT

Article *under review* in the *Plant, Cell and Environment* journal.

Paulo V.L. Souza[1], Liang-Yu Hou[2], Louis Poeker[2], Martin Lehman[2], Humaira Bahadar[1], Adilson P. Domingues-Junior[3], Avilien Dard[4], Laetitia Bariat[4], Jean-Philippe Reichheld[4], Joaquim Albenisio G. Silveira[1], Alisdair R. Fernie[3], Stefan Timm[5], Peter Geigenberger[2**], Danilo M. Daloso[1**]

[1] LabPlant, Departamento de Bioquímica e Biologia Molecular, Universidade Federal do Ceará, Fortaleza 60451-970, Brazil

[2] Ludwig-Maximilians-University Munich, Faculty of Biology, 82152 Planegg-Martinsried, Germany.

[3] Max Planck Institute of Molecular Plant Physiology, Am Mühlenberg 1, D-14476 Golm, Germany

[4] Laboratoire Génome et Développement des Plantes, Unité Mixte de Recherche 5096, Centre National de la Recherche Scientifique, Université de Perpignan Via Domitia, Perpignan, France

[5] University of Rostock, Plant Physiology Department, Albert-Einstein-Straße 3, D-18059 Rostock, Germany

****Correspondence to:** daloso@ufc.com and geigenberger@bio.lmu.de

Running head: Characterization of plants lacking NTR proteins

Abstract

Plants contain three NADPH-thioredoxin reductases (NTR) located in the cytosol/mitochondria (NTRA/B) and the plastid (NTRC) with important metabolic functions. However, mutants deficient in all NTRs remained to be characterized. Here, we generated and characterized the triple Arabidopsis *ntrabc* mutant alongside with *ntrc* and *ntrab* mutants. Similar to the *ntrc* mutant, plants lacking all NTRs showed reduced growth and substantial metabolic alterations. However, *ntrabc* showed higher effective quantum yield of PSII under both continuous and fluctuating light conditions, suggesting a functional interaction between chloroplastic and extra-chloroplastic NTRs in photosynthesis regulation. The redox states of ASC/DHA in the light and glutathione (GSH/GSSG) in the night were altered in *ntrabc* plants. The activities of antioxidant enzymes were strongly reduced in all mutants, especially at night, which led to an over-accumulation of H_2O_2 in this time-period. Although the triple *ntrabc* mutant revealed reduced plant growth, it could complete its full development, indicating that the NTR system is not essential for full Arabidopsis development.

Key words: Metabolic regulation, H_2O_2, redox metabolism, NADPH thioredoxin reductase

Introduction

Plants have an unprecedented redox system that allow these organisms to rapidly respond to changes in environmental cues (Geigenberger, Thormählen, Daloso, Danilo M, *et al.*, 2017). Light absorption rapidly alters the redox state of the chloroplasts by increasing the level of redox active molecules such as NAD(P)H, reduced ferredoxin (Fdx) and H_2O_2 (Elsässer *et al.*, 2020; Ugalde *et al.*, 2021). H_2O_2 is a powerful oxidant, acting as an important regulator of plant metabolism by modulating gene expression and altering enzyme activity through the oxidation of Cys residues in redox-sensitive proteins (Foyer *et al.*, 2020). This process is counter-balanced by thioredoxins (TRXs), ubiquitous proteins involved in redox regulation of plant metabolism by modulating Cys thiol–disulphide exchange in target proteins (Fonseca-Pereira, da *et al.*, 2021). Plant redox metabolism is thus orchestrated by redox reactions, which aid plants to rapidly respond to changes in environmental signals (Meyer *et al.*, 2021b).

TRXs have two redox-active conserved Cys residues, in which thiol moieties are modified according to the redox state of the cell (Buchanan, 2016a). Plant TRXs depend on reducing power derived from TRX reductases, which use either photosynthetically Fdx or NADPH as electron donors, according to the subcellular location (Meyer *et al.*, 2009). In the chloroplasts, Fdx and NADPH are respectively used by Fdx-dependent TRX reductases (FTRs) and the NADPH-dependent TRX reductase C (NTRC), which also harbour a TRX domain in its structure (Evans, Buchanan e Arnon, 1966; Serrato *et al.*, 2004). Although NTRC and FTRs comprise distinct pathways, they act cooperatively regulating chloroplastic metabolism by activating different TRX isoforms present in this organelle (Thormählen *et al.*, 2015b; Yoshida e Hisabori, 2016a). Plants further possess two other NTRs, namely NTRA and NTRB, which are the major TRX reductases outside of the plastids (Laloi *et al.*, 2001; Reichheld *et al.*, 2007, 2005). Therefore, NTR proteins are key for the reduction of several TRX isoforms found in different subcellular compartments. In turn, reduced (active) TRXs can (de)activate several redox-regulated enzymes in the cell, some of which are related to important physiological process such as photosynthesis, starch synthesis and (photo)respiration (Cejudo, González e Pérez-Ruiz, 2021; Martí, Jiménez e Sevilla, 2020).

Compared to animal cells, plants have a higher number of different TRX and TRX reductase isoforms, residing in different subcellular compartments (Foyer e Noctor, 2020). Whilst only one TRX reductase is found in mammalian mitochondria, plants possess two NTR proteins (NTRA and

NTRB) in this organelle, as result of a genetic duplication (Blanc *et al.*, 2000; Reichheld *et al.*, 2005). This leads to a higher robustness of the plant redox network compared to animal cells. For instance, whilst the knockout of the mitochondrial TRX reductase is lethal for mammalian cells (Conrad, Jakupoglu, C, *et al.*, 2004), Arabidopsis plants lacking either NTRC or both NTRA and NTRB are smaller than WT plants, but still viable (Daloso, Danilo M *et al.*, 2015; Reichheld *et al.*, 2007). The reduced growth of the *ntrc* mutant has been associated to its lower photosynthetic capacity and impairments in carbohydrate metabolism, especially under fluctuating light conditions (Serrato *et al.*, 2004; Thormählen *et al.*, 2017). Furthermore, NTRC has an important role in the regulation of 2-Cys peroxiredoxins (PRXs), an important component of the reactive oxygen species (ROS) scavenger system (Ojeda, Pérez-Ruiz e Cejudo, 2018; Pérez-Ruiz *et al.*, 2017). Thus, the reduced growth of *ntrc* plants may be also related to a disturbed ROS metabolism, which may have consequences for several non-plastidial metabolic pathways (Sousa *et al.*, 2019). On the other hand, the restricted growth of the double *ntrab* mutant may be associated to the alterations observed in the carbon metabolism within the cytosol and mitochondria (Daloso, Danilo M *et al.*, 2015).

Previous protein-protein interaction analysis has shown that NTRC interacts with proteins involved in sulphur and nitrogen assimilation, photorespiration and protein synthesis (González *et al.*, 2019), providing evidence that the physiological role of NTRC may be wider than currently known. Furthermore, it has been shown that glutathione can reduce plant TRXs *in vitro* and that NTRA/NTRB and glutathione reductase (GR) act in cooperation (Marty, Bausewein, Müller, Bangash, Moseler, Schwarzländer, Müller-Schüssele, *et al.*, 2019; Marty, L. *et al.*, 2009; Reichheld *et al.*, 2007, 2005). These results indicate that the plant NTR/TRX system is highly connected to other redox players, including glutathione and ascorbate metabolisms (Calderón *et al.*, 2018b). In fact, co-expression and protein-protein interaction network analyses demonstrated that the different components of the chloroplast redox network are highly connected with each other (Souza *et al.*, 2019a). However, it remains unclear whether the deficiency of NTRA and NTRB has additional consequences for the *ntrc* mutant, and *vice versa*, and whether the complete lack of the entire NTR system is severely affecting plant growth, development and viability.

As the whole plant metabolism and, in special, redox reactions operate in a highly integrated and dynamic manner in response to endogenous and environmental changes, it is crucial to understand the interactions that occur between the three plant NTR isoforms. Considering this, we have obtained a triple NTR mutant (*ntrabc*) by crossing the *ntrc* single mutant with the double

ntrab mutant in Arabidopsis. We characterized these plants alongside with wild type (WT), *ntrc* and *ntrab* mutants by analysing the regulation of growth, photosynthesis and both primary and redox metabolisms under different environmental conditions. Our metabolite profiles results indicate the NTR fundamental role to maintained of redox homeostasis of the metabolism during the day and night. Furthermore, although NTRs, alone or in combination, are crucial to maintain normal growth rates under constant or fluctuating light conditions, our data highlights that NTR isoforms display complementary and redundant functions to allow metabolic acclimation to environmental changes, while they are not essential for full plant development.

Material and methods

Plant material and growth conditions

Seeds from *Arabidopsis thaliana* (Arabidopsis) L. Columbia (Col-0) and T-DNA insertional mutants *ntrc* (SALK_012208) and *ntrab* (NTRA SALK_539152, NTRB SALK_545978) were obtained from SALK collection (http://signal.salk.edu/) and characterized previously (Daloso, Danilo M *et al.*, 2015; Reichheld *et al.*, 2007; Serrato *et al.*, 2004; Thormählen *et al.*, 2015b). The triple *ntrabc* mutant was obtained by crossing the single *ntrc* with *ntrab*. Seeds were germinated as described previously (Fonseca-Pereira, da *et al.*, 2020) and sown in soil containing sand, vermiculite, and organic substrate Topstrato® (1:1:1). Plants were grown under 120 μmol photons m^{-2} s^{-1} and different photoperiods (8:16 or 12:12 h light:dark).

Growth analysis

Plants were harvested to determine plant size (cm^2) and fresh and dry weights (mg). The size of entire rosettes was measured using the software Photoshop (Adobe Photoshop®). Prior to the measurement of dry weight, the entire rosette was dried out in an oven (60°C) for 48 h.

Protein extraction and immunoblots

Arabidopsis protein extracts were prepared by grinding approximately 150 mg of fresh weight leaf material in liquid nitrogen and resuspended in extraction buffer (25 mM Tris HCl, pH

7.6, 75 mM NaCl, 1 mM DTT, 1 mM phenylmethylsulfonyl fluoride, and 0.1% Nonidet P-40). After centrifugation (15 min, 13,000 rpm, 4°C), protein concentrations from the supernatant were determined using the Protein Assay kit (Bio-Rad). Proteins were separated by SDS-PAGE and transferred to Immobilon-P membranes (Amersham Pharmacia). Rabbit polyclonal antibodies against NTRB (Reichheld *et al.*, 2007) and NTRC (Serrato *et al.*, 2004) were diluted 1:10,000 for protein gel blotting. Goat anti-rabbit antibodies conjugated to horseradish peroxidase (Amersham Pharmacia) were used as secondary antibodies and revealed with enhanced chemiluminescence reagents (Amersham Pharmacia).

Pulse-amplitude-modulation (PAM) measurements of chlorophyll *a* fluorescence

Plants were dark-acclimated for 30 min and then transferred into an image PAM (MAXI version, WALZ) instrument. Plants were treated with 150 µmol photons $m^{-2}s^{-1}$ for 20 min followed by darkness for 10 min. For the measurement under FL, plants were treated with 4 min low light followed by 4 cycles of FL comprising 1 min high light phases (500 µmol photons $m^{-2}s^{-1}$) and 6 min low light phases (50 µmol photons $m^{-2}s^{-1}$), and then the dark for another 5 min. The emission of florescence was documented by the image PAM and used to estimate the effective quantum yield of photosystem II [Y(II)], non-photochemical quenching (NPQ) and the reduction of plastoquinone pool (1-qL), as described earlier (Thormählen *et al.*, 2017).

GC-TOF-MS-based metabolite profiling analysis

Polar metabolites were extracted from leaves harvested at end of the day (ED) and end of the night (EN) and derivatized following a well-established gas chromatography- *time of flight* -mass spectrometry (GC-TOF-MS) platform (Lisec *et al.*, 2006). Metabolites were identified using the TagFinder 4.1 software and the Golm Metabolome Database (Kopka *et al.*, 2005; Luedemann *et al.*, 2008). The data presented corresponds to the intensity of specific fragments of the metabolites normalized by the fresh weight (g) used for metabolite extraction and the intensity of the internal standard (ribitol/^{13}C-Sorbitol) added during the extraction (Lisec *et al.*, 2006).

Determination of reduced and oxidized glutathione and ascorbate contents

The contents of oxidized (DHA), reduced (ASC) and total ascorbate (DHA + ASC) was determined as described previously (Kampfenkel, Montagu, Van e Inzé, 1995). In brief, leaves harvested at ED and EN were ground to a powder using liquid nitrogen. The method is based on the reduction of Fe^{+3} into Fe^{+2} by ASC and spectrophotometric detection of the Fe^{+2} complex bound to 2,2'-pirydine, being monitored by decrease of the ASC absorbance at 525 nm. Both ASC and DHA forms were expressed as μmol mg^{-1} fresh weight (FW) calculated from ASC standard curve. GSH was measured by the GSH reductase (GR)-dependent reduction of 5,5′-dithiol-bis (2-nitrobenzoic acid), DTNB with some adaptation (Griffith, 1980). In brief, the total glutathione (GSH +GSSG) was determined through the reaction dependent of 1 U of Glutathione Reductase (GR), 0.15 mM of NADPH, reaction buffer 100 mM -sodium phosphate buffer (pH = 7.0)- , and 6 mM DTNB. GSH was measured using 0.15 mM of NADPH, reaction buffer 100 mM -sodium phosphate buffer (pH = 7.0)- , and 6 mM DTNB, while GSSG was calculated by -Total Glutathione (GSH + GSSG) – GSH = GSSG. The content of GSH and GSSG was expressed as μmol g^{-1} FW and calculated using a standard curve of GSH. In addition, the ascorbate and glutathione redox states were calculated by ASA or DHA / ASA + DHA * 100 and GSH or GSSG / GSH + GSSG *100, both results expressed in percentage

Determination of superoxide dismutase, catalase and ascorbate peroxidase activities

Total proteins were extracted by adding 1 ml of potassium phosphate buffer (100 mM; pH 7.0) containing EDTA (final concentration of 1 mM) in tubes containing powder of frozen leaves. The homogenate was centrifuged at 15,000 *g* at 4°C for 15 min, and the resulting supernatant was used for the determination of all enzymatic activities. The total content of soluble proteins was measured according to Bradford (Bradford, 1976). All enzymatic activities were determined spectrophotometrically. Superoxide dismutase activity (SOD) was determined based on the inhibition of tetrazolium chloride (NBT) nitro blue chloride photoreduction (Giannopolitis e Ries, 1977). The unit of SOD activity (U) was defined as the amount of enzyme needed to inhibit 50% of NBT photoreduction, expressed as U mg^{-1} FW min^{-1}. Catalase activity (CAT) was measured by reduction of H_2O_2 (BEERS e SIZER, 1952; Havir e McHale, 1987). CAT activity was calculated using the molar extinction coefficient of H_2O_2 (40 mM cm^{-1}) and expressed as mmol H_2O_2 mg^{-1} FW min^{-1}. The activity of ascorbate peroxidase (APX) was measured based on the oxidation of

ASC, in a reaction mixture containing 0.45 mM of ASC, 3 mM of H_2O_2, and 50 µl of the protein extract, all diluted in a buffer of potassium phosphate 100 mM (pH 7.0) containing 1 mM EDTA in a final volume of 1.5 ml (Nakano e Asada, 1981). APX activity was expressed in µmol ASC mg^{-1} FW min^{-1}.

Detection of hydrogen peroxide

The H_2O_2 content was quantified using the Red Hydrogen Peroxide / Peroxidase Amplex Assay kit (Life Technologies, Carlsbad, CA, United States) according to the manufacture's protocols. In brief, 100 µl of protein extract was mixed with 100 µl of the Amplex red solution (Amplex-red 0.2 M +HRP 0.2 U + potassium phosphate buffer 100 mM; pH 7.5). The absorbance was measured at 560 nm to quantify the H_2O_2 concentration (Zhou *et al.*, 1997). The results were expressed as nmol H_2O_2 mg^{-1} FW.

Statistical analysis

All measurements were performed with at least four biological replicates. All graphs were generated using GraphPad Prism 9. Heat maps were created using the MeV 4.9.0 software. The genotypes were compared by analysis of variance (ANOVA) followed by Tukey's test or by Student's *t* test ($P < 0.05$). Metabolomics data was analysed by hierarchical clustering analysis (HCA) and principal component analysis (PCA) using either MeV 4.9.0 software or the Metaboanalyst platform. Pearson correlation analysis was also carried out using the Metaboanalyst platform (Pang *et al.*, 2021).

Results

Plant growth is severely impaired in plants lacking the complete set of NTR proteins

We obtained an Arabidopsis mutant lacking all three NTR isoforms (*ntrabc*) through crossing of the single *ntrc* and the double *ntrab* mutant. The deletion of NTR proteins in the *ntrabc* line was confirmed by immunoblotting using antibodies against NTRC and NTRA+B (Figure 6a). The triple *ntrabc* mutant displayed a similar pale-green phenotype as *ntrc* lines if grown under either, medium light (ML) (150 µmol m^{-2} s^{-1}; 12 h day/12 h night) or fluctuating light (FL) (50

μmol m^{-2} s^{-1} for 5 min; 550 μmol m^{-2} s^{-1} for 1 min; 12 h day/12 h night) conditions, respectively (Figure 2a). Furthermore, *ntrabc* plants - similar to *ntrc* - showed reduced plant growth when compared to WT and *ntrab*, as indicated by lower fresh weight (FW), dry weight (DW) and plant size under ML and FL (Figure 7). However, no statistical difference between *ntrc* and *ntrabc* mutants was observed (Figure 7b). Interestingly, although *ntrabc* plants have reduced plant growth, they could complete their life cycle, from vegetative to reproductive stages (Figure 6b). These results collectively indicate that the lack of NTRA and NTRB do not exacerbate the growth restriction caused by the absence of NTRC and highlight that NTR proteins are not essential for full Arabidopsis development.

Impaired photosynthetic capacity in the single *ntrc* mutant is attenuated in the *ntrabc* triple mutant

Plants lacking *ntrc* have reduced photosynthetic capacity (Thormählen *et al.*, 2015b). We therefore investigated whether the additional lack of both NTRA and B causes additional photosynthetic impairment in *ntrabc* plants. During dark-light transitions, both *ntrc* and *ntrabc* were found to have reduced effective quantum yield of PSII (Y(II)) and elevated levels in the reduction of plastoquinone pool (1-qL) and in non-photochemical quenching (NPQ), when compared to WT and *ntrab* (Figures 7c-e). However, during the first 10 min of the transition, Y(II) was surprisingly higher and NPQ lower in *ntrabc* compared to *ntrc* plants (Figures 7c-d). The differences between *ntrabc* and *ntrc* mutants with respect to these photosynthetic parameters were enhanced when plants were analysed in alternating low light (LL) and high light (HL) phases in FL, compared to continuous light (Figure 8). Under these conditions, the photosynthetic levels in the *ntrabc* triple mutant ranged between those of WT and *ntrc* single mutant (Figures 8a-c). These results indicate that during transient changes in light intensity, the photosynthetic phenotype of the *ntrabc* triple mutant is less severe, compared to the *ntrc* single mutant.

Leaf primary metabolism is substantially altered in the *ntrabc* triple mutant with the extent being dependent on the light conditions

We next investigated the consequences of NTRs absence on primary metabolism by analysing the metabolite profiles in leaf samples harvested at the end of the day (ED) and end of the night (EN) using GC-TOF-MS. The metabolite profile of *ntrabc* plants was largely comparable to *ntrc* at ED. Twenty out of forty-five metabolites identified were significantly different in both *ntrc* and *ntrabc*, if compared to WT at ED. This statement is in line with both hierarchical clustering analysis (HCA) (Figure 9a) and principal component analysis (PCA), in which a clear separation of both *ntrc* and *ntrabc* plants from WT and *ntrab* was observed by the PC1 (Figure 9b). On the other hand, nineteen metabolites were significantly different in both *ntrab* and *ntrabc* at EN, if compared to WT (Figure 9a). However, HCA demonstrated that *ntrabc* is more similar to *ntrc* than *ntrab* and the PCA showed no clear separation among the genotypes at EN (Figures 9a,c). Among the metabolites altered in *ntrabc* leaves, considerable differences were found in the abundances of carbohydrates.

The absence of NTRs strongly reduce the activity of antioxidant enzymes, leading to H_2O_2 over-accumulation at night

NTRC is an important hub for the redox metabolism (López-Grueso *et al.*, 2019; Souza *et al.*, 2019a), we next investigated whether H_2O_2 content and the activity of antioxidant enzymes were altered in *ntr* mutants. Interestingly, our results showed that the major alterations were observed at EN, and, to a lesser extent, at ED. The H_2O_2 content and the activity of superoxide dismutase (SOD) was unaltered in *ntrabc* plants at ED, when compared to WT plants (Figures 10a-b). However, all mutants showed lower activity of both ascorbate peroxidase (APX) and catalase (CAT), when compared to WT plants at ED (Figures 10c-d). In contrast, the content of H_2O_2 was higher, while the activity of SOD, APX and CAT was lower in all mutants at EN, if compared to WT (Figures 10e-h). These results collectively indicate that the knockout of NTRs directly affects ROS metabolism, in which reduced activity of ROS-scavenging enzymes leads to an over-accumulation of H_2O_2 at EN.

The relative levels of GSH and GSSG are altered in *ntrabc* plants at night

To further enhance our understanding about the role of NTRs for the regulation of redox metabolism, we quantified the concentrations of ascorbate (ASC), dehydroascorbate (DHA) and oxidized (GSSG) and reduced (GSH) glutathione in leaf samples harvested at ED and EN. No changes in the concentration of ASC or DHA between *ntrabc* and the WT were observed in either ED or EN, although significant changes in these molecules were present in *ntrc* and *ntrab* at EN. At ED, *ntrc* plants showed lower ASC and higher DHA than WT (Figures 11a-f), leading to a decrease in the ASC percentage of the total ASC pool (Figure 12). No major changes in GSH and GSSG between *ntrabc* and the WT was found, with the exception of GSSG which was 6.5-fold higher in *ntrabc* than WT at EN (Figures 11g-h). By analysing the percentage of oxidized DHA and GSSG related to their reduced forms (ASC and GSH), the unique differences between WT and *ntrabc* plants was the percentage of GSH and GSSG found at EN, in which *ntrabc* have higher GSSG and lower GSH compared to the control (Figure 11). By contrast, all parameters were different between *ntrc* and the WT, while *ntrab* showed much lower and higher % of ASC and DHA than the WT at EN (Figure 12).

Interestingly, whilst the level of H_2O_2 was not correlated with redox-related parameters at ED, H_2O_2 was negatively correlated with the activity of CAT and APX at ED and positively correlated with the concentration of GSSG at EN (Figure 13a-b). Furthermore, PCA using H_2O_2 and antioxidant-related parameters revealed a clear separation of the different genotypes at ED (specifically between *ntrc* and *ntrabc*), while that the major differences between WT and the mutants was present at EN (Figures 13c-d). Collectively, these results highlight that NTR proteins are key for the regulation of redox metabolism and to maintain the homeostasis of plant cells, especially in the night.

Discussion

Redox reactions mediated by thioredoxins and thioredoxin reductases are fundamental properties of living cells (Biddau *et al.*, 2018; Cheng *et al.*, 2017; Jakupoglu *et al.*, 2005; Muri *et al.*, 2018). For instance, the absence of NADPH-dependent thioredoxin reductase is lethal for mammalian cells (Conrad, Jakupoglu, C, *et al.*, 2004). In contrast to this, neither the lack of the plastidial NADPH-dependent thioredoxin reductase C (NTRC) nor the lack of both non-plastidial NTRA and NTRB is lethal for plant cells. The enhanced robustness of the plant redox network may

be associated to their higher number of redundant and compensatory redox players, compared to other organisms. However, it is still not completely understood how the plant NTR system is associated to other redox components, such as the metabolism of ROS, NAD(P)(H), ascorbate and glutathione. This is partially due to the lack of information from plants missing the complete set of NTRs. Here, we characterized the triple *ntrabc* mutant to obtain better insights into the role of NTRs for the regulation of photosynthesis, metabolism and plant growth in different environments as well as to investigate how the lack of all NTRs affects plant redox metabolism.

NTR proteins are highly important for photosynthesis and plant growth, but not essential for full Arabidopsis development

We generated an Arabidopsis mutant lacking all NTR isoforms through crossing *ntrab* and *ntrc* mutants. Western blot analysis demonstrated that *ntrabc* plants showed no detectable signals for the NTRA, NTRB and NTRC proteins, indicating a complete knockout in these proteins (Figure 6a). It was previously shown that the *ntrab* and especially the *ntrc* mutant have reduced plant growth, compared to WT (Daloso, Danilo M *et al.*, 2015; Ojeda *et al.*, 2017; Reichheld *et al.*, 2007; Thormählen *et al.*, 2015b). We hypothesized that the additional absence of NTRA and NTRB would cause a more severe growth restriction in the *ntrc* background. The results showed that the *ntrabc* triple mutant have the same pale green phenotype (Figure 7a) and higher Y(II) and lower NPQ than *ntrc* single mutant during dark-light transitions and fluctuating light intensities (Figures 7c-d, 8a-b), indicating increased rather than a decreased photosynthetic performance. Thus, contrary to the expected, the additional lack of NTRA and B did not aggravate photosynthetic and growth impairments caused by NTRC knockout. These results are in line with previous studies showing that extra-plastidial components of the NTR/TRX system (i.e. NTRA, NTRB, TRX *o1* and TRX *h2*) affect photosynthetic efficiency of Arabidopsis plants (Hou, Lehmann e Geigenberger, 2021; Reinholdt, Schwab, Zhang, Reichheld, J., *et al.*, 2019) in different environmental conditions, including drought (Fonseca-Pereira, Da *et al.*, 2019). Although the mechanisms by which extra-chloroplastic redox players regulate photosynthetic efficiency are unclear, it has been shown that glycine decarboxylase (GDC) is deactivated by TRX *o1* and TRX *h2 in vitro* (Fonseca-Pereira, da *et al.*, 2020; Reinholdt, Schwab, Zhang, Reichheld, J., *et al.*, 2019), suggesting that the increased photosynthetic efficiency of the double *trxo1 trxh2* mutant, and

probably the triple *ntrabc* mutant, could be associated to higher photorespiratory fluxes on a short-term (Hou, Lehmann e Geigenberger, 2021), which, in turn, would favour the photosynthetic process during dark-to-light transition and under FL condition (Bourguignon, Neuburger e Douce, 1988; Timm *et al.*, 2012, 2015). It is noteworthy that such operation might be a short-term effect, only occurring when plants experience a dark-to-light transition or undergo fluctuation in light intensity.

Despite their reduced growth, *ntrabc* plants were able to complete their life cycle and produce fertile seeds (Figure 6b). This demonstrates that NTR proteins are not essential for full plant development. This is probably due to the complexity of the plant redox network, in which other redundant or compensatory mechanisms overcome, at least to some extent, the complete absence of an important component of the cellular redox system. The absence of NTRC and NTRA/B is likely, at least to some extent, safeguarded by FTRs and GRs, respectively (Marty, Bausewein, Müller, Bangash, Moseler, Schwarzländer, Müller-Schüssele, *et al.*, 2019; Marty, L. *et al.*, 2009; Reichheld *et al.*, 2007; Yoshida e Hisabori, 2016a). Furthermore, NTRC is a major hub of the plastidial redox network, being directly or indirectly connected to proteins from different redox systems, such as GPX1, tAPX, FTR, GRX, 2-Cys PRX and several TRXs (Souza *et al.*, 2019a). These results highlight that the presence of numerous redundant and compensatory systems is an important characteristic of plants, which was likely acquired through gene duplication, polyploidization, horizontal gene transfer and/or non-random mutations (Bowles, Bechtold e Paps, 2019; Ma *et al.*, 2022; Monroe *et al.*, 2022; Ren *et al.*, 2018).

Plant NTRs are important to maintain the homeostasis of primary metabolism

Despite the strong growth reduction of *ntrabc* plants, this triple mutant is still viable. This raises the question on which mechanisms can compensate the absence of all NTRs and if this mutant have any metabolic reprograming to establish a new redox homoeostasis. To obtain better insights into these questions, we carried out a metabolite profiling analysis in *ntrc*, *ntrab* and *ntrabc* plants harvested at the ED and EN. Interestingly, the results showed that both *ntrc* and *ntrabc* have lower level of soluble sugars (glucose and fructose) (Figure 9). Our metabolite profiling analysis further suggests that the NTR/TRX system plays an important role in redox regulation o nitrogen metabolism enzymes, since glutamine, aspartate, asparagine and glutamate levels were altered in

ntrc and *ntrabc* in ED (Figure 9). It is worth to mention that glutamine and asparagine are the main inter-compartmental transporters of nitrogen in plants, playing a fundamental role in plant development (Gaufichon, Rothstein e Suzuki, 2016; Masclaux-Daubresse *et al.*, 2010). The major pathway of glutamine synthesis is via glutamine synthetase (GS), an enzyme found in cytosol (GS1), and in chloroplast and mitochondria (GS2) (Taira *et al.*, 2004). Although some *in vitro* assays has elected GS as a potential TRX target (Balmer *et al.*, 2004; Ortega, Roche e Sengupta-Gopalan, 1999), the role of TRX for the regulation of GS and other enzymes of the nitrogen metabolism remains unclear. The decrease in glutamine levels in all mutants at ED and in *ntrc* and *ntrabc* at EN is an evidence that the GS 1 or GS2 are redox regulated via the NTR/TRX system. This idea is further corroborated by alteration in the level of (photo)respiration metabolites such as glycine, glycerate, fumarate, citrate, succinate, malate and glycolate in *ntrabc*.

Glycine decarboxylase complex (GDC) is one of the main photo-respiratory enzymes in mitochondria (Reinholdt, Schwab, Zhang, Reichheld, J. P., *et al.*, 2019; Timm *et al.*, 2016). Our It has been shown that the mitochondrial lipoamide dehydrogenase (mtLPD), a subunit found in the GDC, pyruvate dehydrogenase, 2-oxuglutarate dehydrogenase and branched-chain 2-oxoacid dehydrogenase (BCKDC), is deactivated by TRX *o1* and TRX *h2 in vitro* (Fonseca-Pereira *et al.*, 2019; Reinholdt, Bauwe, *et al.*, 2019). Further evidence on the connection between the NTR/TRX system and photorespiration comes from results showing that (i) the rate of oxygen inhibition of photosynthesis was higher in the *trxo1* mutant, when compared to the WT, (ii) the Gly to Ser ratio was higher in the *trxo1* mutant than the WT when transferred from 1500 ppm to 390 ppm of CO_2 concentration, and (iii) the activation of Gly-to-Ser conversion catalysed by GDC and serine hydroxymethyltransferase (SHMT) is slowed down in *trxo1* at onset of illumination (Reinholdt, Bauwe, *et al.*, 2019; Reinholdt, Schwab, Zhang, Reichheld, J. P., *et al.*, 2019). These results collectively suggest that the NTR/TRX system plays a key role for the regulation of the nitrogen metabolism. Future studies are needed to elucidate whether the NTR/TRX system directly regulates enzymes associated to the nitrogen metabolism or if the change in the level of these compounds is due to an indirect effect caused by the lack of NTRs. The *ntrabc* mutant further demonstrated an increase in the level of several TCA cycle metabolites , which might be related to the NTR/TRX-mediated regulation of TCA cycle enzymes previously shown (Schmidtmann *et al.*, 2014). Taken together, our results suggest that the NTR system is very important for the homeostasis of primary metabolism, given that the lack of all NTRs leads to an extensive metabolic reprogramming.

The dark side of redox regulation: the lack of NTRs substantially alters redox metabolism, especially at night

Plant cells have multiple sources of H_2O_2 production and ROS scavenging systems across the cellular organelles (Smirnoff e Arnaud, 2019). We showed that *ntrc*, *ntrab* and *ntrabc* mutants have increased leaf H_2O_2 concentration at EN, while no differences among the genotypes were found at ED (Figures 5a,e). These results suggest that compensatory systems are activated in the mutants to maintain H_2O_2 homeostasis at ED, which could involve GRs, FTRs, GRXs, GPXs, 2-Cys PRXs and other components of the large plant redox system (Calderón *et al.*, 2018b; Marty, Bausewein, Müller, Bangash, Moseler, Schwarzländer, Müller-Schüssele, *et al.*, 2019; Marty, L. *et al.*, 2009; Sousa *et al.*, 2015; Yoshida e Hisabori, 2016a). Although all NTR mutants showed lower activity of APX and CAT than WT at ED, these differences were more prominent at EN (Figure 5c,d,g,h). Furthermore, the redox status of ASC/DHA and GSH/GSSG of NTR mutants was mainly altered at EN (Figure 12). The most drastic changes observed at EN explain the higher accumulation of H_2O_2 in this period, especially CAT and APX activities and the concentration of GSSG that were negatively and positively correlated with H_2O_2 concentration, respectively (Figure 13). These results highlight that NTR proteins are important to maintain redox homeostasis of the cell, especially in the night period, when the ferredoxin-dependent thioredoxin reductase is most likely inactive (Schürmann e Buchanan, 2008).

Concluding remarks

Our results demonstrate a previously unknown role of NTR proteins to be crucial for the regulation of leaf primary metabolism. While this was mainly associated to the lack of NTRC, the additional lack of NTRA and NTRB exacerbated the effects on the redox metabolism. This idea is based in the fact that the triple *ntrabc* showed more drastic changes in redox related parameters compared to WT, *ntrc* and *ntrab*, such as the activity of ROS-scavenging enzymes and the concentration of GSSG at night. Interestingly, during dark-light transitions and in fluctuating light

the *ntrabc* triple mutant displayed improved photosynthetic parameters compared to the *ntrc* single mutant, indicating functional interactions between plastidial and extra-plastidial NTR isoforms during short-term light transients. Overall, our study strengthens the idea that NTR proteins act cooperatively with other redox players, to guarantee the full development of Arabidopsis plants, while they are crucial for optimal functioning of photosynthesis and (photo)respiratory metabolism.

Figures chapter 2:

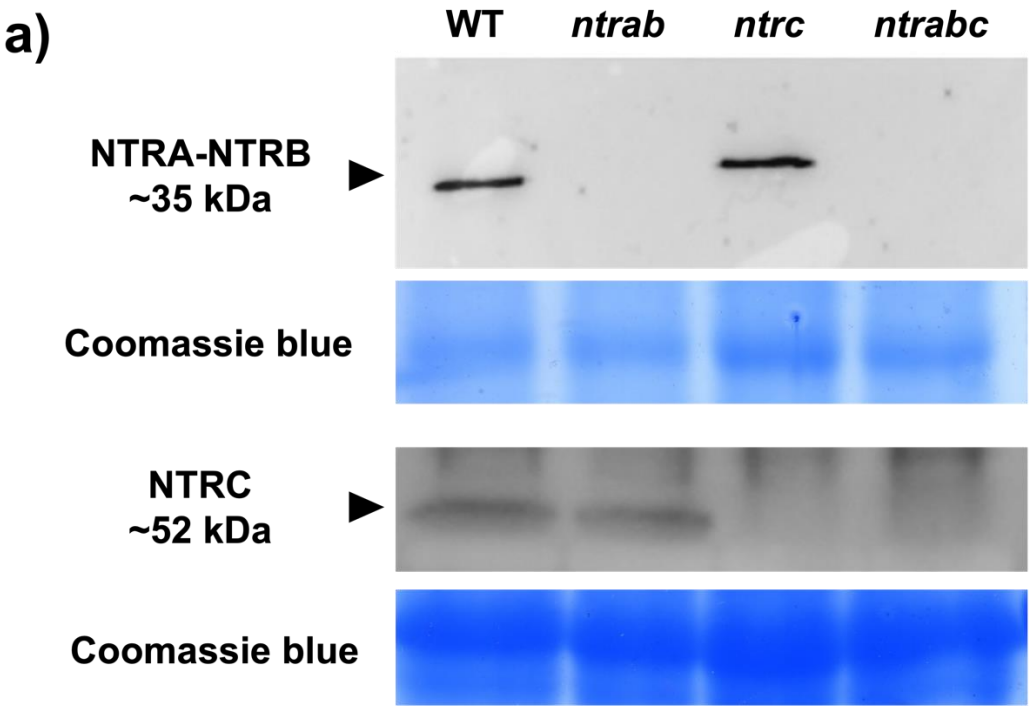

Figure 6- Immunoblot analysis and phenotype of the plants at the reproductive stage. a) Immunoblot detection of NTRC and NTRA/NTRB proteins was carried out in plant extracts of two-week-old *Arabidopsis thaliana* L. wild type (WT) and mutants lacking NTRC (*ntrc*), NTRA and NTRB (*ntrab*) or all NTRs (*ntrabc*). Proteins were separated by SDS-PAGE (10% polyacrylamide) under reducing conditions, then transferred to a nitrocellulose membrane, and incubated with NTRA/NTRB and NTRC antibodies (dilution 1:10.000), followed by incubation with secondary antibody (Sigma secondary antibody anti-rabbit, dilution 1:10,000). The blots were then revealed with enhanced chemiluminescence reagents. b) Phenotype of 49-day old WT, *ntrab*, *ntrc* and *ntrabc* plants grown under 16:8 h photoperiod, highlighting that all mutants were able to complete their life cycle, from vegetative to the reproductive stage

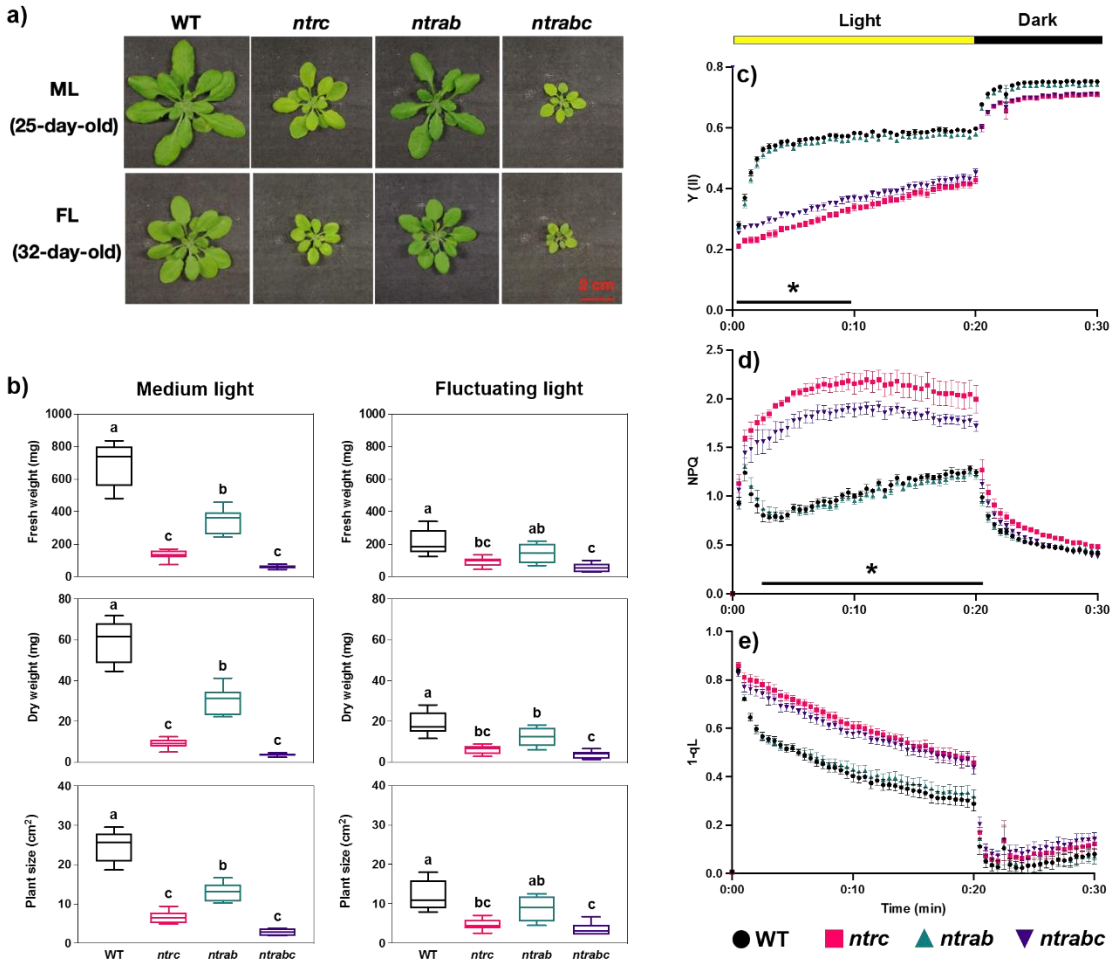

Figure 7- Growth and photosynthetic phenotype of *Arabidopsis thaliana* L. wild type (WT) and mutants lacking NTRC (*ntrc*), NTRA and NTRB (*ntrab*) or all NTRs (*ntrabc*). a) Visual aspects of 25-day-old and 32-day-old Arabidopsis rosettes grown under moderate light (ML) or fluctuating light (FL) conditions, respectively. The setup of ML corresponds to 125 µmol photons m^{-2} s^{-1} (12:12 h photoperiod), while FL represents a loop of low light (50 µmol photons m^{-2} s^{-1} for 5 min) and high light (550 µmol photons $m^{-2}s^{-1}$ for 1 min) phases with the same photoperiod as ML. b) Growth-related parameters determined in WT and NTR mutants grown under ML (left graphs) or FL (right graphs) conditions. After 25 and 35 days under ML or FL conditions, plants were harvested and the fresh weight, dry weight and plant size were determined. Black, pink, green and purple box plots represent averages and standard errors of WT, *ntrc*, *ntrab*, and *ntrabc* genotypes, respectively. Means that do not share a letter are significantly different according to ANOVA and Tukey test analysis ($P < 0.05$) (n=6 ± SE). c-e) Chlorophyll *a* fluorescence analysis. Effective quantum yield of PSII (Y(II)) (c), non-photochemical quenching (NPQ) (d) and the reduction of plastoquinone pool (1-qL) (e) were measured in WT and NTR mutants grown under 125 µmol photons m^{-2} s^{-1} (12:12 h photoperiod). Dark-adapted leaves were transferred to the image PAM instrument (MAXI version, WALZ) and subjected to constant light (150 µmol photons m^{-2} s^{-1}) for 20 min (yellow bars), followed by 10 min in the dark (black bars). The emission of chlorophyll *a* florescence was recorded by the image PAM instrument every 30 seconds and used for the calculation of Y(II), 1-

qL and NPQ. Asterisks indicate time points in which Y(II) and NPQ are statistically different between *ntrc* and *ntrabc* plants by ANOVA and Tukey test ($P < 0.05$) (n = 6).

.

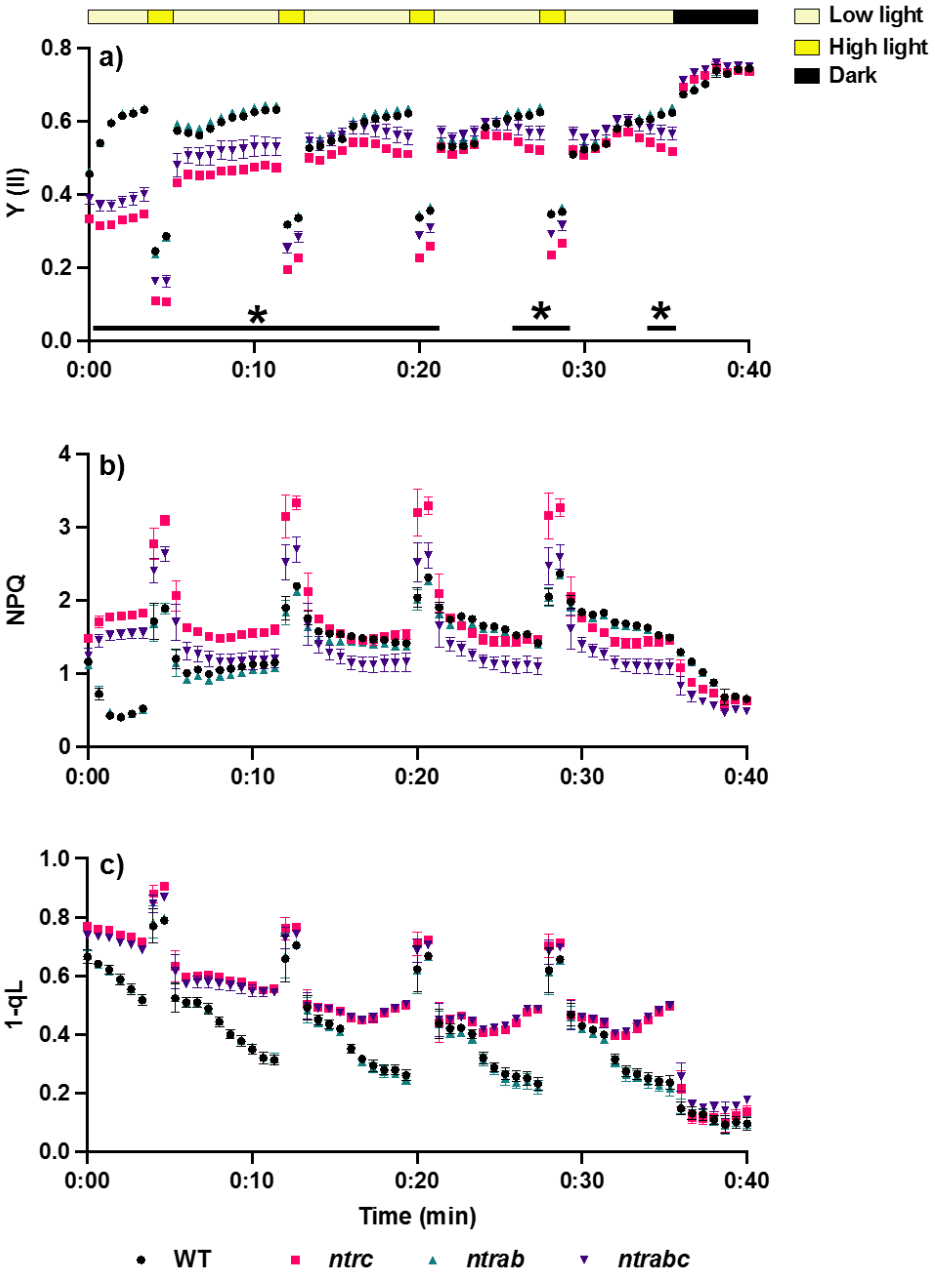

Figure 8- Chlorophyll *a* fluorescence analysis in *Arabidopsis thaliana* L. wild type (WT) and mutants lacking NTRC (*ntrc*), NTRA and NTRB (*ntrab*) or all NTRs (*ntrabc*). Effective quantum yield of PSII (Y(II)) (a), the reduction of plastoquinone pool (1-qL) (b) and non-photochemical quenching (NPQ) (c) were measured in WT and NTR mutants grown under fluctuating light regime (5 min of 50 µmol photons m^{-2} s^{-1} 1 min of 550 µmol photons $m^{-2}s^{-1}$, 12:12 h photoperiod). Dark-

adapted leaves were transferred to the image PAM instrument (MAXI version, WALZ) and subjected to low light (50 μmol photons $m^{-2}s^{-1}$) followed by 4 cycles of FL comprising 1 min high light (500 μmol photons $m^{-2}s^{-1}$) and 6 min low light (50 μmol photons $m^{-2}s^{-1}$), and then the dark for another 5 min. The emission of chlorophyll *a* florescence was recorded by the image PAM instrument every 30 seconds and used for the calculation of Y(II), 1-qL and NPQ. Asterisks indicate time points in which Y(II) and NPQ are statistically different between *ntrc* and *ntrabc* plants by ANOVA and Tukey test ($P < 0.05$) (n = 6).

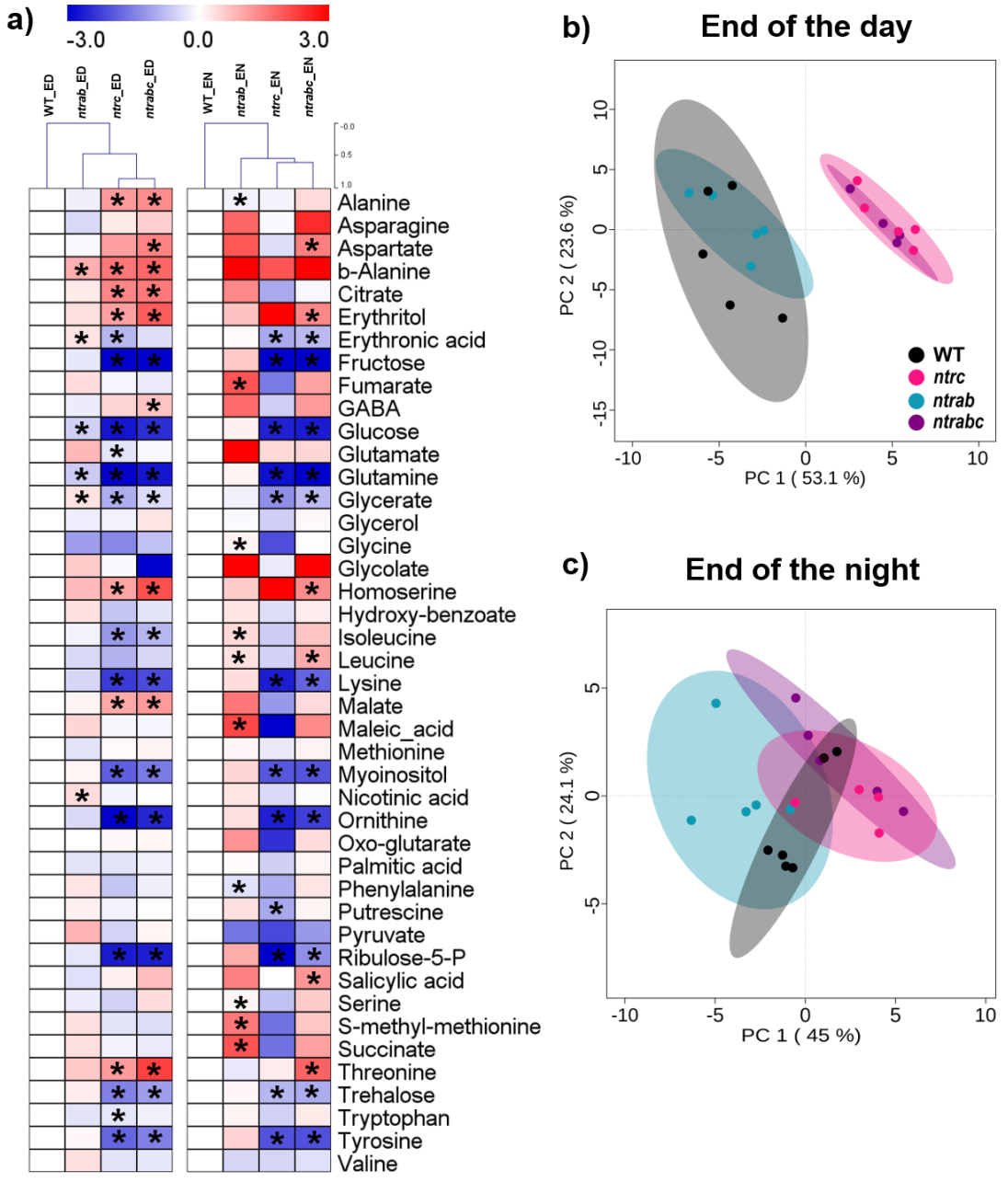

Figure 9- Changes in the metabolite profiling of *Arabidopsis thaliana* L. wild type (WT) and mutants lacking NTRC (*ntrc*), NTRA and NTRB (*ntrab*) or all NTRs (*ntrabc*). a) Heat map representation of the changes in the relative abundance of primary metabolites identified by gas chromatography mass spectrometry (GC-MS) in leaf samples harvested at the end of the day (ED) and the end of the night (EN) of short-day (125 µmol photons m^{-2} s^{-1}; 08:16 h photoperiod) grown plants. The average values of the relative abundance (normalized to Ribitol and fresh weight) were normalized according to the WT values found at ED and EN and log_2 transformed (n = 4). Asterisks (*) indicate values that are significantly different from the WT by the Student's t-test ($P < 0.05$). b-

c) Principal component analysis (PCA) carried out using GC-MS-based metabolite profiling data of WT, *ntrc*, *ntrab*, *ntrabc* harvest at ED (b) or EN (c). The two main components and the percentage variation explained by PC1 and PC2 are represented in the axis of the figures. Heat map and PCA were carried out using MeV and the Metaboanalyst platform, respectively.

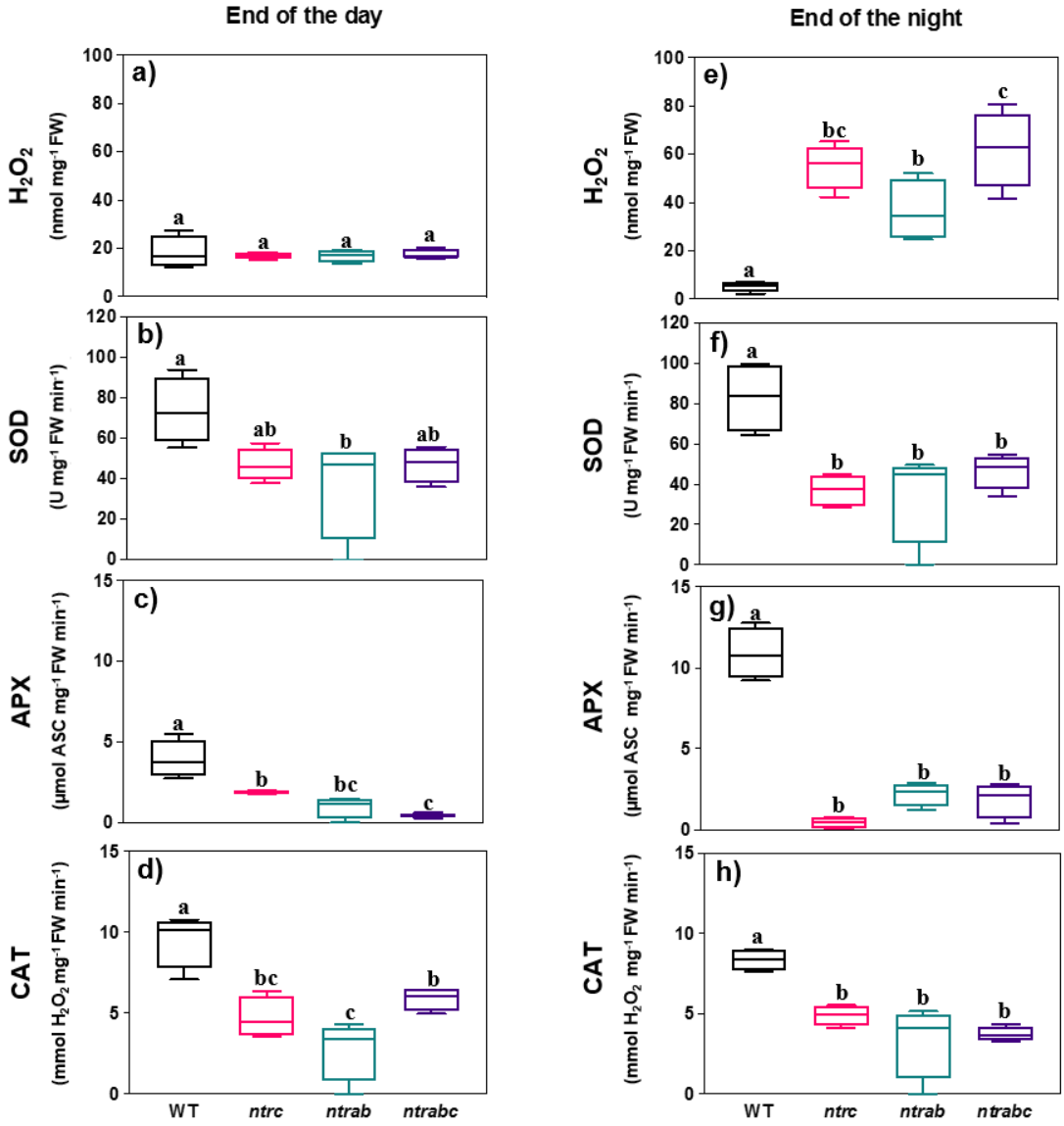

Figure 10- H_2O_2 concentration and activity of antioxidant enzymes in leaves of *Arabidopsis thaliana* L. wild type (WT) and mutants lacking NTRC (*ntrc*), NTRA and NTRB (*ntrab*) or all NTRs (*ntrabc*) harvested at end of the day (ED) (a-d) and end of the night (EN) (e-h) of short-day (125 µmol photons m^{-2} s^{-1}; 08:16 h photoperiod) grown plants. H_2O_2 was quantified by the Amplex red method. The concentration of H_2O_2 and the activities of superoxide dismutase (SOD), ascorbate peroxidase (APX) and catalase (CAT) are expressed in a fresh weight (FW) basis. Black, pink, green and purple box plots represent averages and standard errors of WT, *ntrc*, *ntrab*, and *ntrabc* genotypes, respectively (n = 4). Means that do not share a letter are significantly different according to ANOVA and Tukey test analysis ($P < 0.05$).

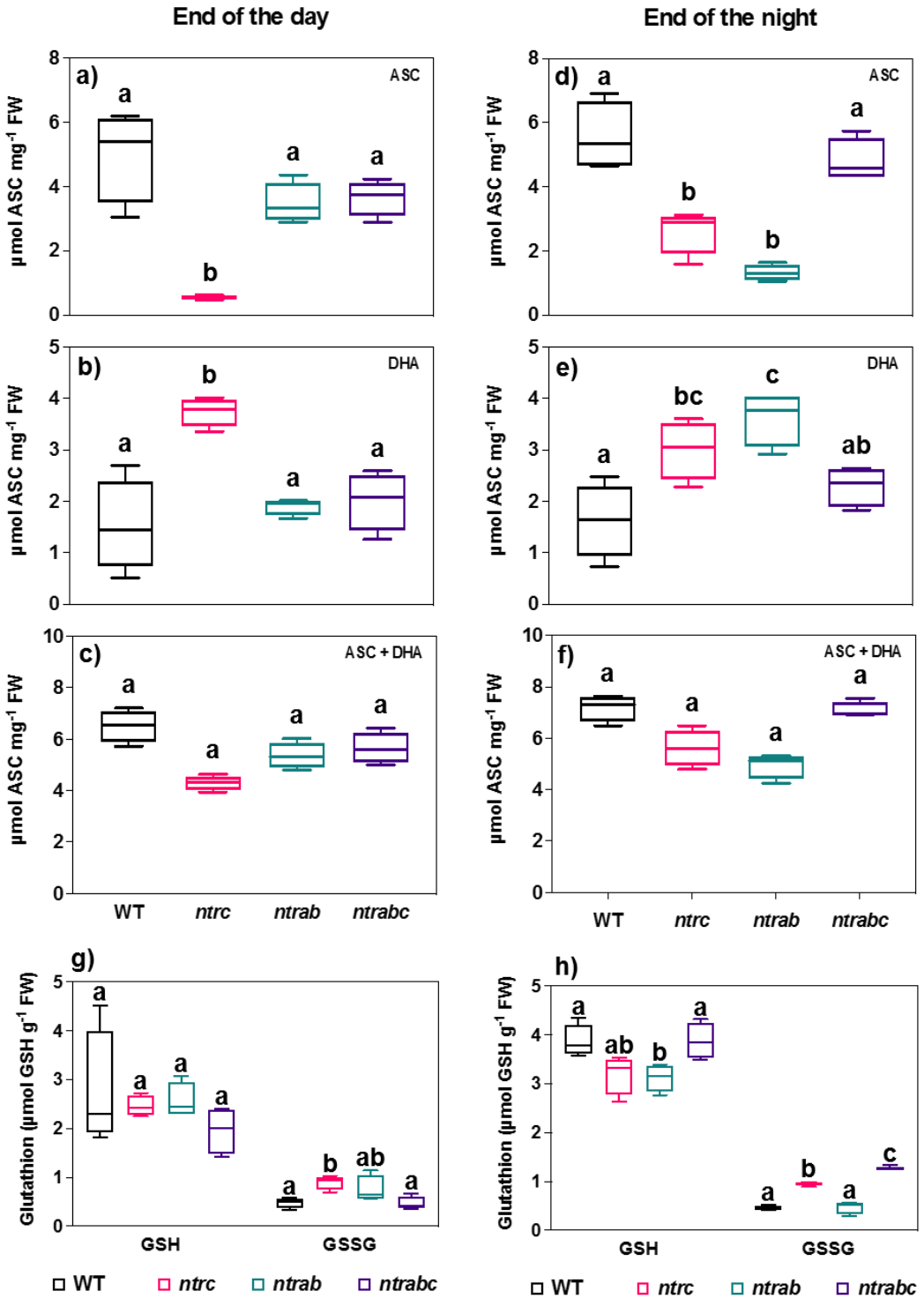

Figure 11- Concentration of ascorbate (ASC), dehydroascorbate (DHA), the sum of them (ASC + DHA), and reduced (GSH) and oxidized (GSSG) glutathione in leaves of *Arabidopsis thaliana* L. wild type (WT) and mutants lacking NTRC (*ntrc*), NTRA and NTRB (*ntrab*) or all NTRs (*ntrabc*) harvested at end of the day (ED) (left panel) and end of the night (EN) (right panel) of short-day (125 µmol photons m^{-2} s^{-1}; 08:16 h photoperiod) grown plants. Black, pink, green and purple box

plots represent averages and standard errors of WT, *ntrc*, *ntrab*, and *ntrabc* genotypes, respectively (n = 4). Means that do not share a letter are significantly different according to ANOVA and Tukey test analysis ($P < 0.05$).

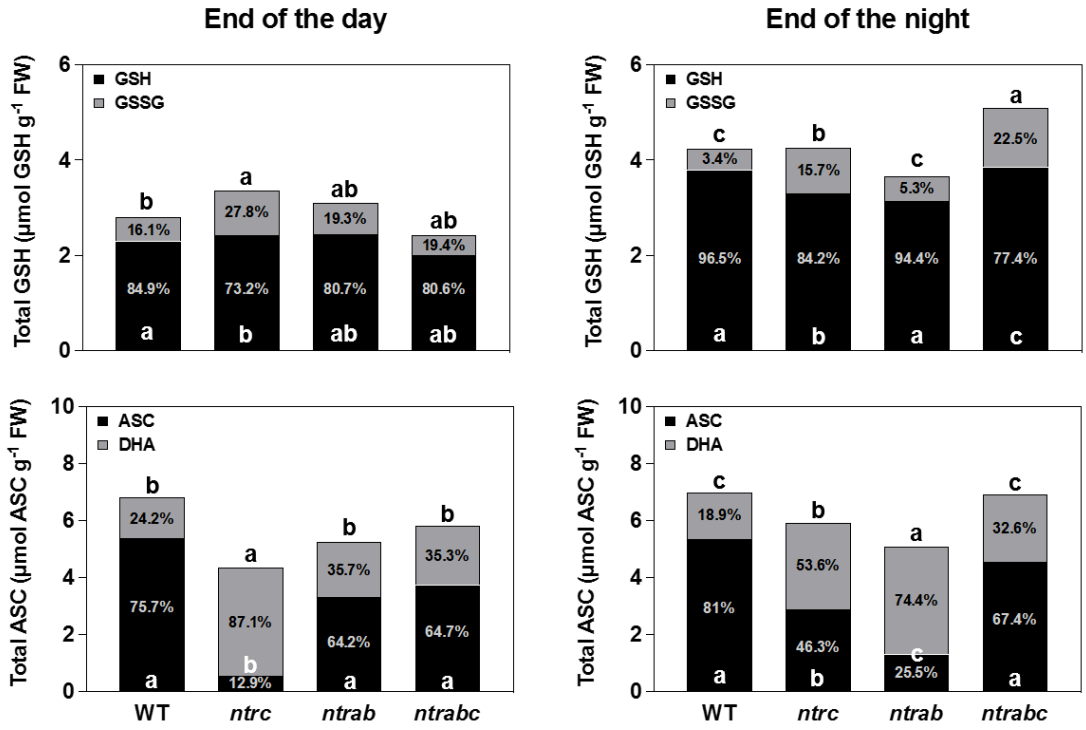

Figure 12- Redox status of glutathione and ascorbate in leaves of *Arabidopsis thaliana* L. wild type (WT) and mutants lacking NTRC (*ntrc*), NTRA and NTRB (*ntrab*) or all NTRs (*ntrabc*) harvested at end of the day (ED) (left figures) and end of the night (EN) (right figures) of short-day (125 µmol photons m^{-2} s^{-1}; 08:16 h photoperiod) grown plants. Genotypes that do not share a letter within each parameter are significantly different according to ANOVA and Tukey test analysis ($P < 0.05$). Abbreviation: ASC, ascorbate; DHA, dehydroascorbate; GSH, reduced glutathione; GSSG, oxidized glutathione.

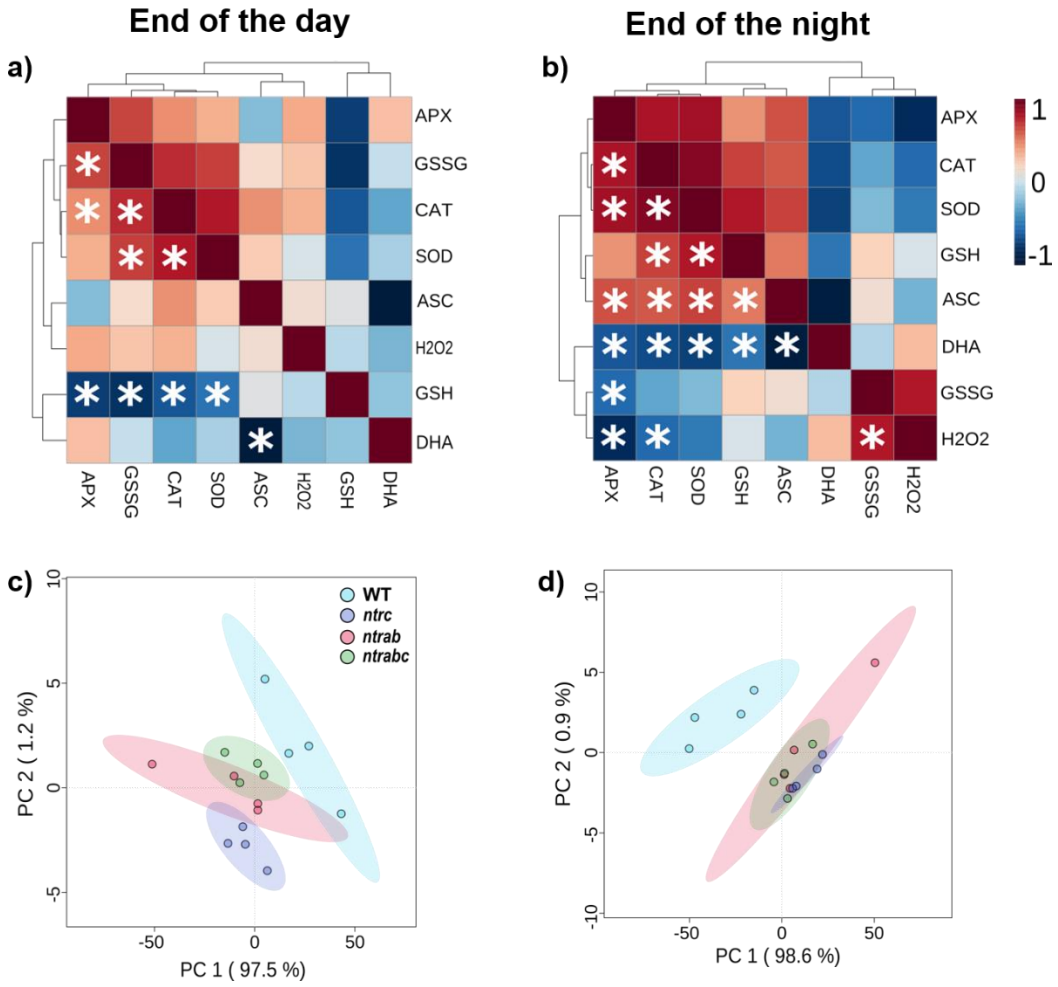

Figure 13- Integrative redox analyses. a-b) Heat map representation of Pearson's correlation analysis between H_2O_2 and components of the antioxidant system. The correlation analysis was carried out using data from all genotypes at end of the day (ED) (left figure) and end of the night (EN) (right figure). Plants were grown under short-day conditions (125 µmol photons m^{-2} s^{-1}; 08:16 h photoperiod). Asterisks (*) indicate significant correlations ($P < 0.05$). These analyses were carried out using the Metaboanalyst platform. c-d) Principal component analysis (PCA) carried out using redox-related parameters (H_2O_2, ASC, DHA, ASC+DHA, ASC (%), DHA (%), GSH, GSSG, GSH+GSSG, GSH (%), GSSG (%), SOD, CAT, APX) observed in leaves of *Arabidopsis thaliana* L. wild type (WT) and mutants lacking NTRC (*ntrc*), NTRA and NTRB (*ntrab*) or all NTRs (*ntrabc*) harvested at end of the day (ED) (a) and end of the night (EN) (b) of short-day (125 µmol photons m^{-2} s^{-1}; 08:16 h photoperiod) grown plants. The two main components and the percentage variation explained by them are represented in the axis of the figures. PCA was carried out using the Metaboanalyst platform. Abbreviations: H_2O_2, hydrogen peroxide; ASC, ascorbate; APX, ascorbate peroxidase; CAT, catalase; DHA, dehydroascorbate; GSH, reduced glutathione; GSSG, oxidized glutathione; SOD, superoxide dismutase.

6 CHAPTER 3: THE MITOCHONDRIAL THIOREDOXIN SYSTEM REGULATES THE REDOX STATUS AND THE METABOLIC FLUXES THROUGHOUT THE GS/GOGAT CYCLE, WHICH IS IMPORTANT FOR PLANT HIGH-LIGHT STRESS ACCLIMATION

Paulo V.L. Souza[1], Vicente T.C.B Alencar[1], Joaquim Albenisio G. Silveira[1], Danilo M. Daloso[1*]

[1] LabPlant, Departamento de Bioquímica e Biologia Molecular, Universidade Federal do Ceará, Fortaleza 60451-970, Brasil

***Correspondence to:** daloso@ufc.com

Running head: TRX/NTR-mediated regulation of glutamine synthetase

Abstract

The glutamine synthetase (GS)/glutamate synthase (GOGAT) cycle is the main pathway to assimilate inorganic ammonium into organic molecules, being thus a hub for the nitrogen metabolism. Recent results suggest that the mitochondrial thioredoxin (mTRX) system can coordinate the fluxes throughout the tricarboxylic acid (TCA) cycle and associated pathways. However, it remains unclear how redox-mediated mechanisms regulate the GS/GOGAT cycle. Here, we carried out several bioinformatics, biochemical, and metabolic analyses to investigate how the TRX system influence the redox status of GS and how the lack of the major components of the mTRX coordinates the metabolic fluxes throughout the GS/GOGAT pathway. For this, we have used plants lacking TRX *o1* (*trxo1*), TRX *h2* (*trxh2*), or both NADPH-dependent TRX reductase A and B (*ntrab*) alongside with the wild type (WT). Substantial metabolic alterations were observed in leaves of the *trxo1* and *ntrab* mutants grown under moderate or high-light (HL) conditions, as compared to the WT. Both *trxo1* and *ntrab* mutants showed higher ^{13}C-enrichment in glutamate and pyroglutamate derived from ^{13}C-pyruvate, suggesting that the mTRX system restrict the metabolic fluxes from the TCA cycle to the GS/GOGAT pathway *in vivo*. The protein content, the activity and the percentage of the reduced band of GS were lower in the *trxo1* mutant, as compared to the WT. Interestingly, the *trxo1* mutant showed stronger reductions in potential quantum yield of the PSII under HL stress, in parallel to higher activities of GS, GOGAT and glutamate dehydrogenase (GDH) and lower level of glutamate and metabolites associated to the (photo)respiratory metabolism, when compared to WT under HL. Our results collectively indicate that the mTRX system regulates the redox status and the metabolic fluxes throughout the GS/GOGAT pathway, which is important for plant HL stress acclimation.

Key word: Thioredoxin *o1*, NADPH$^+$ thioredoxin reductases, glutamine synthetase, high light stress, metabolic regulation.

Introduction.

Due to their sessile lifestyle, plants have developed strategies to avoid or at least to reduce the effects of constraints environmental conditions (Geigenberger e Fernie, 2014). In this context, plants possess an unprecedented and complex redox metabolism, made up of numerous enzymes with signaling, antioxidant and regulatory functions (Mittler *et al.*, 2011; ROWLEY e TAYLOR, 1972). Redox metabolism is governed by oxidative and reductive reactions, which ultimately control the metabolic fluxes through post-translational modifications (PTMs) of enzymes (Daloso, Danilo M *et al.*, 2015; Fonseca-Pereira, da *et al.*, 2020; Meyer *et al.*, 2009). Among the redox mechanisms, thiol switches mediated by thioredoxins (TRXs) and glutaredoxins (GRXs) are important PTMs that (de)activate enzymes and adjust metabolic fluxes according to the prevailing environmental and endogenous conditions (Hägglund *et al.*, 2016; Reinholdt, Bauwe, *et al.*, 2019). For instance, it has been shown that the chloroplastic TRX system is crucial to activate photosynthetic reactions, being thus a great controller of the leaf metabolism in the light. However, it is still unclear how the non-chloroplastic TRX system aid plants to acclimate to high light (HL), which involves the coordination between carbon and nitrogen metabolisms.

TRXs are small ubiquitous proteins with two redox-active cysteine (Cys) residues separated by a pair of amino acids (CXXC). TRXs are found in all organisms from prokaryotes to complex eukaryotes (Buchanan, 2017b; Buchanan *et al.*, 2012; Montrichard *et al.*, 2009). Differently from other organisms, plants have an unprecedented number of TRX isoforms largely distributed throughout plant cell organelles (Buchanan, Gruissem e Jones, 2015; Geigenberger, Thormählen, Daloso, Danilo M., *et al.*, 2017; Schürmann e Buchanan, 2008). In *Arabidopsis thaliana*, TRX *o1* is the most abundant TRX found in the mitochondria (Fuchs *et al.*, 2020b), whilst TRX *h2* was recently found in microsomal fractions (Hou, Lehmann e Geigenberger, 2021). The activity of these non-chloroplastic TRXs depends on reducing power transferred from NADPH-dependent TRX reductases (NTR), namely NTRA and NTRB (Reichheld *et al.*, 2007, 2005). It has been demonstrated that the mitochondrial NTR/TRX system regulates different enzymes of the tricarboxylic acid (TCA) cycle, such as succinate dehydrogenase (SDH), fumarase (FUM), citrate synthase, and isocitrate dehydrogenase (IDH), alongside with the mitochondrial alternative oxidase (AOX) (Daloso et al., 2015; Schmidtmann et al., 2014; Yoshida and Hisabori, 2014). Furthermore, it has been reported that either TRX *o1* or TRX *h2* can deactivate the mitochondrial lipoamide dehydrogenase (mtLPD) *in vitro*, a subunit found in several multi-enzymatic complexes such as

glycine decarboxylase (GDC), pyruvate dehydrogenase (PDH), oxoglutarate dehydrogenase (OGDH), and branched-chain 2-oxoacid dehydrogenase (Fonseca-Pereira, da *et al.*, 2020; Reinholdt, Schwab, Zhang, Reichheld, J. P., *et al.*, 2019). These studies collectively indicates that that the non-chloroplastic NTR/TRX system acts as a key regulator of the metabolic fluxes throughout the TCA cycle and associated pathways, providing important insights into the mechanisms on how the (photo)respiratory metabolism is regulated in light (Fonseca-Pereira, da *et al.*, 2021). Further studies have recently demonstrated that the metabolic fluxes derived from glycolysis and the CO_2 assimilation mediated by phospho*enol*pyruvate carboxylase (PEPc) toward glutamate are restricted by the mitochondrial NTR/TRX system in either illuminated or dark-exposed leaves(Lima *et al.*, 2021; Porto *et al.*, 2022). This suggests that the mitochondrial NTR/TRX system acts as a negatively regulator on the fluxes toward glutamate *in vivo*. However, despite the recent efforts in unveiling the function of the non-chloroplastic TRX system for the regulation of the primary metabolism, few studies have deeply investigated how this system regulates the interplay between carbon and nitrogen metabolisms.

Nitrogen is a fundamental element for plant growth and development (Good, Shrawat e Muench, 2004; Jones *et al.*, 2005). Nitrogen fertilization and its assimilation into plant metabolism has been associated as a key factor for the increased crop yield achieve by the green revolution (Khush, 2005; Wu *et al.*, 2020). In plants, the glutamine synthetase (GS)/ glutamate synthase (GOGAT) cycle is the main pathway that incorporates inorganic nitrogen into organic molecules (Masclaux-Daubresse *et al.*, 2010). Arabidopsis has two GS isoforms, one exclusively found in the cytosol (GS1) and the GS2, which is dually located in chloroplasts and mitochondria (McNally *et al.*, 1983; Taira *et al.*, 2004). GS1 and GS2 are encoded by five (GLN1;1-5) and by an exclusive gene (GLN2), respectively, which are regulated by light and nitrogen availability (Martinelli *et al.*, 2007; McNally *et al.*, 1983; Oliveira e Coruzzi, 1999). GS is fundamental to assimilating NH_4^+ from different sources such as primary root nitrogen assimilation, nitrogen remobilization in sink and source tissues and those released by photorespiration, specifically the NH_4^+ released by the GDC-serine hydroxymethyltransferase (SHMT) complex (Obata *et al.*, 2016; Taira *et al.*, 2004). The comprehension of the regulatory mechanisms of GS assumes a pivotal role in engineering the central metabolism design, since it has been shown that the overexpression of the GS1 gene does not result in a substantially increase in GS activity (Gallais e Hirel, 2004; Habash *et al.*, 2007). In part, this is because the failure in assimilation of nitrogen through the

glutamine synthetase, due to the higher ATP demand, which is approximately estimated around 15% of the cellular ATP budget (Seger *et al.*, 2009). Moreover, it has already established that GS is heavily regulated at gene, transcript, and protein level. At protein level, GS is regulated by several PTMs, such as phosphorylation, oxidation, tyrosine nitration, and S-nitrosylation, and is allosterically inhibited by ATP and P_i, while glutamate activates the enzyme (Finnemann e Schjoerring, 2000; Melo *et al.*, 2011; Rhee, Chock e Stadtman, 1989; Thomsen *et al.*, 2014). As the main consequences, despite many works had successfully overexpression GS1, all these regulators mechanisms served to guarantee that glutamine synthetase activity in the transgenic plants was maintained at wild-type levels (Sweetlove, Nielsen e Fernie, 2017). In this aspect, gene editing of proteins/enzymes that act on GS PTMs can play a fundamental role in increasing GS activity. However, a full comprehension of the agents that act on GS PTMs walk side by side in engineering GS in the central metabolism edition.

In addition, GS is sensitive to [DTT], being thus a candidate to be regulated by redox-mediated mechanisms (Choi, Kim e Kwon, 1999). Indeed, previous studies have reported that TRX could reduce GS in *Canavalia lineata* and *Chlamydomonas reinhardtii in vitro* (Florencio, Gadal e Buchanan, 1993; Tischner e Schmidt, 1982). This idea is further supported by affinity chromatography (Motohashi *et al.*, 2001; Yoshida *et al.*, 2013), and interactome analysis, which showed that TRX *h3* interacts with GS2 (Souza *et al.*, 2019b). Despite these evidence, how redox-mediated mechanisms regulate GS isoforms and what is the impact of this to underpin the metabolic fluxes throughout the GS/GOGAT cycle remains to be determined. Taking this into account, here we have investigated whether the TRX system can regulate GS activity and the metabolic fluxes throughout the TCA and the GC/GOGAT cycles. We have carried out several bioinformatics analyses and an extensive biochemical and metabolic characterization of enzymes and metabolites associated to the TCA and the GS/GOGAT cycles using Arabidopsis plants lacking TRX *o1*, TRX *h2* or both NTRA and NTRB.

Material and Methods

Plant material and growth conditions

Arabidopsis thaliana wild-type (WT) and T-DNA insertion mutants lacking TRX *h2* (*trxh2)* (SALK_079507), TRX *o1* (*trxo1*) (SALK 04279), NTRA (SALK_539152), and NTRB

(SALK_545978) were collected from SALK collection (http://signal.salk.edu/) and characterized previously (Daloso, Danilo M *et al.*, 2015; Fonseca-Pereira, da *et al.*, 2020; Reichheld *et al.*, 2007). The double *ntrab* mutant was obtained by crossing the single *ntra* and *ntrb* mutants (Reichheld et al., 2007). Seeds were germinated as described previously (Fonseca-Pereira *et al.* 2019) and sown in soil containing sand, vermiculite, and organic substrate Topstrato® (1:1:1). Plants were grown under 120 – 150 μmol photons m^{-2} s^{-1} and grown under short-day photoperiod (8h light: 16h dark), 35-45% of relative humidity, temperature 22-25ºC. Rosettes were collected and frozen in liquid nitrogen for further analysis, as described in the legend of each figure.

We further carried out an experiment subjecting WT and the TRX mutants to a short high-light (HL) stress treatment. For this, 8-week old plants were grown under the same conditions described above and later divided into two groups; the control group, which was submitted to a growth light (GL) condition (120-150 μmol photons $m^{-2}s^{-1}$), and HL stress group, which was submitted to 550-600 μmol photons m^{-2} s^{-1}. After 8h under GL or HL, whole rosettes were harvested and immediately frozen in liquid nitrogen. Samples were stored at -80°C until further analysis. We used four biological samples per treatment/genotype.

Pulse-amplitude-modulation (PAM) measurements of chlorophyll *a* fluorescence

In vivo chlorophyll *a* fluorescence parameters were estimated using DUAL PAM 100 (Halz, Germany) using fully expanded leaves from WT, *trxh2*, *trxo1*, and *ntrab*. The potential quantum yield of photosystem II (PSII) ($F_v/F_m = (F_m - F_o)/F_m$) was estimated from dark-adapted leaves. F_m and F_o parameters represents the maximum and minimum fluorescence of dark-adapted leaves, respectively (Genty, Briantais e Baker, 1989).

Bioinformatics analysis

Different bioinformatics approaches were used to investigate whether GS, GOGAT and GDH are possibly regulated by TRXs. We started searching for conserved Cys residues in amino acid sequences of these enzymes from different plant species. Amino acid sequences of GS, GDH, and GOGAT were collected from National Bank Information Biotechnology (NCBI), aligned using

Clustal W (https://www.ebi.ac.uk/research), and visualized using the GeneDoc software. Conserved Cys residues in the protein sequences were used to predict possible disulfide bond formation in the proteins by using the DIANNA 1.1 web server (Ferrè & Clote, 2005). DIANNA algorithm provides a probability of a disulfide bond formation among different Cys residues, according to a score ranging from 0 (low probability) to 1 (high probability).

Molecular docking

Molecular docking analysis was used to predict protein-protein interaction between GS isoforms and TRX *o1* and TRX *h2*. The molecular docking is an *in silico* analysis that provides a physical interaction among a binder, which for instance can be a peptide or even a complex protein, and a receptor that usually is a protein. Given that the non-plastidial NTRs do not possess a TRX domain in their sequences, as the chloroplastic homologous NTRC, it is highly unlikely that NTRs A and B will directly regulates GS. For this reason, we did not carry out molecular docking analysis between NTRs and GS isoforms. The TRX *o1* crystal from *Arabidopsis thaliana* L. was collected directly from the protein data bank (PDB; https://www.rcsb.org/). Unfortunately, the protein crystals from Arabidopsis TRX *h2*, GS1, and GS2 are not available yet. To overcome this obstacle, we decided to build protein homologous to these proteins. Firstly, we ran a protein blast (https://blast.ncbi.nlm.nih.gov/Blast.cgi) using Arabidopsis sequences of GS isoforms and TRX *h2* as bait to find PDB crystal proteins with a higher degree of similarity with them. Posteriorly, we used the swiss-modelling platform (https://swissmodel.expasy.org/) to build 3D protein models of GS isoforms and TRX *h2*. For this, we used the templates **2d3a** for GS2, **7v4h** for GS1, and **6x0B** for TRX *h2*, which represents the homologous protein crystals with higher similarity to each bait. The models created were evaluated by both QMEAN and GMQE scores (Benkert, Tosatto e Schomburg, 2008). Posteriorly, we ran a protein-protein docking analysis using two friendly online docking platforms namely Cluspro (https://cluspro.org/) and haddock (https://wenmr.science.uu.nl/haddock2.4) (Kozakov *et al.*, 2013; Vajda *et al.*, 2017; Zundert, van *et al.*, 2016). Cluspro and haddock use different algorithms to generate different clusters, which are translated into different forms of interaction between ligand and receptor. These programs generate two scores namely Z-score (haddock) and lower energy score (cluspro), which define the best position of the ligand to the receptor. The lower is the values of Z-score and energy score,

greater is the interaction prediction between ligand and receptor. We used both TRX *o1* and TRX *h2* 3D models as ligands and the 3D models of GS isoforms as receptors. We further ran a protein-protein docking analysis using TRX *h2* 3D model and TRX *o1* crystal with all GS 3D model subunits using the cluspro platform. In haddock, we ran a docking between the TRX *h2* 3D model with one subunit of GS1 and GS2 3D model. We chose the clusters with lower energy and Z scores. The docking figures were created using the Discovery studio 2021 program (https://www.3ds.com).

GC-MS-based metabolomics analysis

Extraction, derivatization, and gas chromatography coupled to mass spectrometry (GC-MS) analysis was carried out exactly as described previously (Lisec *et al.*, 2006). Briefly, leaf samples were powdered using liquid nitrogen, weighed and aliquoted to 2 mL tubes (30-50 mg of fresh weight per sample). The extraction was carried out by adding 700 µl of pure methanol and 30 µl of ribitol, which is used as an internal quantitative standard. Samples were shaken (10 min, 70 °C, 950 rpm) and centrifuged (10 min, 11,000 *g*). The supernatant was transferred to a tube (2 mL), where 375 µl of cold chloroform and 750 µl of water were added and later centrifuged (15 min, 10,000 *g*). Then, 150 µl from the upper (polar) phase was transferred to a tube (1.5 mL) and dried in a speed vac. Samples were derivatized by adding 40 µl of methoxyamine hydrochloride (20 mg ml^{-1}) dissolved in pure pyridine, shaken (950 rpm, 2 h, 37 °C), and added 70 µl of *N*-Methyl-*N*-(trimethylsilyl) trifluoroacetamide (MSTFA). Samples were shaken again for 30 min under 37 °C and then transferred to glass vials for GC-MS analysis. Chromatograms were analysed using the Xcalibur 2.1 software (Thermo Fisher Scientific). Metabolite identification was carried out by using the Golm Metabolome Database (http://gmd.mpimp-golm.mpg.de/) (Kopka *et al.*, 2005). Peak areas of the mass fragments were normalized based on the fresh weight of the sample, followed by normalization by the amount of the internal standard (ribitol).

^{13}C-pyruvate labelling experiment

Leaves of 6-week-old *A. thaliana* plants were detached and the petiole was immediately submerged in 5 mM MES-TRIS buffer pH 6.15, when another cut was made to avoid embolism.

Petioles were submerged in the same buffer containing 15 mM [U^{13}C]-pyruvate (Cambridge Isotope Laboratories) and submitted to light (120-150 µmol m^{-2} s^{-1}) or darkness for 0, 30, and 60 minutes. After that, leaves were removed from the tubes and immediately frozen in liquid nitrogen, as described previously (Daloso, Danilo M *et al.*, 2015). Samples were stored at -80°C until further GC-MS analysis.

The analysis of the chromatograms and the metabolite identification were carried out as described above. The relative isotopologue abundance (RIA) in fragments obtained from metabolites of, or associated to, the TCA cycle was carried out as described previously (Lima *et al.*, 2018). Given that pyruvate degradation by the PDH complex releases two carbons into the TCA cycle (Le, Lee e Millar, 2021), we have investigated the M2/M0 ratio in metabolites of, or associated to, the TCA cycle. The M2 isotopologue reflects the incorporation of two ^{13}C incorporated into the metabolite fragments, reflecting therefore the two carbons of the acetyl-CoA that enters the TCA cycle from PDH activity.

Protein extraction and immunoblots

Arabidopsis proteins were extracted from 8-week-old fresh leaves. Around 150 mg of fresh weight was ground to powder using a mortar with liquid nitrogen. Subsequently, 1ml of extraction buffer (Potassium Phosphate 100 mM + EDTA 1%) was added to a 2mL tubes containing grinded samples and then centrifuged at 14,000 *g* for 15min. The supernatant was collected and the pellet was discarded. The protein extracts were stored at -80^{o}C until the day of analysis. Bradford method was used to evaluate the total soluble protein content (Bradford, 1976). To immunoblot GS detection, leaf protein fractions were separated by sodium dodecyl sulfate-polyacrylamide gel electrophoresis (SDS-PAGE) with 10% acrylamide gel concentration, using 25 ug of protein. After the separation by SDS-PAGE, the proteins were transferred to a nitrocellulose membrane (Towbin, Staehelin, & Gordon, 1979). The nitrocellulose membrane was incubated with skinned milk to block unspecific protein binding for 3 hr. After that, the membranes were washed with TRIS - buffered saline (TBS) containing 1% (w/v) Bovine serum albumin (BSA) and 0.1% (v/v) Tween-20 TBS buffer and then incubated with the primary antibodies cited above for 12 h. The membranes were then washed with TBS buffer and incubated with a secondary antibody (Sigma secondary antibody anti-rabbit, dilution 1:20,000). The blots were revealed by colorimetric

assay with BCIP/NBT. The protein content was quantified using monoclonal mono-specific antibodies for both GS isoforms. To quantify the protein level, we made a protein content gradient (75% and 100%) with WT samples. The protein amount in the mutants was thus quantified based on the optical density related to the grey gradient.

Enzyme activity analysis

Approximately 200 mg of fresh weight of Arabidopsis leaves from 8-week-old plants was ground to powder using a mortar with liquid nitrogen. Posteriorly, 1 ml of extraction buffer (TRIS - HCl 0,2 mM pH 7,8, EDTA 1 mM and $MgCl_2$ 1 mM) was added to the mortar and mix with an aliquot of the sample. The homogenate was centrifuged at 15.000 *g* at 4ºC per 15 min. The resultant supernatants were used to determine enzyme activity spectrophotometrically. Bradford method was used to evaluate the total soluble protein content (Bradford, 1976).

GS activity is based on the biosynthesis of γ-glutamyl hydroxamate, which uses hydroxylamine instead of ammonium. The reaction was prepared in a 2 ml tube with the addition of 200 µL of biological extract, 200 µL of reaction buffer (TRIS - HCl 0.2 M pH 7.8), 200 µL of 0.4 M sodium glutamate, 100 µL of 80 mM ATP and 100 µL of 0.2 M $MgSO_4$. The reagents were incubated at 35 °C for 2 min. After that, 100 µL of hydroxylamine was added to the enzymatic extract. After 6 minutes, the samples were taken from the thermo-mixer and 500 µL of $FeCl_3$ was added. Subsequently, the extract was centrifuged at 14,000 *g* for 10 min at room temperature to precipitate proteins. The absorbance was measured at 540 nm. GS activity was calculated through the standard curve of γ-glutamyl hydroxamate (GGH) being expressed by GGH µmol FW^{-1} mg $Prot^{-1}$ h^{-1} (Hirel e Gadal, 1980; O'Neal e Joy, 1974).

The activity of glutamate dehydrogenase (GDH) and glutamate synthase (GOGAT) are based on NADH oxidation being monitored by UV spectrophotometer at 340 nm (Matoh, Ida e Takahashi, 1980). The difference between GDH and GOGAT is based on the composition of reaction buffers. The reaction buffer for GDH is composed by TRIS - HCl 62.5 mM pH 7.4 + α-ketoglutarate 8.75 mM + ammonium chloride 12.5 mM (Kwinta e Bielawski, 1998), while the GOGAT reaction buffer is composed by TRIS - HCl 62.5 mM pH 7.4 + 2.5 mM EDTA + 12.5 mM glutamine + 25 mM α-ketoglutarate. The reaction began with the addition of 1600 µL of reaction buffer, followed the addition of 200 µL of biological extract and 200 µL of 2.5 mM NADH. The

reaction is monitored at 340 nm during 6 min. Both GDH and GOGAT activity are expressed by µmol FW^{-1} mg $Prot^{-1}$ h^{1}.

GS redox status

Frozen samples were ground to a powder in liquid nitrogen and proteins were precipitated with 10% (v/v) trichloroacetic acid. The samples were incubated on ice for 20 min followed by centrifugation at 16,200 *g* at 4°C for 10 min. The pellets were washed with acetone, collected in alkylation buffer (2% SDS, 50-mM TRIS - HCl, pH 7.8, 2.5% glycerol, and 4 M urea) with 10-mM methyl-maleimide polyethylene glycol (MM-PEG_{24}) and incubated for protein thiol alkylation at room temperature for 20 min (Naranjo *et al.*, 2016). The protein extracts were separated by SDS-PAGE (15% polyacrylamide), transferred to a nitrocellulose membrane (Towbin, Staehelint e Gordon, 1979), and incubated with skinned milk to block unspecific protein binding for 3 hr. The protein content was quantified using monoclonal monospecific for both GS isoforms (1 and 2) antibodies (1:2,000). Posteriorly, the membranes were washed with TBS buffer and then incubated with the primary antibodies cited above for 12 hr. After that, the membranes were washed with TBS buffer and incubated with secondary antibody for 3 hours (Sigma secondary antibody anti-rabbit, dilution 1:20,000). The blots were revealed by BCIP/NBT. Blot images were taken using the Major Science gel photo-documentation system and quantified by SmartView Pro 1200 Imager System Version 1.0.03 program. The intensities of both oxidized and reduced protein bands were quantified based on an optical density gradient. The results are demonstrated as the intensity of each oxidized and reduced band as well as the ratio between them within each genotype, normalized by the fresh weight (FW) used in the gel shift protein extraction.

Statistical analysis

Significant differences between mutants and the WT were determined by Student's *t*-test ($P < 0.05$) or by analysis of variance (ANOVA) followed by Tukey's test ($P < 0.05$). Metabolite profiling data were analysed by principal component analysis (PCA) using the Metaboanalyst platform (Chong, Wishart e Xia, 2019). Heat maps were created using the MeV 4.9.0 software.

Results

Bioinformatics analysis suggests that GS, GDH and GOGAT are redox regulated by TRXs

We have previously shown that bioinformatic analysis is a prominent approach to raise proteins that are possible TRX targets (Daloso, Danilo M *et al.*, 2015; Fonseca-Pereira, da *et al.*, 2020, 2021). We then decided to investigate whether enzymes of the nitrogen metabolism have conserved Cys residues in their amino acid sequence, form disulfide bonds and can interact with TRXs. Interestingly, all GS1 Arabidopsis isoforms own conserved Cys residues, especially on 91, 160, and 179 Cys residues, with exception of the GLN1.2 sequence that possess a Ser instead of Cys residue at the 179 amino acid (Figure supplementary S1). The alignment between GS1 and GS2 sequences from Arabidopsis and other plant species demonstrated that several Cys residues are conserved between different plant species (Figure S2 and S3). Similarly, we identified several conserved Cys residues on GOGAT and GDH sequences between Arabidopsis and different plant species (Figure S4 and S5).

We next decided to investigate which of these Cys residues from Arabidopsis GS, GDH and GOGAT amino acid sequences may form a disulfide bond by using the Dianna web server platform. Our results demonstrated that four out of five GS1 isoforms (Gln1;1, Gln1;2, Gln1;3, Gln1;4) have Dianna scores below 0.2, which indicates a low probability to forming a disulfide bond among two Cys residues. In contrast, GS1 (Gln 1:5) and GS2 had high probability to form a disulfide bond between the Cys pairs 92-228 (score > 0.99) and 150-306 (score > 0.97), respectively (Table 1). Both GDH isoforms (1 and 2) and the GOGAT (GLU 1) amino acid sequence have Dianna score higher than 0.97 between different pair of Cys residues, suggesting that these sequences also have high probability of disulfide bond formation. These results suggest that GS, GOGAT, and GDH can be redox regulated and highlights which Cys residues may form disulfide bonds.

Molecular docking analysis suggests that GS isoforms interact with TRXs o1 and h2

Molecular docking is a well-established *in silico* analysis widely used in biochemical studies (Attique *et al.*, 2019; Kurkcuoglu *et al.*, 2018; Soni e Madhusudhan, 2017), but rarely explored to identify proteins that interact with TRXs. We then used molecular docking to predict protein interactions between TRX *h2* and TRX *o1* with GS isoforms. We first ran a molecular

docking using the TRX *o1* crystal and TRX *h2* model as ligands (Table S2) and GS1 and GS2 as receptors using two friendly docking platforms, namely haddock and Cluspro platforms. Both haddock and cluspro platforms build clusters based in different possible interactions between the receptor and the ligand and provide two scores, the lower energy score (Cluspro) and the Z-score (Haddock). Lower scores indicate the best position of interaction between the receptor and the ligand. We then chose the clusters with the lowest Z and energy scores (Tables S3 and S4). Interestingly, the molecular docking built in both platforms shows an interaction between TRX *o1*/*h2* and GS isoforms (Figures S6-S8). It is worth mentioning that the docking between TRX *o1*/*h2* and GS1 showed that both TRXs were close to 228 Cys residues. On the other hand, the docking between the TRX *o1/h2* and GS2 showed that the TRXs are closer to 306 Cys residues. Both 228 Cys in GS1 and 306 in GS2 were predicted to form a disulfide bridge according to Dianna web server platform (Table 1).

Leaf metabolic alterations induced by the lack of TRX *o1*, TRX *h2* and NTRA/B

We next carried out a metabolite profiling analysis in leaf samples harvested at the end of the day (ED) and at the end of the night (EN) using a well-established GC-TOF-MS platform (Lisec *et al.*, 2006, 2015). Principal component analysis (PCA) indicates that both the *trxo1* and the double *ntrab* mutants have stronger metabolic alterations rather than the *trxh2* mutant, when compared to the WT in both EN and ED conditions (Figures 14a-b). This is corroborated by hierarchical clustering analysis (HCA), which showed that the metabolic changes observed in the double *ntrab* mutant are more similar to the *trxo1* rather than the *trxh2* (Figure 15). The lack of TRX *o1*, TRX *h2*, and NTRA/B substantially altered the level of amino acids, organic acids and sugars, especially at ED. These changes were more drastic in the double *ntrab* mutant, in which seventeen out of the thirty-one metabolites identified were significantly different from the WT (Figure 15). All mutants have higher content of valine, leucine and homoserine than the WT at ED. Metabolites of, or associated to, the (photo)respiratory metabolism such as glycine, serine, glycerate as well as those from the TCA cycle (citrate, malate, succinate and fumarate) showed significant difference in at least one of the mutants in either ED or EN. Moreover, the lack of TRXs directly affects the level of metabolites from the nitrogen metabolism. For instance, lower level of proline was found in both *trxo1* and *ntrab* at ED, while tyrosine was lower only in the *trxo1*, as compared to the WT at ED.

The level of glutamine increased in the *ntrab* at ED and decreased in *trxo1* in both ED and EN, when compared to the WT. Additionally, in ED the level of glutamate was substantially higher (up to 33 and 85-fold) in both *trxo1* and *ntrab*, when compared to the WT (Figure 15). This result indicates that the level of glutamate and glutamine is substantially altered in NTR/TRX mutants, in agreement with our previous studies (Daloso, Danilo M *et al.*, 2015; Fonseca-Pereira, da *et al.*, 2020; Lima *et al.*, 2021).

The lack of the mitochondrial NTR/TRX system increase the fluxes from pyruvate to glutamate in both dark and light-exposed leaves

Our metabolite profiling analysis suggests that the fluxes toward glutamate/glutamine are altered in the NTR/TRX mutants. However, it is important to highlight that changes in metabolite content does not necessarily correlates with changes in metabolic fluxes, and *vice-versa* (Williams *et al.*, 2008). We then decided to investigate whether the lack of TRX *o1*, TRX *h2*, or NTRA/B alter the metabolic fluxes from the TCA cycle toward glutamate. It is noteworthy that the tracer (^{13}C-labelled substrate) to be used and the conditions in which plant tissues will be submitted are two critical steps in ^{13}C-metabolic flux analysis (^{13}C-MFA) (Lima *et al.*, 2018). Previous ^{13}C-MFA demonstrated that the fluxes throughout the TCA cycle and glutamate synthesis are inhibited in the light (Abadie *et al.*, 2017a; Gauthier, Paul P G *et al.*, 2010; Szecowka *et al.*, 2013). Among the mechanisms that aid to explain the light-inhibition of these metabolic pathways, it is well-known that the activity of pyruvate dehydrogenase (PDH) represents an important limiting point, given that this enzyme is inhibited by phosphorylation in the light (Tovar-Méndez, Miernyk e Randall, 2003; Zhang *et al.*, 2021). Taking these points into account, we then performed the ^{13}C-labelling experiment using uniformly ^{13}C-labeled pyruvate ([U^{13}C]-pyruvate) as tracer in leaves subjected to either dark or light conditions.

PDH converts pyruvate (three carbons) into acetyl-CoA (AcCoA) (two carbons), releasing a molecule of CO_2. AcCoA is substrate for a wide range of metabolic pathways, including the TCA cycle (Souza, de *et al.*, 2020) (Figure 16a). We then followed the ^{13}C-distribution derived from PDH by analyzing the ratio between M2 and M0 isotopologues (M2/M0) in glutamate and metabolites of the TCA cycle (Figure 16a). The intensity of the M2 isotopologue represents metabolite fragments with the addition of two ^{13}C-labelled carbons, while M0 indicates fragments

with the natural ^{13}C abundance (Figure 16b). Thus, increases in the M2/M0 ratio, compared to the time 0 of each genotype (i.e. samples not subjected to ^{13}C-labelling), indicates increased ^{13}C-metabolic fluxes toward the correspondent metabolite. No significant alteration in citrate and fumarate M2/M0 ratios was observed in either dark-exposed or illuminated leaves from all genotypes (Figures 17a-b). Similarly, no increase in M2/M0 ratio was observed in malate in WT, *trxh2* and *ntrab* under either dark or light conditions, while *trxo1* showed higher M2/M0 ratio after 60 min in the dark (Figure 17e). Despite these slight changes in the ^{13}C-enrichment in TCA cycle metabolites, substantial increases in M2/M0 in glutamate and pyroglutamate were observed in the mutants, especially in *trxo1* and *ntrab*, while no increases in this ratio was observed in WT (Figure 17c-d). For instance, we observed an increase in the glutamate M2/M0 ratio in leaves of *trxo1* and *ntrab* after 60 min of dark or light exposure. The pyroglutamate M2/M0 ratio increased in *trxh2* after 30 min of darkness, in *trxo1* after 30 min of illumination, and in *ntrab* after 60 min of darkness or illumination (Figure 17c-d).

The activity of GS/GOGAT cycle enzymes are altered in plants lacking NTRA/B, -TRX h2 or TRX o1

The metabolic results of NTR/TRX mutants showed substantial alterations in metabolites associated to the GS/GOGAT cycle, which can be due to modifications at enzyme activity level. We then next investigated whether the activity of key GS/GOGAT cycle enzymes namely GS, GOGAT and GDH are altered in samples harvested at ED and EN. The activity of GOGAT was lower in all mutants, while GS was lower in *trxh2* and *trxo1*, and GDH was lower in *trxo1* and *ntrab*, when compared to WT at ED (Figure 18a-c). In addition, at EN the activity of GS was lower in all mutants, while both GDH and GOGAT activities were higher only in *trxo1*, when compared to the WT (Figure 18d-f).

The content of GS1 and GS2 proteins are lower in illuminated leaves of the mutants

Our previous bioinformatics, biochemical and metabolic analyses strongly suggest that GS may be redox regulated by TRXs. We next performed different biochemical analysis to deeply investigate this hypothesis. We first carried out a western blot analysis in leaf proteins harvested at

ED and EN, using specific antibodies for GS1 and GS2 isoforms. All mutants showed lower GS1 and GS2 contents at ED, when compared to WT (Figures 19a-c). At EN, the protein content of GS1 was higher and lower in *trxo1* and *ntrab* mutants than the WT, respectively (Figure 19d). We did not detect any signal of GS2 at EN neither in WT nor in the mutants, which is likely associated to the dark-mediated protein degradation of GS2 (Figure 19e) (Oliveira e Coruzzi, 1999).

The redox status of GS is altered in the NTR/TRX mutants

GS is known to be sensitive to DDT concentration, a well-described reductant agent (Choi, Kim e Kwon, 1999). However, neither the changes in the activity nor in the content of GS found in the NTR/TRX mutants guarantee that the redox status of GS was altered. Thus, to obtain better insights on the mechanisms by which TRX regulates GS, we next investigated whether the absence of TRX o1, TRX h2, and NTRA/B altered the redox status of GS by carrying out a gel shift analysis in leaf protein samples harvested at ED and EN. We have used $mmPEG_{24}$ as an SH group marker agent, which increase the molecular weight (MW) of the labelled (reduced) proteins by covalent pegylation of the Cysteine residues. Given this increase in the MW caused by the $mmPEG_{24}$ and the similarity between the MW of GS1 and GS2 isoforms, the reduced band of GS1 ends overlapping with the reduced band of GS2, not enabling the distinction of these isoforms in the gel shift analysis (Figure 20a). This analysis reflects therefore the redox status of GS, except at night in which the GS2 protein was not detected (Figure 20e). The percentage of reduced and oxidized GS bands were higher in both *trxh2* and *ntrab* and lower in *trxo1* at ED (Figures 20b-c). However, the ratio between reduced to oxidized bands was lower only in the *trxh2* mutant at ED (Figure 20d). Interestingly, *trxh2* and *trxo1* mutants also showed higher and lower percentage of both reduced and oxidized GS bands at EN, respectively, as compared to the WT. The *ntrab* showed lower percentage of the reduced GS band at EN, while no difference was observed in the oxidized, as compared to the WT (Figures 20e-f). The reduced to oxidized ratio of GS bands was higher in *trx h2* and lower in *ntrab*, as compared to the WT at EN (Figure 20g). These results indicate that the redox status of GS is altered in the NTR/TRX mutants, which could be associated to a direct effect of the lack of NTR/TRXs, suggesting a direct involvement of TRXs in the regulation of GS, or, alternatively, by an indirect effect caused by disruption in the homeostasis of redox metabolism.

High light stress-mediated changes in nitrogen metabolism depends on the mitochondrial NTR/TRX system

Our results provided compelling evidence indicating that the absence of NTR/TRXs substantially alter the nitrogen metabolism. However, it remains unclear what is the physiological relevance of the NTR/TRX-mediated regulation of the GS/GOGAT metabolic pathway. Given the importance of this pathway as a sink to the excess of reducing power originated from high-light (HL) stress periods (Brestic *et al.*, 2014; Guilherme *et al.*, 2019), we then subjected the genotypes investigated here to a short (08 h) HL stress period. Plants were grown under a short photoperiod (08:16 h light/dark) and ~120 μmol photons m^{-2} s^{-1} for 8 weeks and then subjected to 08 h of HL (~550 μmol photons m^{-2} s^{-1}), from the beginning until the end of the day (ED). The HL treatment corresponds therefore to one day of HL. HL-stressed plants were compared to plants harvested at the end of the night (EN), i.e. before the start of the HL stress treatment, and with plants also harvested at ED but subjected to 08 h of grown light (GL, ~120 μmol photons m^{-2} s^{-1}) condition. The impact of the HL stress was evaluated at physiological, biochemical and metabolic levels.

HL stress imposition reduced the potential quantum yield of the photosystem II (PSII) (F_v/F_m) only in *trxo1* and *trxh2* mutants (Figure 21a). As expected, HL stress leads to a higher GS activity in WT leaves. Similar increase was observed in *trxh2*. Interestingly, *trxo1* showed the highest HL-mediated increase in GS activity and the *ntrab* showed much higher GS activity than the WT under GL, which was maintained high under HL (Figure 21b). By contrast to GS, the activity of GOGAT was substantially reduced in WT leaves under HL stress. GOGAT activity was lower under GL and unresponsive to HL in all mutants (Figure 21c). No changes in GDH activity were observed in WT and *ntrab*, while it decreased in *trxh2* and increased in *trxo1* in response to HL. The *trxo1* mutant showed the highest GDH activity under HL. These analyses indicate that HL stress greatly affect the activity of GS/GOGAT related enzymes, with a stronger impact in the *trxo1* mutant.

PCA using metabolite profiling data from plants harvested at EN and ED under GL and HL conditions highlights that the HL-induced changes in primary metabolism were more drastic in WT and in the double *ntrab* mutant, as indicated by the clearest separation of the ED-HL from EN and ED-GL samples in these genotypes (Figure 22). However, when the data of ED-GL and ED-HL are normalized by the values found at EN in each genotype, we observed that the changes in *trxo1* and *ntrab* are very similar to each other, as demonstrated by the HCA (Figure 23). Several

metabolites related to the (photo) respiratory and the nitrogen metabolisms presented an opposite behavior in *trxo1* and *ntrab*, compared to WT. For instance, while the levels of homoserine, glycerate, serine, fumarate, glutamate and tryptophan were higher in WT after HL stress, as compared to ED-GL WT samples, they were lower in both *trxo1* and *ntrab*, when compared to ED-GL samples of each genotype (Figure 23). PCA using this normalized data showed that *trxo1* and *ntrab* were clearly separated from the WT by the PC1 (Figure 24). Biplot analysis of the PCA highlighted that the HL-induced accumulation of glutamate in the WT is the main responsible for the distinction between the WT and *trxo1* and *ntrab* mutants (Figure 24). This analysis further highlighted that proline and pyruvate also contributed to the separation between WT and *trxo1*, as indicated by the arrows toward *trxo1* (Figure 24b). Intriguingly, the level of proline decreased only in the WT after HL (Figure 25) and was negatively correlated with glutamate in the WT, *trxh2* and *trxo1* (Figure 25). Furthermore, several metabolites were positively correlated with glutamate in the mutants, while none was positively (P <0.05) in the WT and glutamate was negatively correlated with pyruvate and alanine only in the WT (Figure 25). These results suggest that the mitochondrial NTR/TRX system is important to modulate the connection between carbon and nitrogen metabolisms, which is important for plant HL acclimation.

Discussion

The green revolution was characterized by substantial increases in crop yield, which was especially due to the advances in plant nitrogen fertilization (Evans e Lawson, 2020). However, the overuse of nitrogen fertilizers is harnessing natural environments. Finding environmental friendly strategies to improve plant nitrogen use efficiency assumes therefore a paramount importance to maintain or improve crop yield at lower cost for the environment (Waqas, Hawkesford e Geilfus, 2023). At the plant metabolism point of view, nitrogen assimilation depends on the reactions of, or associated to, the GS/GOGAT cycle (Liu, Hu e Chu, 2022). It is thus reasonable to hypothesize that the establishment of new crop cultivars and the development of environmental friendly strategies for crop cultivation in the current climate change scenario will likely depends on our fully understanding regarding the functioning of this cycle (Hirt *et al.*, 2023; Li *et al.*, 2018). However, how the metabolic fluxes throughout the GS/GOGAT cycle are regulated remains not completely understood, which is in part associated to the complex regulation of its

constituent enzymes (Sweetlove, Nielsen e Fernie, 2017). For instance, GS is known to be regulated by several transcriptional and post-translational mechanisms, including reduction by DTT, a well-established reductant agent (Choi, Kim e Kwon, 1999). This suggests that GS is redox regulated by redoxins. Indeed, recent results highlight that GS possess several biochemical characteristics such as the presence of conserved Cys residues in their amino acid sequences and a high probability to form disulfide bonds that makes this enzyme a potential target of TRXs (Porto *et al.*, 2022). Furthermore, the accumulation of glutamate and glutamine was altered in NTR/TRX mutants (Fonseca-Pereira, da *et al.*, 2020; Lima *et al.*, 2021; Porto *et al.*, 2022), strengthening the idea that this pathway is redox regulated by the TRX system. Here, we carried out an extensive metabolic and protein characterization to better understand the role of the NTR/TRX system for the regulation of the GS/GOGAT cycle and its importance for plant high-light (HL) stress acclimation.

Bioinformatics analyses strongly suggest an important role of NTR/TRXs in the regulation of nitrogen metabolism enzymes

Arabidopsis GS is a homo octameric isozyme with a native molecular weight of approximately 320 and 380 kDa for the cytosolic (GS1) and mitochondria/chloroplastic (GS2) isoforms (LEA *et al.*, 1990). Beyond being sensitive to DDT and $FeCl_3$, which *per se* strongly suggest that GS be redox regulated (Choi, Kim e Kwon, 1999; Ortega, Roche e Sengupta-Gopalan, 1999), previous *in vitro* assays in *Canavalia lineata* and *Chlamydomonas reinhardtii* demonstrated that the activity of GS and GOGAT were higher in the presence of TRXs plus DDT (Choi, Kim e Kwon, 1999; Florencio, Gadal e Buchanan, 1993; Tischner e Schmidt, 1982). TRX affinity chromatography studies have also proposed that GDH and GOGAT are TRX targets (Balmer *et al.*, 2004; Motohashi *et al.*, 2001; Yoshida *et al.*, 2013). Here, we have used different bioinformatics approaches and demonstrated that both GS isoforms, GOGAT, and GDH own conserved Cys residues in different plant species. We further demonstrated that GS1 and GS2 have high probability to form disulfide bonds among 92-228 and 150-306 Cys residues, respectively. Interestingly, our TRX *o1*/*h2*-GS1/2 molecular dockings demonstrated that both TRX *o1* and *h2* were close to 228 Cys residue of GS1 and 306 Cys residue of GS2, both Cys residues were predicted to form a disulfide bridge through Dianna web server. In addition, GOGAT (GLU1) and

GDH isoforms also demonstrated a high probability to form disulfide bonds (Table S1). Our results coupled to previous reports suggest that GS, GOGAT and GDH are likely regulated by TRXs.

The mitochondrial NTR/TRX system regulates the interplay between carbon and nitrogen metabolisms

Plant carbon and nitrogen metabolisms are closely linked, and the synergistic dependence of both metabolisms is essential for plant growth, development and abiotic stress acclimation (Fernie e Morgan, 2013; Lehmann *et al.*, 2015; Szal e Podgórska, 2012). The synthesis of amino acids strongly depends on carbon skeletons derived from glycolysis and the TCA cycle, which makes the respiration process a hub for the interplay between carbon and nitrogen metabolisms (Hildebrandt *et al.*, 2015). In this context, it has been shown that the mitochondrial NTR/TRX system is an important player for the regulation of the metabolic fluxes throughout the TCA cycle and associated pathways (Daloso, Danilo M *et al.*, 2015; Fonseca-Pereira, da *et al.*, 2020; Lima *et al.*, 2021; Porto *et al.*, 2022; Reinholdt, Schwab, Zhang, Reichheld, J. P., *et al.*, 2019). However, the precise elucidation of the specific role of TRX isoforms has been a great challenge in plant biology, mainly due to the high number of TRX isoforms and the presence of other compensatory redox mechanisms found in plants (Schwarzländer e Fuchs, 2019; Souza, Paulo V L *et al.*, 2018).

In the last decade, extraordinary efforts have been made to elucidate the role of the non-chloroplastic NTR/TRX system (Daloso, Danilo M *et al.*, 2015; Fonseca-Pereira, da *et al.*, 2020; Meyer *et al.*, 2012), especially for the regulation of two important metabolic pathways namely photorespiration and respiration. Mitochondria has two TRX o isoforms (*o1* and *o2*), while the exact TRX *h2* sublocalization is still uncertain. Previous studies suggested that TRX *h2* would be located at the mitochondria in Arabidopsis and *Populus trichocarpa* (Gelhaye et al., 2004; Meng et al., 2010), and also associated with the endoplasmic reticulum (ER)-Golgi membrane system in Arabidopsis (Traverso et al., 2013). However, recent cell fractionation and immunoblot analyses demonstrated that TRX *h2* is found at the microsomal fraction (Hou et al., 2021). This suggests that TRX *h2* is found in the endomembrane system rather than mitochondria or cytosol. However, previous studies highlight that certain metabolic changes are similar between *trxh2* and *trxo1* mutants (Hou et al., 2021), as also observed here (Figure 15). Thus, although these proteins are probably located in different cell compartments, they share some mechanism in the redox control

of primary metabolism, which can be associated to similar alterations in in the metabolism of other redox players such as NAD(P)(H), ROS, glutathione and ascorbate (Hou et al., 2021). However, our results indicate that TRX o1 rather than TRX *h2* has greater influence on the regulation of GS/GOGAT pathway, especially in illuminated leaves.

In the presence of light, the chloroplastic TRX system acts as positive regulators of photosynthetic enzymes (Buchanan, 2016b; Yoshida e Hisabori, 2021). On the other hand, respiration is partially inhibited in the light, which seemingly involves the inactivation of enzymes mediated by the non-chloroplastic NTR/TRX system and other transcriptional and post-translational mechanisms (Fonseca-Pereira, da *et al.*, 2021). For instance, it has been reported that the PDH complex is inhibited by phosphorylation in the light (Kromer, 1995; Zhang *et al.*, 2021) and that the mtLPD, a subunit shared by several enzymatic complexes including PDH, GDC and OGDH, is deactivated by TRX *h2* and TRX *o1 in vitro* (Fonseca-Pereira, da *et al.*, 2020; Reinholdt, Bauwe, *et al.*, 2019). In this scenario, the light-triggered inhibition of PDH decreases the conversion of pyruvate into acetyl-CoA (AcCoA) and thus the input of carbons into the TCA cycle via this pathway. The synthesis of glutamate highly depends on carbons derived from the TCA cycle (Calderon e Mora, 1989; Fontaine *et al.*, 2012). Thus, plants have alternative mechanisms such as the entrance of carbons from previously stored citrate and the activities of alanine amino transferase and malic enzyme that converts alanine and malate into pyruvate inside the mitochondria, respectively (Le *et al.*, 2022; Le, Lee e Millar, 2021; Le e Millar, 2022) (Figure 16). These mechanisms collectively contribute to overcome the PDH-inhibition barrier and maintain the C6-branch of the TCA cycle running, which leads to the synthesis of 2-oxoglutarate (2-OG), the immediate substrate of the GS/GOGAT cycle (Abadie *et al.*, 2017b; Tcherkez *et al.*, 2012). Our results showed that the level of glutamate is substantially increased in both *trxo1* and *ntrab* mutants (Figure 15), highlighting that the mTRX system is key for the connection between carbon and nitrogen metabolisms.

It has been previously shown that succinate dehydrogenase (SDH) and fumarase (FUM) are inhibited by TRX *o1 in vitro*, while citrate synthase and isocitrate dehydrogenase (IDH) are activated by TRX *o1* (Daloso, Danilo M *et al.*, 2015; Noguchi e Yoshida, 2008; Schmidtmann *et al.*, 2014). As expected, the level of TCA cycle metabolites such as citrate, fumarate, malate, and succinate were substantially altered in both *trx o1* and *ntrab* mutants, further strengthening the role of TRX *o1* and NTRA/B in controlling the metabolic fluxes throughout the TCA cycle. Moreover,

it was recently demonstrated that the fluxes from ^{13}C-glucose and the PEPc-mediated ^{13}C-HCO_3 assimilation toward glutamate and glutamine, respectively, are higher in illuminated leaves of the *trxo1* mutant than the WT (Lima *et al.*, 2021; Porto *et al.*, 2022). Here, our ^{13}C-pyruvate labelling experiment demonstrated that the M2/M0 ratio of glutamate have increased in dark-exposed and illuminated leaves of both *trxo1* and *ntrab* mutants over time, and this was not observed in WT or *trxh2* mutant (Figure 17). The lack of increases in the ^{13}C-enrichment in glutamate in the WT could be explained by the inhibition of the PDH and/or by the time of labelling (60 min), given that longer time (240 min) under [U^{13}C]-pyruvate was sufficient to label glutamate in illuminated Arabidopsis leaves (Daloso, Danilo M *et al.*, 2015; Lima *et al.*, 2021). By contrast, the increase in M2/M0 ratio of glutamate and pyroglutamate in *trxo1* and *ntrab* suggests that the mitochondrial NTR/TRX system restrict the flux from pyruvate to glutamate *in vivo* in both dark and light conditions, as previously suggested (Porto *et al.*, 2022). Our results collectively indicate that the mitochondrial NTR/TRX system plays an important role in regulating the TCA cycle-derived carbon flux toward glutamate synthesis.

Redox regulation of enzymes associated to glutamate metabolism

GS has two isoforms with distinct physiological roles (Gaufichon, Rothstein e Suzuki, 2016). The mitochondrial and chloroplastic GS2 has been described to play an essential role in the assimilation of the NH_4^+ released by the GDC complex (Taira *et al.*, 2004), while the cytosolic GS1 is important to maintaining the nitrogen remobilization to sink organs and during senescence (Ishiyama *et al.*, 2004; Masclaux-Daubresse *et al.*, 2010). The absence of GS2 leads to severe deleterious effects, being lethal to some plant species (Hachiya *et al.*, 2021; Wallsgrove *et al.*, 1987), while plants lacking GS1 causes severe growth impairment (Guan, Møller e Schjoerring, 2015; Oliveira e Coruzzi, 1999). It is clear therefore that these isoforms are highly important for plant growth and that their function goes beyond NH_4^+ assimilation (Liu, Hu e Chu, 2022). Understanding the mechanisms by which GS is regulated is key for plant metabolic engineer (Sweetlove, Nielsen e Fernie, 2017). Here, our data strongly suggests that GS is directly or indirectly regulated by TRXs, especially under illuminated conditions. Evidence supporting this idea are several folds. First, the protein content of both GS1 and GS2 decreased in all mutants at ED (Figures 19b-c). Second, GS activity was lower in both *trxo1* and *trxh2* mutants, compared to

the WT at ED (Figure 18a). Third, the redox status of GS was substantially altered in all mutants (Figure 20). Intriguingly, however, the intensity of the reduced band of GS was higher in *trxh2* and *ntrab* and lower in *trxo1* mutants, when compared to the WT at ED (Figure 20a). This result *per se* suggests that TRX *o1* and TRX *h2* would act activating and deactivating GS *in vivo*. This antagonistic role of TRX *o1* and TRX *h2* has also been observed in the regulation of fumarase (FUM), in which the addition of TRX *h2* and TRX *o1* to the enzymatic assay increased and decreased the activity of FUM (Daloso, Danilo M *et al.*, 2015). However, a more complex picture raises in the case of GS, given that the changes in the redox status do not explain the activity in the mutants, which could be associated to a yet not understood mechanism present in the mutants.

Another intriguing response is the increase in the intensity of the reduced band in the *ntrab* double mutant at ED, but not at EN (Figure 20a). NTRA and NTRB are enzymes found in nucleus, cytosol and mitochondria (Bashandy *et al.*, 2010; Meyer *et al.*, 2008; Møller e Rasmusson, 1998). Despite the importance of NTRA and B in reducing (activating) non-chloroplastic TRXs, it has been reported that glutathione reductases (GR) can compensate the lack of these two NTRs (Marty, Bausewein, Müller, Bangash, Moseler, Schwarzländer, Müller-Schüssele, *et al.*, 2019; Marty, L. *et al.*, 2009; Reichheld *et al.*, 2007). This could explain the increase in the reduced band of GS in the *ntrab* double mutant, in which another compensatory mechanism (e.g. GRs) could compensate the lack of the non-chloroplastic NTRs. However, the reduced band is lower at EN in the *ntrab* double mutant, similar to the observed in the *trxo1* mutant (Figure 20e). Given that the gel shift analysis did not discriminate GS isoforms, thanks to the superposition of the oxidized and reduced bands of GS1 and GS2, our results suggest that GS could be differentially regulated according to its location in the cell or with the prevailing environmental condition. Further proteomics and enzymatic analyses using isolated GS isoforms are now needed to better understand its redox regulation.

Our results further showed that the activities of GS, GOGAT and GDH were lower in *trxo1* than the WT at ED, while GS was lower and both GOGAT and GDH were higher in *trxo1* than the WT at EN (Figure 16). The activity of these enzymes collectively modulates the level of 2-OG, Glu and Gln. The *trxo1* mutant had higher and lower levels of Glu and Gln at ED. This could be associated to a lower conversion of Glu to 2-OG and Gln to Glu, given that the decrease in the activity of GDH and GOGAT was more severe (44% and 28%, respectively) than the decrease in GS (22%) in this mutant at ED, when compared to the WT. The higher content of glutamate in the

trxo1 could be also explained by a higher availability of 2-OG, which is in turn explained by the higher metabolic fluxes throughout the TCA cycle previously shown in this mutant (Daloso, Danilo M *et al.*, 2015; Florez-Sarasa, Obata, Del-Saz, Nï¿½stor Fernï¿½ndez, *et al.*, 2019; Porto *et al.*, 2022). Given that no difference has been observed in the accumulation of glutamate at ED and EN in the *trxh2* mutant, as compared to the WT in these conditions (Figure 15), and no ^{13}C-enrichment was observed in this metabolite in this mutant (Figure 16c), it seems that the regulation of the TCA cycle fluxes toward glutamate is dependent on the mitochondrial NTR/TRX system rather than TRX *h2*.

On the role of the NTR/TRX-mediated regulation of the GS/GOGAT cycle for plant high-light stress acclimation

Light is a fundamental environmental cue for plants (Giovagnetti e Ruban, 2015). Light absorption by plant photosynthetic pigments and its conversion into chemical energy is the basis of earth life (Ruban, 2015). However, the excess of light absorption can damage photosystems and organic molecules, ultimately leading to cell death (Johnson e Ruban, 2011; Takahashi *et al.*, 2010). Plants have then developed mechanisms to avoid high-light (HL) stress-mediated photoinhibition, which involves not only changes in chloroplast processes but also activation of several metabolic pathways out of the chloroplast, especially the (photo)respiratory metabolism in mitochondria and peroxisomes (Giovagnetti e Ruban, 2015; Pintó-Marijuan e Munné-Bosch, 2014). For instance, we have previously shown that the activities of both GS and nitrate reductase (NR) are substantially increased in cotton plants under HL stress and that this is dependent on the NO_3 availability (Guilherme *et al.*, 2019). The upregulation of these enzymes coupled to increases in photorespiration protected cotton plants from the excess of light absorbed (Guilherme *et al.*, 2019). These pathways are then important sink of reducing power produced in the chloroplasts under photoinhibitory conditions. In parallel, it has been previously shown that the mitochondrial lipoamide dehydrogenase (mtLPD), the L subunit of glycine decarboxylase complex (GDC), an important protein of the photorespiratory metabolism, is regulated by both TRX *h2* and TRX *o1 in vitro* (Fonseca-Pereira *et al.*, 2019; Reinholdt, Schwab, Zhang, Reichheld, J., *et al.*, 2019). Taking this into account, we then decided to investigate the role of the NTR/TRX system-mediated regulation of the GS/GOGAT/GDH cycle for plant acclimation to a short HL stress. Our

photochemical results showed that the decrease in F_v/F_m was more severe in the *trxo1* mutant, as previously shown (Florez-Sarasa, Obata, Del-Saz, Nï¿½stor Fernï¿½ndez, *et al.*, 2019; Reinholdt, Bauwe, *et al.*, 2019). Interestingly, the HL stress-mediated increases in GS activity was stronger in *trxo1*, which also showed higher activities of GOGAT and GDH under HL, compared to all other genotypes (Figures 21c-d). The increased GS activity under HL is in contrast to the decreased GS activity under HL in barley (Brestic *et al.*, 2014), but corroborates the increases in GS activity described in cotton (Guilherme *et al.*, 2019), highlighting that the modulation of GS activity may range according to the species and/or the level of the HL stress. Furthermore, the increased GS activity under HL (Figure 21b) contrast with the lower GS activity found in the *trxo1* mutant under non-stress condition (Figure 18a), highlighting that the effects of the lack of TRX *o1* on GS may range according to the environmental condition.

The GC-MS-based metabolite profiling analysis showed that the HL-mediated metabolic responses of both *trxo1* and *ntrab* were very distinct from those observed in the WT, as evidenced by the clear separation of these genotypes by the PC1 (Figure 22a). This was associated to a differential accumulation of glutamate, proline, pyruvate and metabolites associated to the TCA cycle and photorespiration (Figure 22b). Interestingly, the levels of glutamate, fumarate, homoserine, methionine, lysine and serine were substantially higher in ED-HL than ED-GL in the WT, and this was not observed in any mutant studied here. By contrast, the level of these metabolites and others from nitrogen (asparagine) and photorespiration (glycolate) was lower in *trxo1* and/or *ntrab* under HL than GL conditions (Figure 21). Given that these metabolic alterations were minor or not observed in the *trx h2* mutant, it strengthens the idea discussed above that the regulation of (photo)respiration and the glutamate metabolism is more dependent on the mitochondrial NTR/TRX system rather than the TRX h2. Indeed, it has been shown that the *trxo1* is more sensitive to HL (Florez-Sarasa, Obata, Del-Saz, Nï¿½stor Fernï¿½ndez, *et al.*, 2019) and that the photosynthetic acclimation to step-wise increases in light intensity is disrupted in *trxo1* (Reinholdt, Bauwe, *et al.*, 2019). The phenotype of the *trxo1* mutant under HL has been associated to a slower conversion of glycine to serine catalyzed by GDC and SHMT, suggesting that the TRX-mediated regulation of photorespiration is necessary for plant HL acclimation (Reinholdt, Bauwe, *et al.*, 2019). Beyond confirming this hypothesis, our metabolic data from HL-stressed plants further suggest that the lack of the mitochondrial NTR/TRX system alter the connection between carbon and nitrogen metabolisms. For instance, glutamate was negatively correlated with pyruvate

only in WT plants (Figure 25), suggesting that the increased level of glutamate is associated to the reductions in pyruvate under HL (Figure 23), but this response is lost in the mutants, especially in *trxo1* and *ntrab*.

Conclusion

We have provided compelling evidence indicating that the enzymes of the nitrogen metabolism, especially GS, is directly or indirectly regulated by the mitochondria NTR/TRX system (Figure 13). This idea is supported by *in silico* (bioinformatics), *in vitro* (enzymatic), and *in vivo* (metabolic) analyses. Whilst our molecular docking analysis strongly corroborate previous *in vitro* studies showing that GS is a redox sensitive enzyme (Florencio, Gadal e Buchanan, 1993; Motohashi *et al.*, 2001; Tischner e Schmidt, 1982; Yoshida *et al.*, 2013), the increased ^{13}C-enrichment in glutamate derived from ^{13}C-pyruvate indicates that the TRX *o1*/NTRA/B system coordinate the fluxes from the tricarboxylic toward the GS/GOGAT cycle, which is important for plant HL stress acclimation.

The main Figures chapter 3

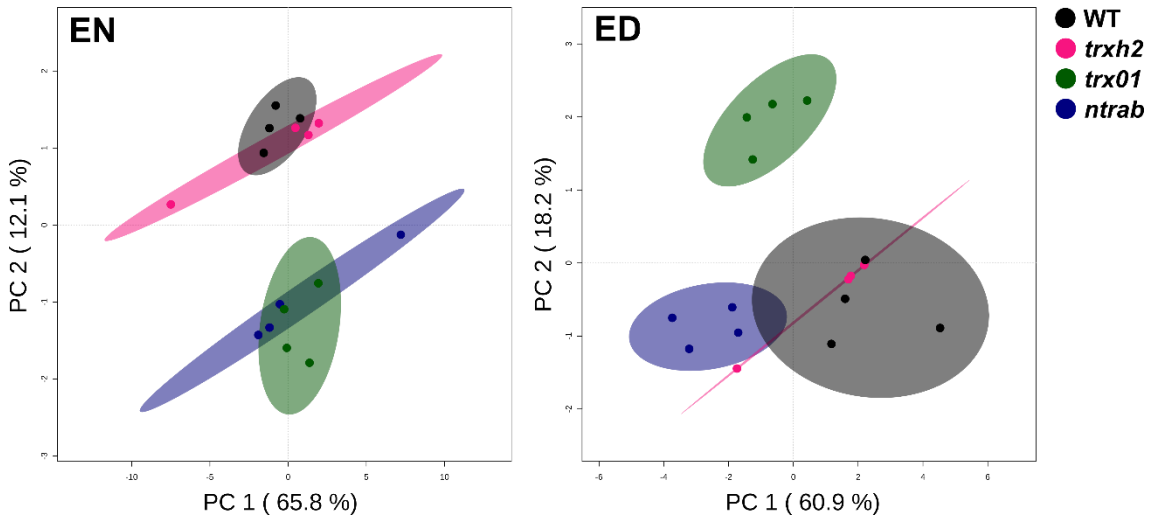

Figure 14. Principal component analysis (PCA) carried out using GC-MS-based metabolite profiling data of leaves from the wild type (WT) and the *trxh2*, *trxo1*, and *ntrab* mutants harvest at the end of the night (EN) (a) and end of the day (ED) (b). The two main components and the percentage variation explained by PC1 and PC2 are represented in the axis of the figures. PCA was carried out using the Metaboanalyst platform.

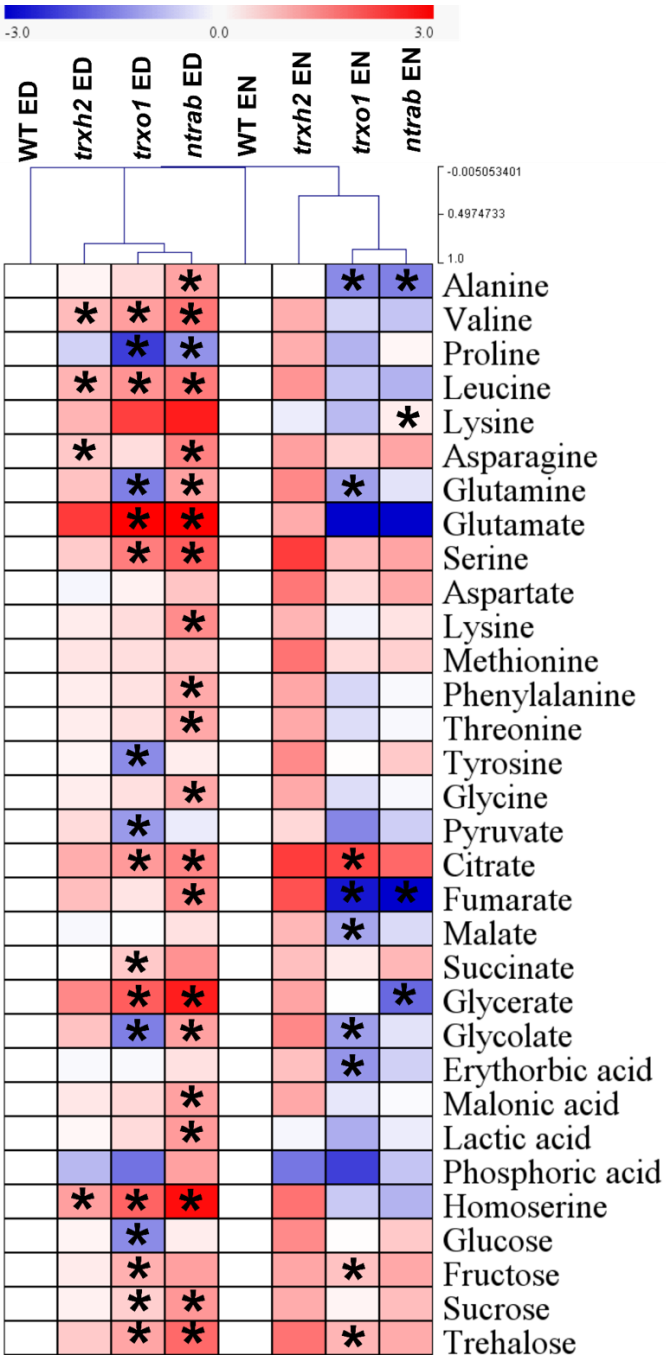

Figure 15. Heatmap representation of the GC-MS-based metabolite profiling carried out in leaves from the wild type (WT) and the *trxh2*, *trxo1*, and *ntrab* mutants harvest at the end of the night (EN) (a) and end of the day (ED) (b). The average values of the metabolite level (normalized to Ribitol and fresh weight) were normalized according to the WT values found at ED and EN $\log_2$ transformed (n=4). Red and blue colors represent increased and decreased abundance in primary metabolites related to the WT at ED and EN. Asterisks (*) indicate values that are significantly different from the WT in each condition by the Student's t-test ($P < 0.05$)

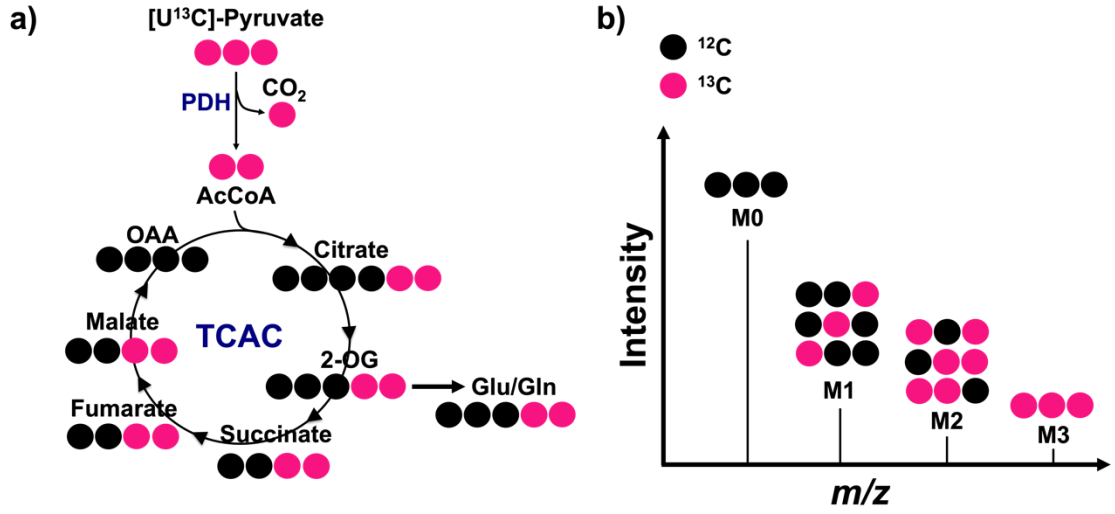

Figure 16. Schematic representation of the distribution of carbons derived from pyruvate degradation mediated by pyruvate dehydrogenase (PDH) throughout the tricarboxylic acid cycle (TCAC) and glutamate metabolism. a) Simplified schematic representation of the TCAC describing the incorporation of two ^{13}C-labelled carbons (pink spheres) derived from uniformly ^{13}C-labelled pyruvate [(U^{13}C]-pyruvate) into the TCAC glutamate (Glu)/glutamine (Gln). b) Schematic representation of the natural ^{13}C-abundance of a hypothetical metabolite fragment composed of three carbons obtained by GC-MS analysis. M0 represents the fragment with no ^{13}C, while M1, M2 and M3 contain the incorporation of 1, 2 or 3 ^{13}C, respectively. Black and pink spheres represent respectively ^{12}C and ^{13}C in both figures.

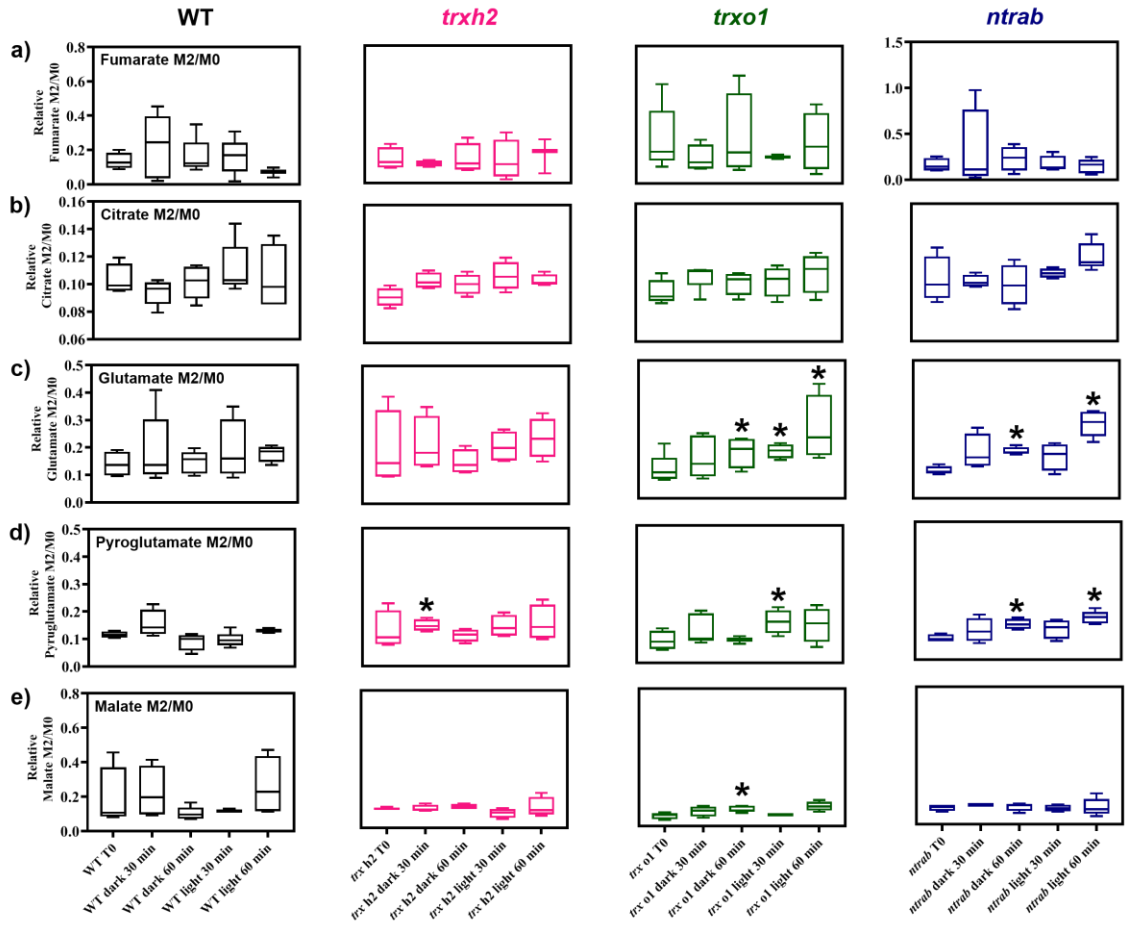

Figure 17. Box plots representing the M2/M0 isotopologues ratio in fumarate (a), citrate (b), glutamate (c), pyroglutamate (d) and malate (e)**.** M0 and M2 represent the isotopologues of a fragment of the metabolites with 0 and 2 ^{13}C incorporated. Detached leaves of wild type (WT) and knockout mutants (*trxo1*, *trxh2*, and *ntrab*) of *Arabidopsis thaliana* L. were subjected to 15 mM [U^{13}C]-pyruvate for 0, 30 and 60 min under light (120 - 150 µmol m^{-2} s^{-1} photosynthetic photon flux density) or darkness conditions. The WT, *trxo1*, *trxh2*, and *ntrab* are represented by black, pink, green, and blue colors, respectively. Asterisks (*) indicate values that are significantly different from the time 0 of each genotype by the Student's t-test ($P < 0.05$)

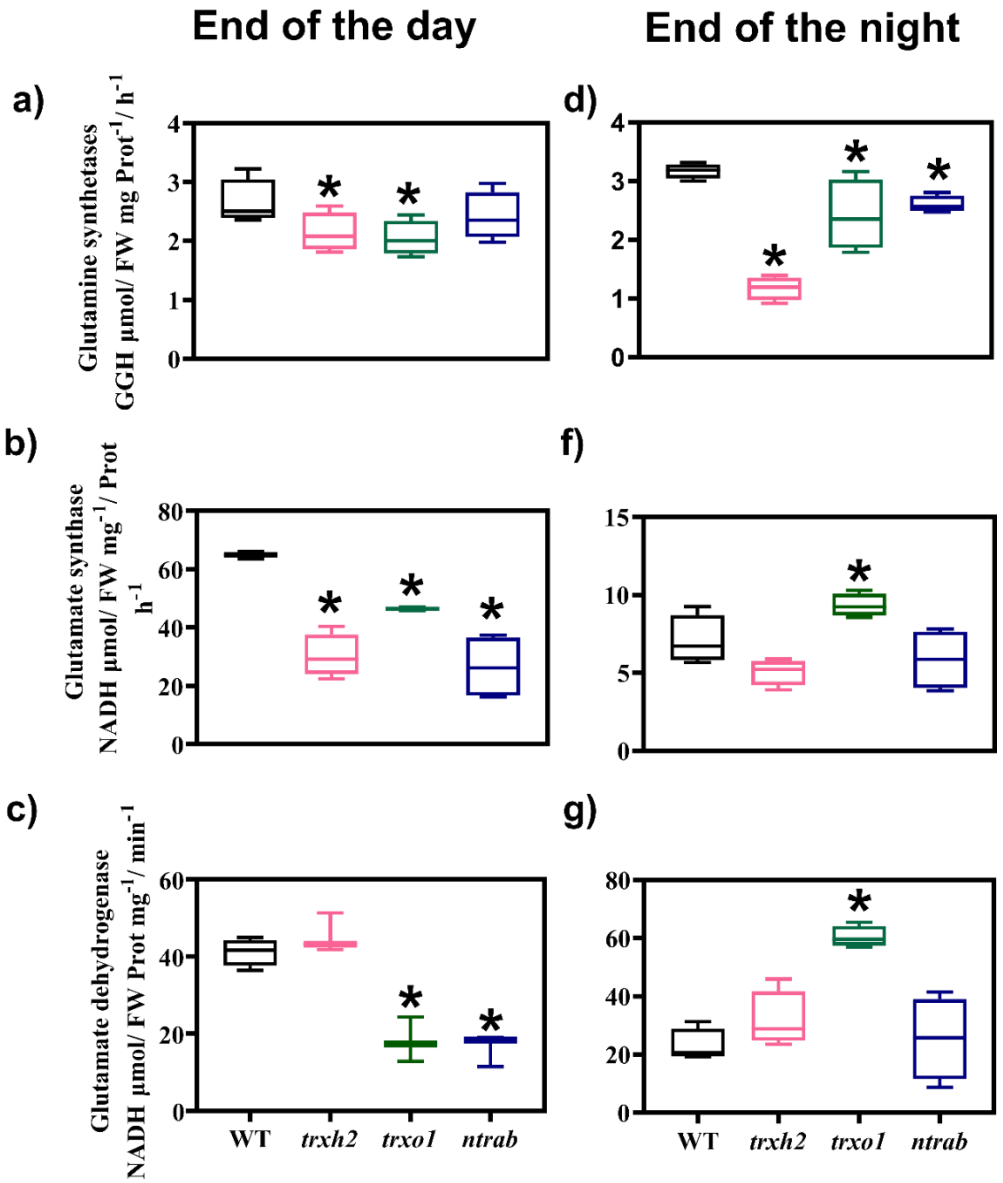

Figure 18. Activity of enzymes related to the nitrogen metabolism carried out in leaves of *Arabidopsis thaliana* L. wild type (WT) and mutants lacking TRX h2 (*trxh2*), TRX o1 (*trxo1*), and NTRA & NTRB (*ntrab*) harvested at end of the day (ED) (a-c) and end of the night (EN) (e-f) of short-day (125 µmol photons m^{-2} s^{-1}; 08:16 h photoperiod) grown plants. The activity of glutamine synthetase (a,d) (GS), glutamate synthase (GOGAT) (b,e), and glutamate dehydrogenase (GDH) (c,f) are expressed by mg of fresh weight (FW) per protein $^{-1}$ hour^{-1}. Black, pink, green and blue box plots represent averages and standard errors of WT, *trx h2*, *trx o1*, and *ntrab* genotypes, respectively (n = 4).Asterisks (*) indicate values that are significantly different from the WT in each condition by the Student's t-test ($P < 0.05$)

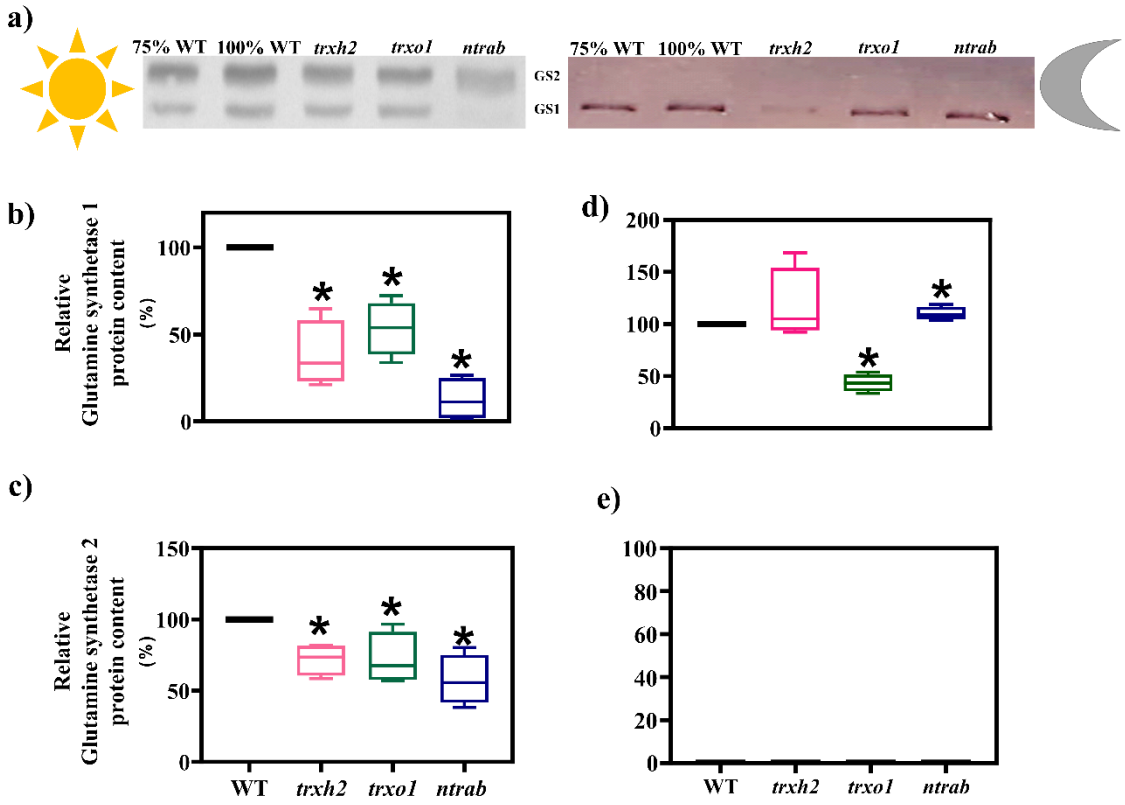

Figure 19. Immunoblot analysis of glutamine synthetase (GS) isoforms carried out in leaves of *Arabidopsis thaliana* L. wild type (WT) and mutants lacking TRX h2 (*trxh2*), TRX o1 (*trxo1*), and NTRA & NTRB (*ntrab*). GS was identified using specific antibodies for both GS isoforms in leaf protein extracts from the wild type (WT) and *trxh2*, *trxo1*, and *ntrab* mutants harvested at end of the day (ED) or end of the night (EN). The content of GS subunits was determined by comparing the intensity of the band found in the mutants compared to a protein amount gradient found in WT samples (75% and 100%). 25 µg of total protein content corresponding to 100% in all genotypes. GS2 was not detected at EN, which is associated to the dark-mediated degradation previously documented for this isoform. Asterisks (*) indicate values that are significantly different from the WT in each condition by the Student's t-test ($P < 0.05$)

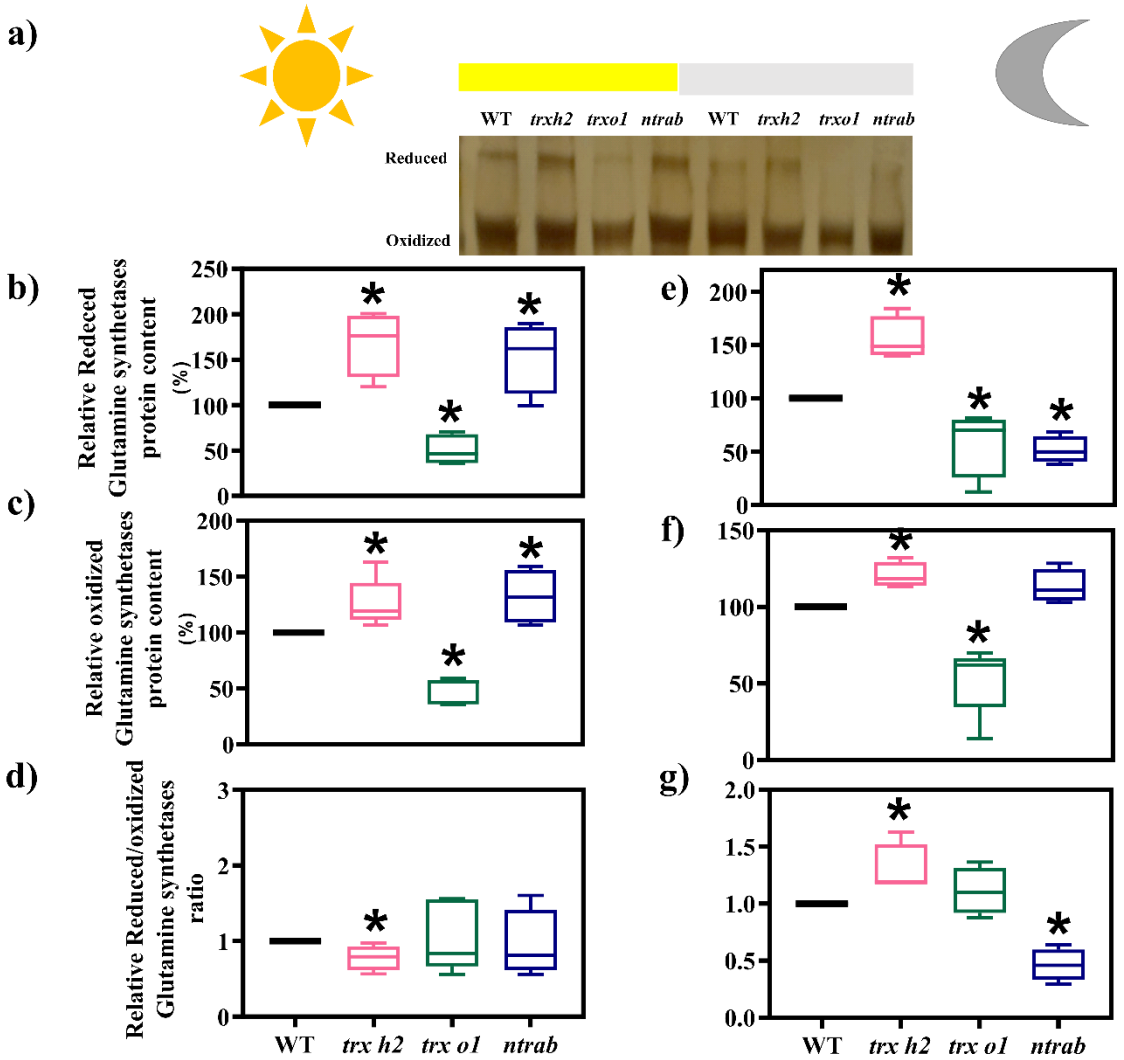

Figure 20. Gel shift analysis of glutamine synthetase (GS) isoforms carried out in leaves of *Arabidopsis thaliana* L. wild type (WT) and mutants lacking TRX h2 (*trxh2*), TRX o1 (*trxo1*), and NTRA & NTRB (*ntrab*). Total leaf proteins were extracted in the presence of 10% TCA and protein thiols were alkylated with 10-mM mm-PEG_{24}. Proteins were resolved in SDS-PAGE (15% polyacrylamide) under non-reducing conditions, transferred to nitrocellulose membrane, and probed with GS antibody (dilution 1:2,000), followed by incubation with secondary antibody (Sigma secondary antibody anti-rabbit, dilution 1:20,000). The blots were revealed by BCIP/NBT. The data represent the protein bands of both oxidized and reduced bands from leaf samples harvested at the end of the day (ED) and the end of the night (EN), normalized by the fresh weight (FW) used in the protein extraction. Asterisks (*) indicate values that are significantly different from the WT in each condition by the Student's t-test ($P < 0.05$)

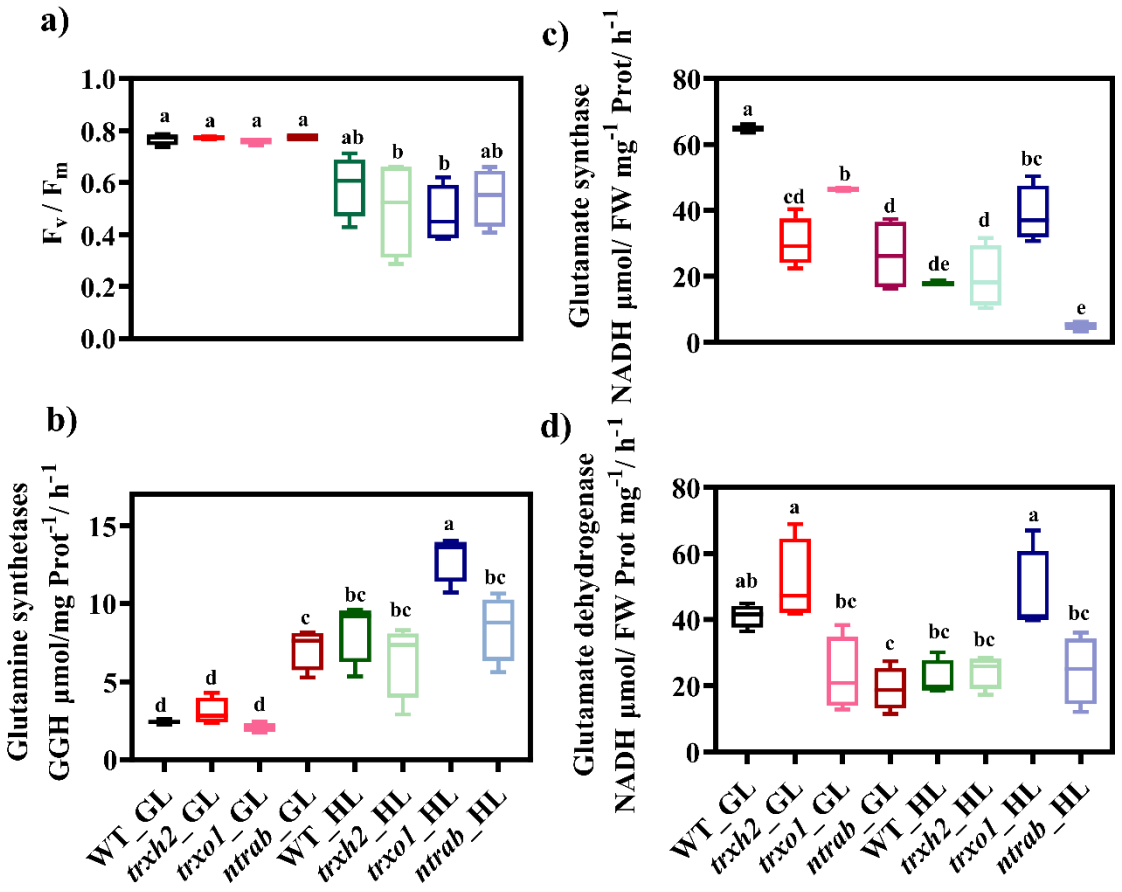

Figure 21. Photochemical and enzymatic analyses of *Arabidopsis thaliana* L. wild type (WT) and mutants lacking TRX h2 (*trxh2*), TRX o1 (*trxo1*), and NTRA & NTRB (*ntrab*) under grown (GL) and high-light (HL) conditions. a) Potential quantum yield of the photosystem II (Fv/Fm) measured in dark-adapted leaves. b-d) The activity of glutamine synthetase (b) (GS), glutamate synthase (GOGAT) (c), and glutamate dehydrogenase (GDH) (d) were measured in leaf samples harvested at the end of the day from plants subjected to 08 h of GL or HL. Enzyme activity is expressed by mg of fresh weight (FW) per protein $^{-1}$ hour^{-1}. Means that do not share a letter are significantly different according to ANOVA and Tukey test analysis ($P < 0.05$).

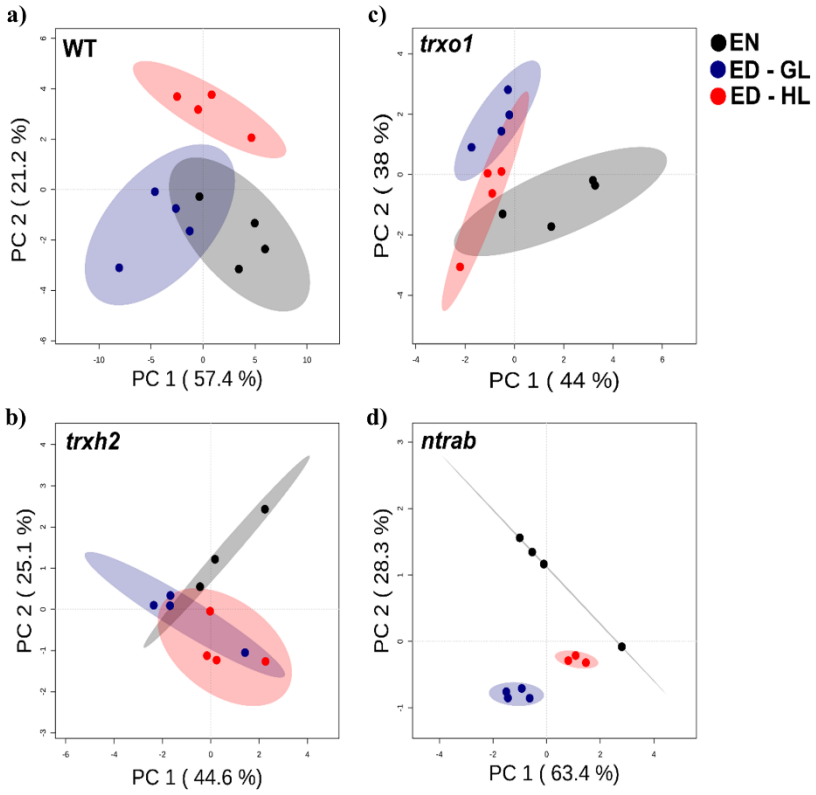

Figure 22. Principal component analysis (PCA) carried out using GC-MS-based metabolite profiling data of leaves from the wild type (WT) and the *trxh2*, *trxo1*, and *ntrab* mutants harvest at the end of the night (EN) and end of the day (ED) from plants exposed to 08h of growth light (~120 µmol photons m^{-2} s^{-1}) (ED-GL) or high-light (HL) (~550 µmol photons m^{-2} s^{-1}) conditions. The two main components and the percentage variation explained by PC1 and PC2 are represented in the axis of the figures. PCA was carried out using the Metaboanalyst platform.

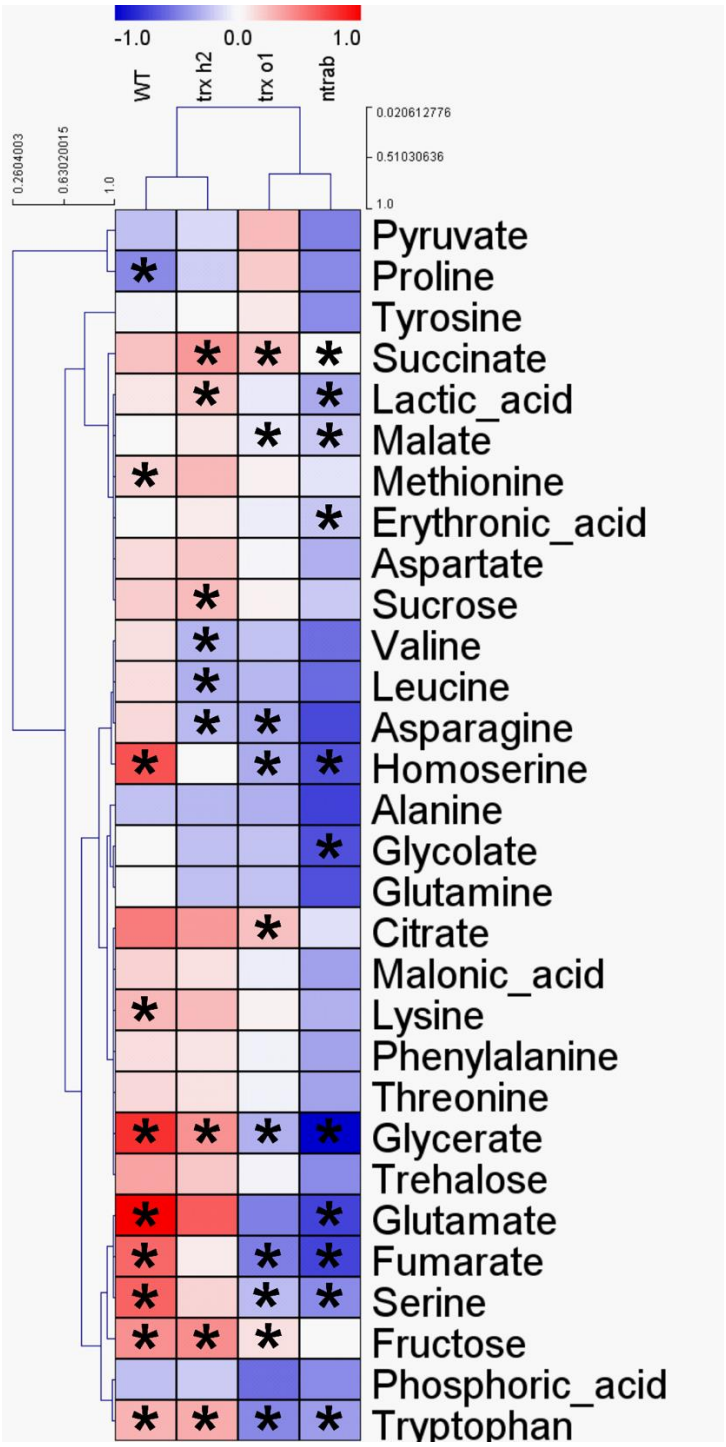

Figure 23. Heatmap representation of the GC-MS-based metabolite profiling carried out in leaves from the wild type (WT) and the *trxh2*, *trxo1*, and *ntrab* mutants harvest at the end of the day (ED) from plants exposed to 08h of growth light (~120 µmol photons m^{-2} s^{-1}) (ED-GL) or high-light (HL) (~550 µmol photons m^{-2} s^{-1}) conditions. The average values of the metabolite level (normalized to Ribitol and fresh weight) found in ED-GL and ED-HL were first normalized according to the values found at EN in each genotype. After that, the values of the ED-HL were normalized according to those of the ED-GL and log_2 transformed. Red and blue colors represent

increased and decreased abundance in primary metabolites found in ED-HL related to ED-GL in each genotype. Asterisks (*) indicate values that are significantly different between increased and decreased abundance in primary metabolites found in ED in each genotype by the Student's t-test ($P < 0.05$)

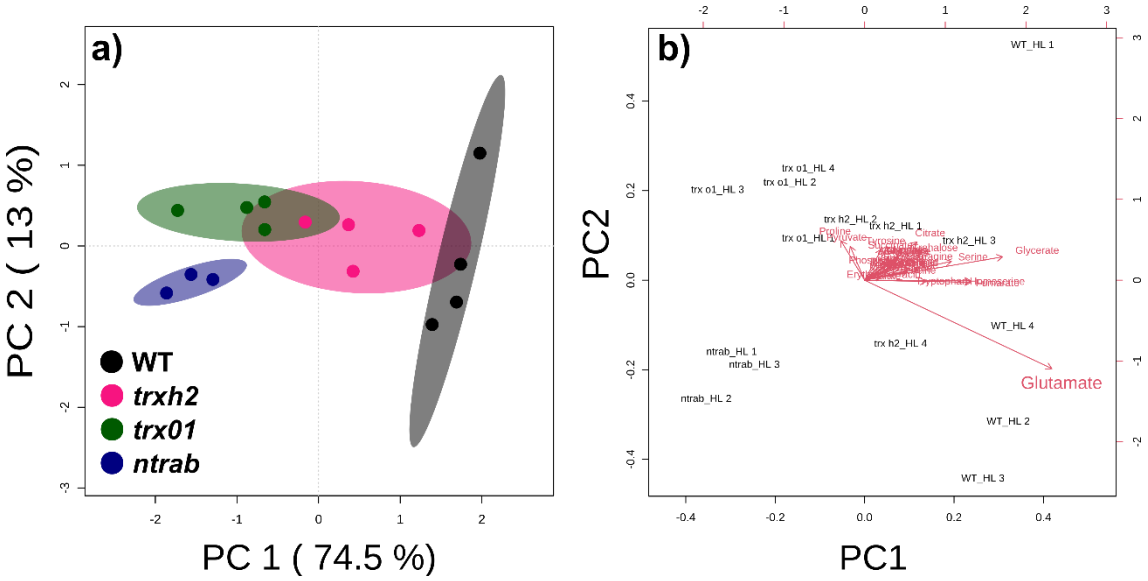

Figure 24- Principal component (PCA) (a) and biplot (b) analysis of the disposed in the figure 10. The two main components and the percentage variation explained by PC1 and PC2 are represented in the axis of the figures. Both analyses were carried out in Metaboanalyst platform.

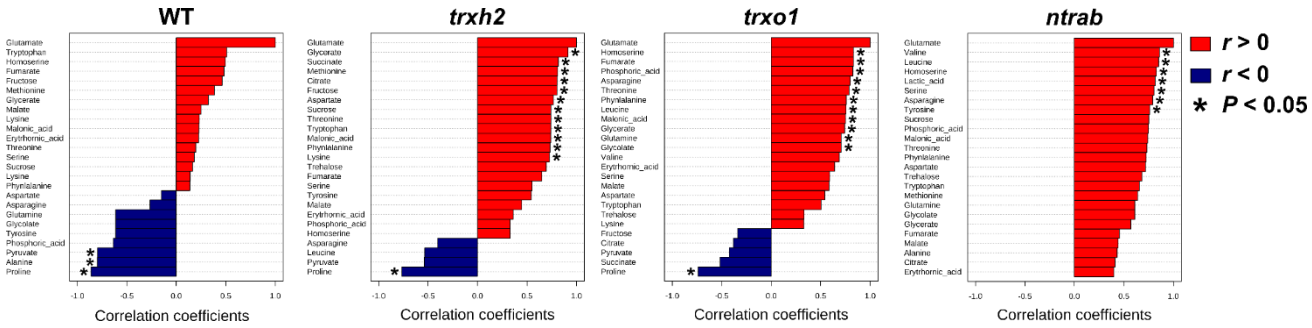

Figure 25. Pattern search analysis showing the top 25 correlated metabolites with glutamate, according to a Pearson correlation analysis. Positive and negative Pearson correlation coefficients (*r*) are highlighted in red and blue colors, while –asterisks (*) indicate significant *r* ($P < 0.05$). Pattern search analysis was carried out using the Metaboanalyst platform.

Supplementary Figures Chapter 3

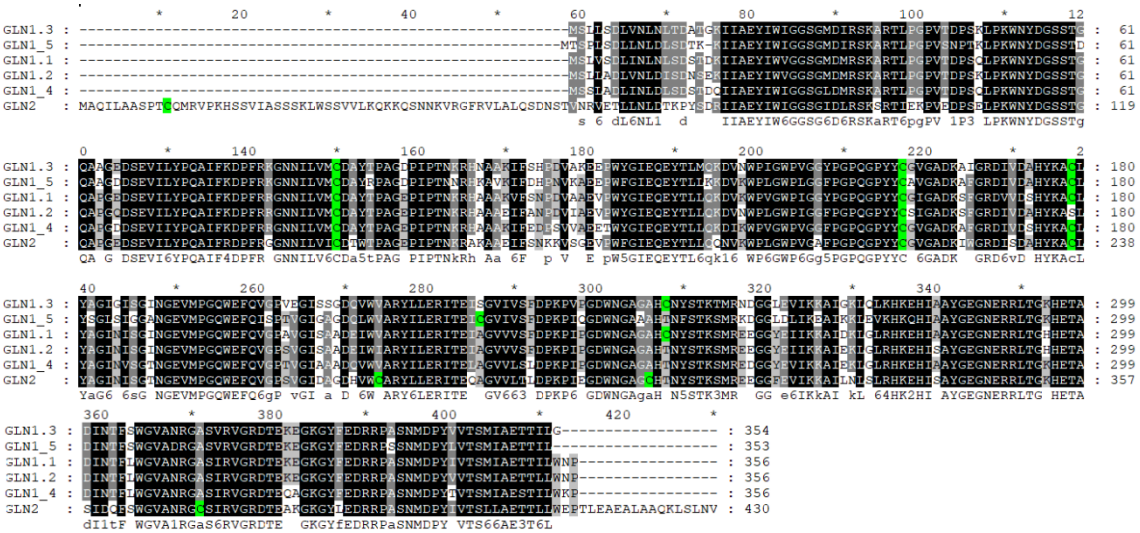

Figure S1. Alignment of amino acid sequences of glutamine synthetases 1 (GS1) and 2 (GS2) isoforms. The amino acid sequences from Arabidopsis thaliana L. were obtained from the National Center for Biotechnology Information (NCBI) (https://www.ncbi.nlm.nih.gov/), aligned using the ClustalW platform (https://www.genome.jp/tools-bin/clustalw) and visualized using the GeneDoc® software. Cys residues are highlighted in green. The following sequences from Arabidopsis thaliana were used: NCBI ID: GS2, NP_001031969.1; GLN1.1, sp|Q56WN1.2; GLN1.2, AEE34474.1; GLN1.3, NP_188409.1;GLN1.4, NP_568335.1; GLN1.5, AEE32297.1.

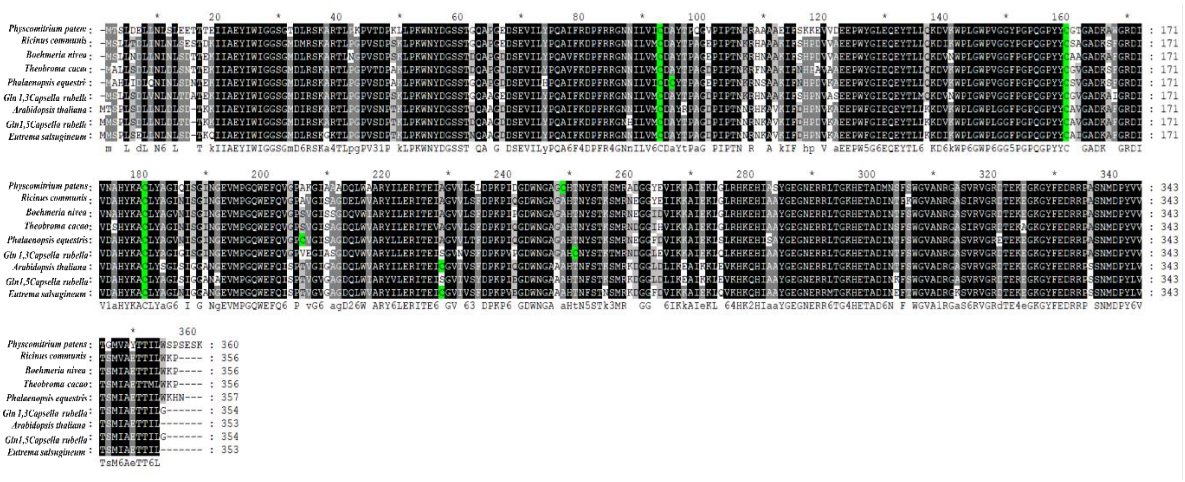

Figure S2. GS1 cys conserved residues between different organisms. Amino acid GS1 sequences were obtained from the National Center for Biotechnology Information (NCBI). Through the Blatst platform tool (https://blast.ncbi.nlm.nih.gov/Blast.cgi), we chosen the GS2 homologous protein sequences from different species, which had higher similarity in protein sequence in comparison with *At*GS1. Subsequently, the alignment between *At*GS1 and the homologous GS1 from different organisms was performed using the clustaw platform (https://www.ebi.ac.uk/Tools/msa/clustalw2/), the alignments were analyzed using the GeneDoc platform program. Sequences NCBI I.D: NP_175280.1 -*Arabidopsis thaliana*; XP_006306121.1 - *Capsella rubella*; XP_006393403.1 - *Eutrema salsugineum*; XP_024359357.1 - *Physcomitrium patens*; XP_020584530.1 - *Phalaenopsis equestris*; AJD14834.1 - *Boehmeria nivea*; EOX99143.1 - *Theobroma cacao*; XP_048229468.1 - *Ricinus communis*; XP_006298020.1 - *Capsella rubella*.

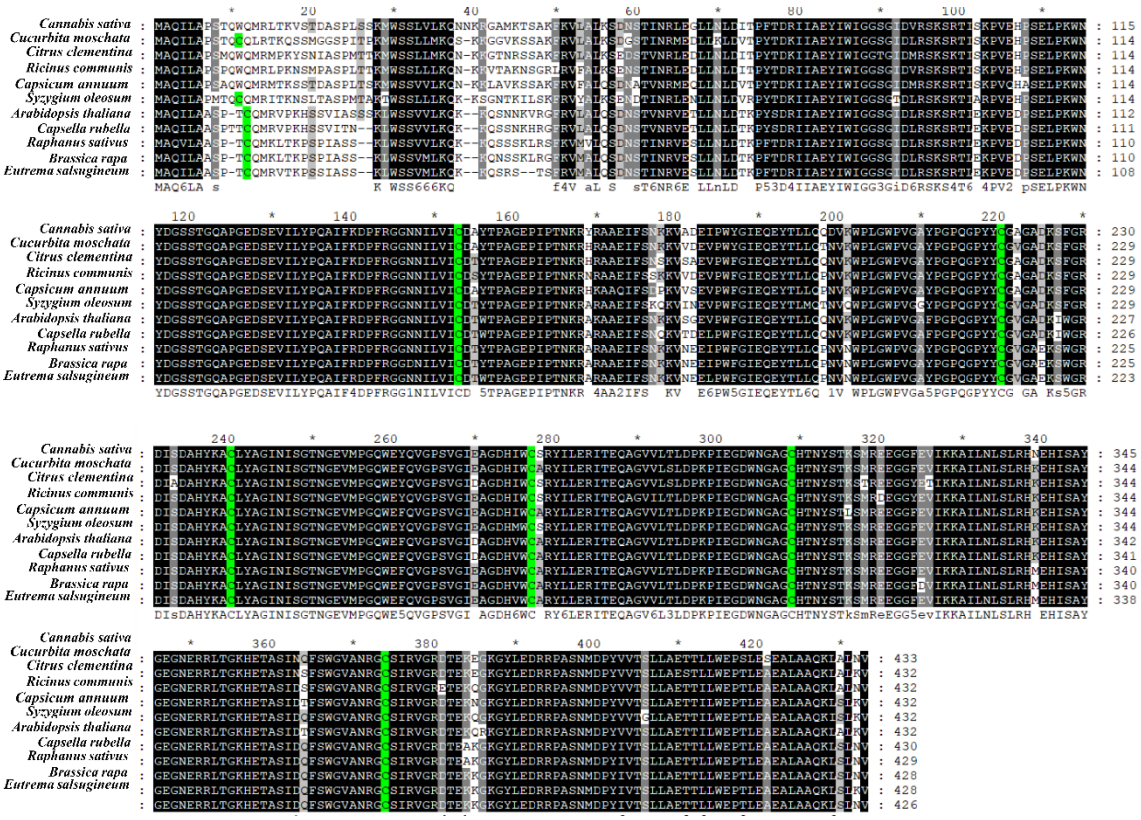

Figure S3. GS2 cys conserved residues between different organisms. Amino acid GS2 sequences were obtained from the National Center for Biotechnology Information (NCBI). Through the Blatst platform tool (https://blast.ncbi.nlm.nih.gov/Blast.cgi), we chosen the GS2 homologous protein sequences from different species, which had higher similarity in protein sequence in comparison with *At*GS2. Subsequently, the alignment between *At*GS2 and the homologous GS2 from different organisms was performed using the clustaw platform (https://www.ebi.ac.uk/Tools/msa/clustalw2/), the alignments were analyzed using the GeneDoc platform program. Sequences NCBI I.D: NP_001031969.1-*Arabidopsis thaliana*; XP_006282617.1-*Capsella rubella*; XP_018451685.1-*Raphanus sativus*; XP_006395952.1-*Eutrema salsugineum*; XP_009108017.1-*Brassica rapa*; NP_001310696-*Ricinus communis*; XP_006419778.1-*Citrus clementina*; XP_030476294.1-*Syzygium oleosum*; XP_002516801.1-*Ricinus communis*; XP_030507192-*Cannabis sativa*; NP_001311524-*Capsicum annuum*; XP_022953350-*Cucurbita moschata.*

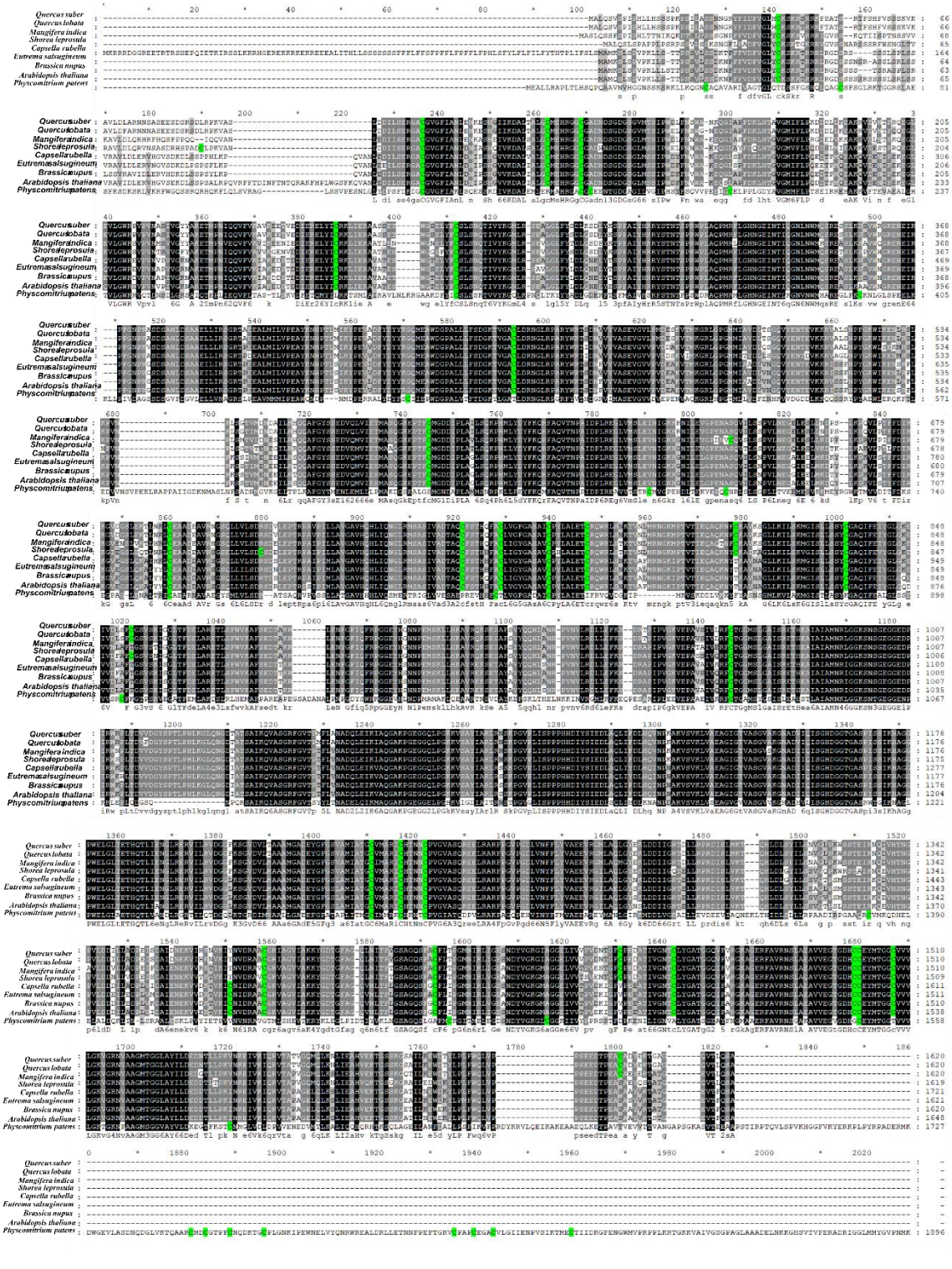

Figure S4. GOGAT (GLU1) cys conserved residues between different organisms. Amino acid GOGAT sequences were obtained from the National Center for Biotechnology Information (NCBI). Through the Blatst platform tool (https://blast.ncbi.nlm.nih.gov/Blast.cgi), we chosen the GOGAT homologous protein sequences from different species, which had higher similarity in protein sequence in comparison with *At*GOGAT. Subsequently, the alignment between

*At*GOGATand the homologous GOGAT from different organisms was performed using the clustaw platform (https://www.ebi.ac.uk/Tools/msa/clustalw2/), the alignments were analyzed using the GeneDoc platform program. Sequences NCBI I.D: NP_850763.1 -*Arabidopsis thaliana*; EOA19780.1 - *Capsella rubella*; XP_013668394.1 - *Brassica napus*; XP_006398870.1 - *Eutrema salsugineum*; XP_023892191.1 - *Quercus suber*; GKV41679.1 - *Shorea leprosula*; XP_030925863.1- Quercus lobata; XP_044478376.1 - Mangifera indica; XP_024395288.1 1- *Physcomitrium patens*.

a)

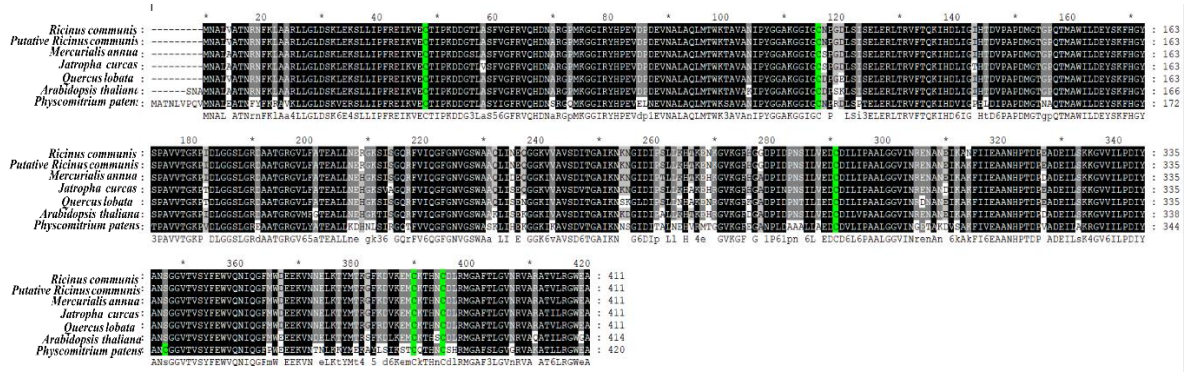

b)

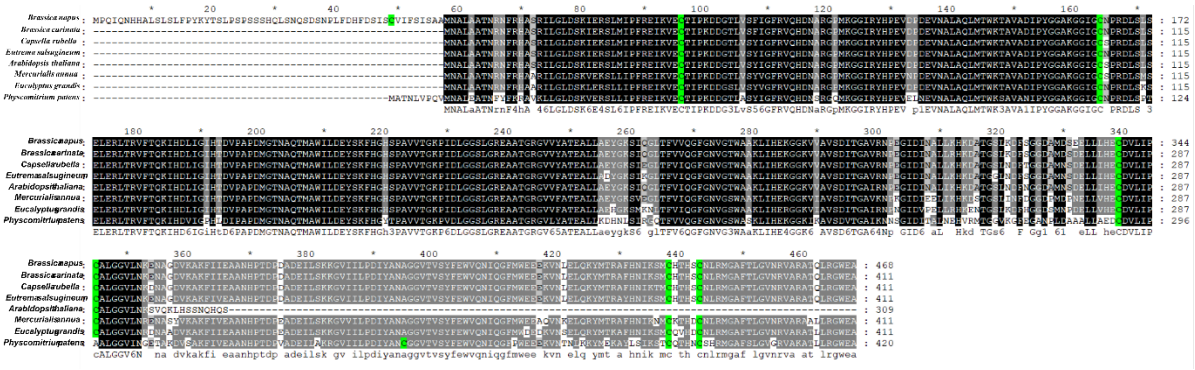

Figure S5. GDH cys conserved residues between different organisms. a) GDH 1 alignment between *AT*GDH 1 and homologous GDH 1 from diferents species. b)) GDH 2 alignment between *AT*GDH 2 and homologous GDH 2 from differents species. Amino acid GDH sequences were obtained from the National Center for Biotechnology Information (NCBI). Through the Blatst platform tool (https://blast.ncbi.nlm.nih.gov/Blast.cgi), we chosen the GDH1 and GDH 2 homologous protein sequences from different species, which had higher similarity in protein sequence in comparison with *AT*GDH. Subsequently, the alignment between *AT*GDH and the homologous GDH from different organisms was performed using the clustaw platform (https://www.ebi.ac.uk/Tools/msa/clustalw2/), the alignments were analyzed using the GeneDoc platform program. Sequences NCBI I.D: XP_024382943.1 -*Physcomitrium patens;* XP_030927431.1 - *Quercus lobata*; XP_002525427.2 - *Ricinus communis*; XP_012070451.1 - *Jatropha curcas*; XP_050206241.1- *Mercurialis annua*; 6YEH_A-*Arabidopsis thaliana*; *Physcomitrium patens*– XP_024382943.1; NP_001119184.1 - *Arabidopsis thaliana*; XP_006287548.2 - *Capsella rubella*; XP_006399227.1-*Eutrema salsugineum*; XP_013743201.1 - *Brassica napus*; KAG2262865.1-*Brassica carinata*; XP_050225579.1- *Mercurialis annua*; XP_010062756.2-*Eucalyptus grandis*.

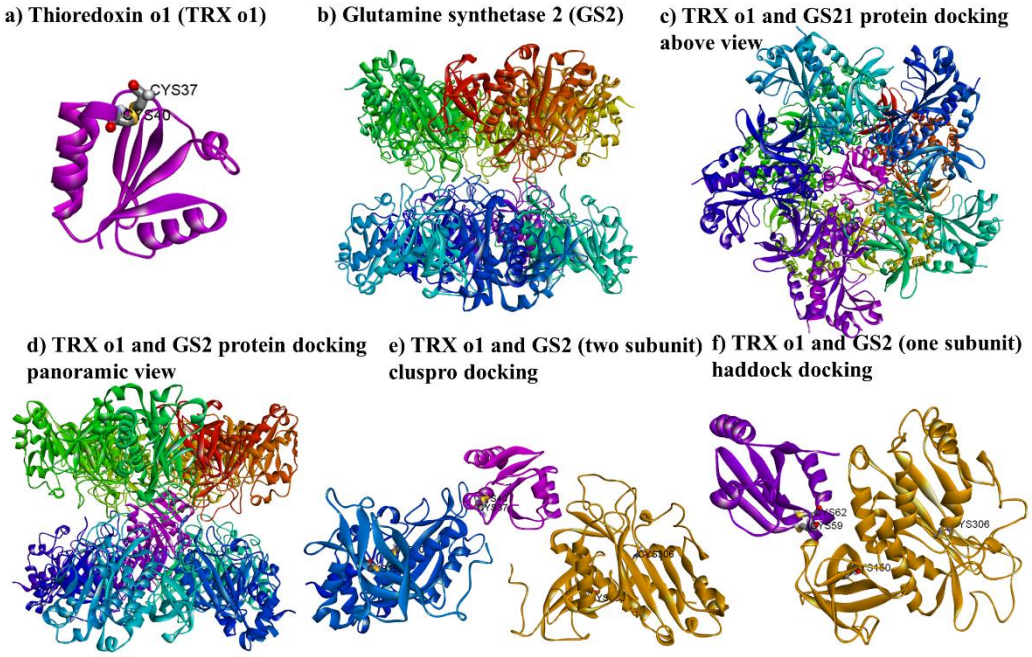

Figure S6- GS2 and TRX o1 molecular docking. The molecular docking of GS2 and TRX o1 were carry out in Cluspro and Haddock online platforms, using the TRX o1 crystal, 6g61, collected directly from PDB and the GS2 3D model built in swiss protein platform. A) Molecular cluspro docking GS2 and TRX o1 with overhead view. B) Molecular cluspro docking GS2 and TRX o1 panoramic image. C) GS2 and TRX o1 molecular docking between two subunits of GS2 with TRX o1. Molecular Docking haddock GS2 and TRX o1, using only subunit of GS2. The cys residues are stick-shaped label. The dockings were visualized on Discovery Studio program 2021.

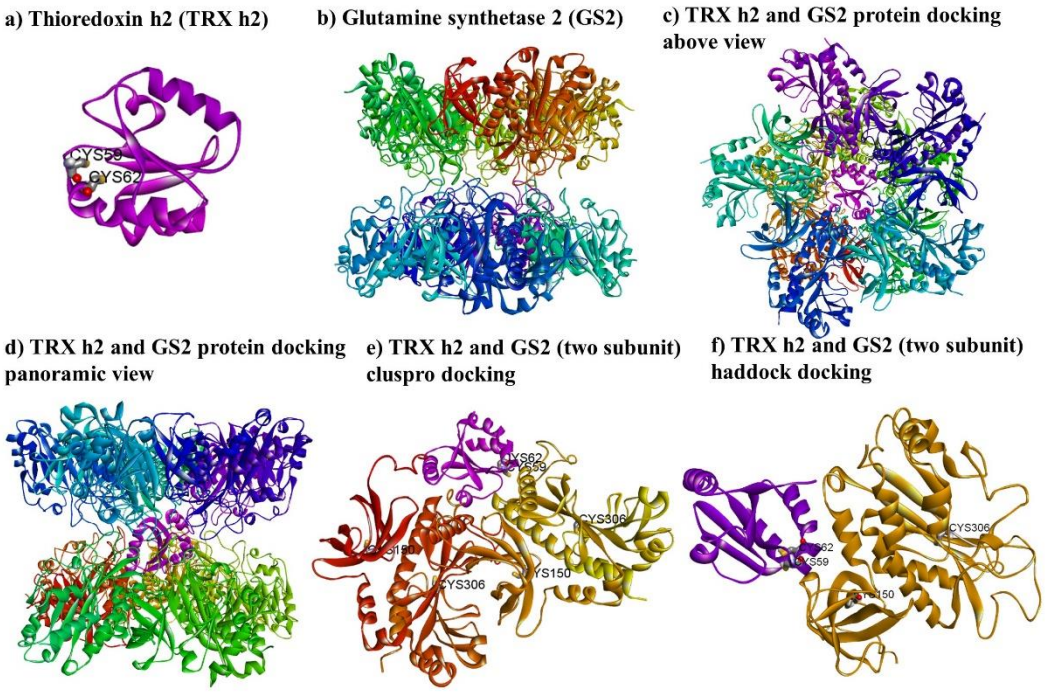

Figure S7- GS2 and TRX h2 molecular docking. The molecular docking of GS2 and TRX h2 were carry out in Cluspro and Haddock online platforms, using the TRX h2 3D model and the GS2 3D model built in swiss protein platform. A) Molecular cluspro docking GS2 and TRX h2 with overhead view. B) Molecular cluspro docking GS2 and TRX h2 panoramic image. C) GS2 and TRX h2 molecular docking between two subunits of GS2 with TRX h2. Molecular Docking haddock GS2 and TRX h2, using only subunit of GS2. The cys residues are stick-shaped label. The dockings were visualized on Discovery Studio program 2021.

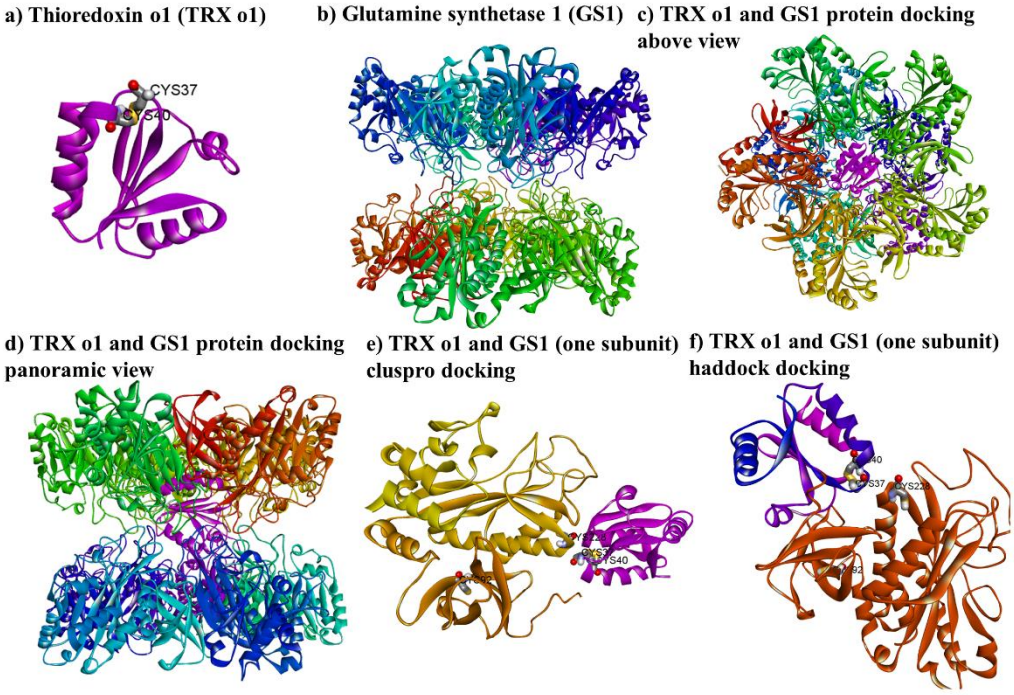

Figure S8- GS1 and TRX o1 molecular docking. The molecular docking of GS1 and TRX o1 were carry out in Cluspro and Haddock online platforms, using the TRX o1 crystal, 6g61, collected directly from PDB and the GS1 3D model built in swiss protein platform. A) Molecular cluspro docking GS1 and TRX o1 with overhead view. B) Molecular cluspro docking GS1 and TRX o1 panoramic image. C) GS1 and TRX o1 molecular docking between two subunits of GS1 with TRX o1. Molecular Docking haddock GS1 and TRX o1, using only subunit of GS1. The cys residues are stick-shaped label. The dockings were visualized on Discovery Studio program 2021.

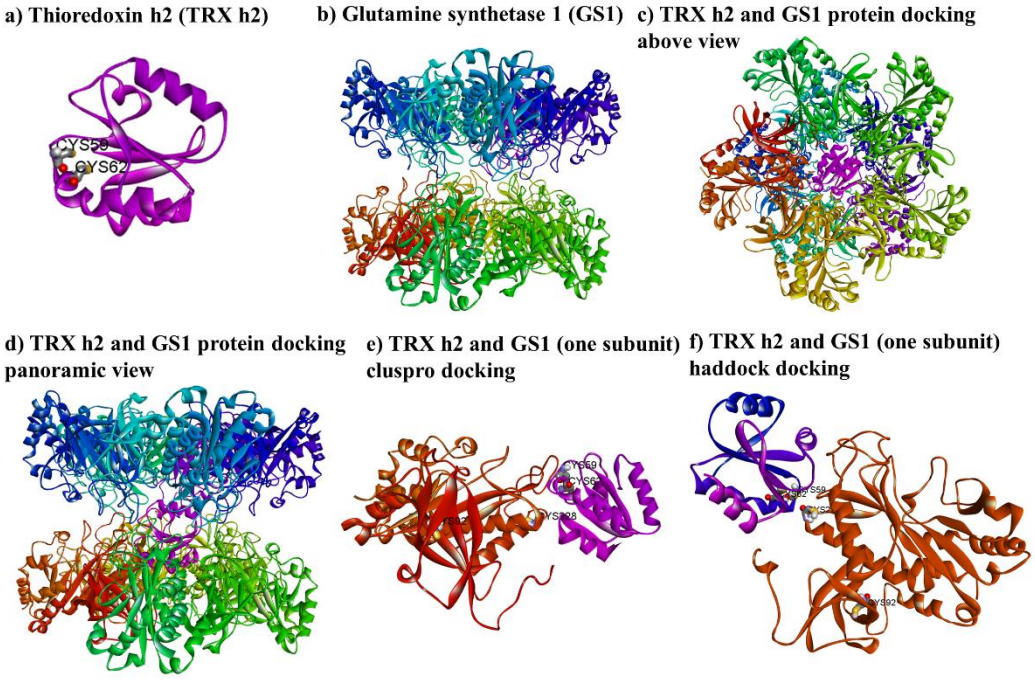

Figure S9- GS1 and TRX h2 molecular docking. The molecular docking of GS1 and TRX h2 were carry out in Cluspro and Haddock online platforms, using the TRX h2 3D model and the GS1 3D model built in swiss protein platform. A) Molecular cluspro docking GS1 and TRX h2 with overhead view. B) Molecular cluspro docking GS1 and TRX h2 panoramic image. C) GS1 and TRX h2 molecular docking between two subunits of GS1 with TRX h2. Molecular Docking haddock GS1 and TRX h2, using only subunit of GS1. The cys residues are stick-shaped label. The dockings were visualized on Discovery Studio program 2021.

Table Chapter 3

Table 1. DIANNA's program disulfide bond prediction. The enzymes chosen are involved in N-metabolism. The gene number assertions are given in this table. The DIANNA program gives a score according to (Ferrè & Clote, 2005). The prediction of disulfide bond formation was carried out by the DIANNA web server program. DIANNA algorithm provides a probability of a disulfide bond formation among different Cys residues, according to a score ranging from 0 (low probability) and 1 (high probability).

Protein name	Gene abbreviation	Number accession (TAIR)	Disulfide bridge prediction	Score Dianna web server (0-1)
Glutamine Synthetase 2	Gln2	At5g35630	11-306	Higher than 0,97
			150-306	Higher than 0.97
Glutamine Synthetase 1	Gln1;1	At5g37600	-	Bellow than 0,2
	Gln1;2	At1g66200	-	Bellow than 0,2
	Gln1;3	At3g17820	-	Bellow than 0,2
	Gln1;4	At5g16570	-	Bellow than 0,2
	Gln1;5	At1g48470	92 - 228	0,99
Glutamate Dehydrogenase subunit α and β	GDH1	At5g18170	39 – 282	0.99
	GDH2	At5g07440	107 - 282	0.99
			107 - 288	0.99
			107 - 282	0.99
Glutamate synthase (GLU1)	Glu1	At5g53460	132-168	Higher than 0,97
			132-1490	Higher than 0,97
			282-479	Higher than 0,97

Table S1- The 3D proteins models parameters. Homologous protein 3D models of GS1, GS2, and TRX h2 were build using the swiss-model platform, using the 7v4h 1 ,2d3a and 6x0B templates for GS2 and TRX h2, respectively. The protein models were evaluated by two parameters, Qualitative Model Energy Analysis (QMeans) and Global Model Quality Estimation score (GMQE). The resulting GMQE is expressed as a number between 0 and 1, reflecting the expected accuracy of a model built, in which higher numbers indicate higher reliability. On the other hand, QMEAN is a scoring function based on different geometrical properties and provides both global (i.e., for the entire structure) and local (i.e., per residue) absolute quality estimates.

Protein	**Templete**	**X-ray Crystal species**	**Similar with *A.t* sequence**	**QMeans**	**GMQE**
Glutamine synthetase 2	2d3a	*Z*ea *mays*	56%	0.40	0.76
Glutamine synthetase 1	7v4h 1	*Glycine max*	81.25%	0.83	0.88
Thioredoxin h2	6x0B	*Nicotiana alata*	53%	0.83	0.73

Table S2- Cluspro parameters. Cluspro is an online platform specialized in molecular docking, specifically protein-protein docking (Kozakov *et al.*, 2013; Vajda *et al.*, 2017). Thus, we provided the protein crystals collected from PDB. We collected 6g61crystal for *AtT*RX o1. For GS2, GS1 and TRX h2 we created homologous protein 3D models. We did three cluspro dockings: GS2 and TRX h2, GS2 and TRX o1, GS1 and TRX o1, and GS1 and TRX h2. Cluspro provides different clusters, which are translated into different ways in which ligands (TRXs) interact with the receptor (GS2 and GS1), and also the lower energy scores which can help in the interpretation of the data. Thus, the lower energy score may indicate the better positional prediction of the ligand to the receptor docking.

Protein – protein docking	**Cluster balance chosen**	**Center**	**Lower energy score**
GS2 and TRX h2	6	-1.108.9	-1.173.4
GS2 and TRX o1	0	-993.3	-1.255.5
GS1 and TRX h2	8	-760.6	-956.4
GS1 and TRX o1	8	-1.024	1.024.6

Table S3- Haddock parameters- Haddock is an online platform specialized in molecular docking, specifically protein-protein docking (Zundert, van *et al.*, 2016). Thus, we provided the protein crystals collected from PDB. We collected 6g61 for *AtT*RX o1. For GS2, GS1 and TRX h2 we created homologous protein 3D models. We did four cluspro dockings: GS2 and TRX h2, GS2 and TRX o1, GS1 and TRX o1, and GS1 and TRX h2. Unlike with cluspro dockings, in haddock platform we just ran a docking between a subunit (GS2 and GS1) and the TRX o1 and TRX h2. The haddock algorithm generates different parameters, which translate into different positions between ligands (TRXs) and receptors (GS2 and GS1). Z-score is a good parameter to define the best clusters, since the lower the Z-score value define the better the prediction of binding between ligand and receptor. Here are the clusters chosen based on the lowest Z-scores, which refer to figuresS6-S9.

HADDOCK parameters	**GS2 and TRX h2** Cluster 1	**GS1and TRX h2** Cluster 9	**GS2and TRX o1** Cluster 8	**GS1and TRX o1** Cluster 8
HADDOCK score	-85.8 +/- 2.7	-80.0 +/- 16.8	-72.8 +/- 3.0	-85.7 +/- 9.2
Cluster size	51	4	6	6
RMSD from the overall lowest-energy structure	0.7 +/- 0.4	0.9 +/- 0.5	14.0 +/- 0.2	0.9 +/- 0.6
Van der Waals energy	-37.8 +/- 4.5	-26.8 +/- 4.2	-36.9 +/- 3.8	-42.8 +/- 6.0
Electrostatic energy	-236.4 +/- 24.6	-271.4 +/- 81.8	-191.7 +/- 19.0	-195.8 +/- 30.7
Desolvation energy	-4.2 +/- 1.3	-0.0 +/- 1.0	-3.0 +/- 1.5	-4.1 +/- 2.7
Restraints violation energy	34.3 +/- 19.5	11.3 +/- 8.0	53.8 +/- 14.1	3.7 +/- 2.9
Buried Surface Area	1364.5 +/- 10.3	1563.0 +/- 136.1	1344.1 +/- 26.3	1668.7 +/- 160.0
Z-Score	**-1.9**	**-1.5**	**-1.5**	**-1.4**

7 GENERAL CONCLUSION AND FUTURE PERSPECTIVES

Our works have provided new insights into the role of the NTR/TRX system in the regulation of plant metabolism. The characterization of the triple mutant showed that the NTR system is highly important for plant growth, but not essential for plant development. We further demonstrated that the mitochondrial NTR/TRX system is important for the regulation of nitrogen metabolism enzymes, especially GS redox regulation, and that this mechanism aid plants to acclimate to high-light stress condition. In brief, we hope to publish the last two papers in a journal with a high impact factor, given that both papers systematically and significantly contribute to the understanding of redox metabolism, as well as presenting the important potential for biotechnological use to obtain plants more yield and adapt to change in the environment.

REFERENCES

ABADIE, C.; LOTHIER, J.; BOEX-FONTVIEILLE, E.; CARROLL, A.; TCHERKEZ, G. Direct assessment of the metabolic origin of carbon atoms in glutamate from illuminated leaves using 13C-NMR. **New Phytologist**, *[s.l.]*, v. 216, n. 4, p. 1079–1089, 2017a.

Direct assessment of the metabolic origin of carbon atoms in glutamate from illuminated leaves using13C-NMR. **New Phytologist**, *[s.l.]*, v. 216, n. 4, p. 1079–1089, 2017b.

ABADIE, C.; TCHERKEZ, G. In vivo phosphoenolpyruvate carboxylase activity is controlled by CO 2 and O 2 mole fractions and represents a major flux at high photorespiration rates. **New Phytologist**, *[s.l.]*,v. 221, n. 4, p. 1843–1852, 2019.

AINSWORTH, E. A.; ROGERS, A. The response of photosynthesis and stomatal conductance to rising [CO2]: Mechanisms and environmental interactions. **Plant, Cell and Environment**, *[s.l.]*, v. 30, n. 3, p. 258–270, 2007.

ARAÚJO, W. L. *et al.* Antisense Inhibition of the Iron-Sulphur Subunit of Succinate Dehydrogenase Enhances Photosynthesis and Growth in Tomato via an Organic Acid–Mediated Effect on Stomatal Aperture. **The Plant Cell**, *[s.l.]*, v. 23, n. 2, p. 600–627, 2011.

ARAÚJO, W. L.; NUNES-NESI, A.; FERNIE, A. R. Fumarate: Multiple functions of a simple metabolite. **Phytochemistry**, *[s.l.]*,v. 72, n. 9, p. 838–843, 2011.

ARAÚJO, W. L.; NUNES-NESI, A.; NIKOLOSKI, Z.; SWEETLOVE, L. J.; FERNIE, A. R. Metabolic control and regulation of the tricarboxylic acid cycle in photosynthetic and heterotrophic plant tissues. **Plant, Cell & Environment**, *[s.l.]*, v. 35, n. 1, p. 1–21, 2012.

ASHTON, A. R.; HATCH, M. D. Regulation of C4 photosynthesis: Physical and kinetic properties of active (dithiol) and inactive (disulfide) NADP-malate dehydrogenase from Zea mays. **Archives of Biochemistry and Biophysics**, *[s.l.]*, v. 227, n. 2, p. 406–415, 1983.

ATTACHA, S.; SOLBACH, D.; BELA, K.; MOSELER, A.; WAGNER, S.; SCHWARZLÄNDER, M.; ALLER, I.; MÜLLER, S. J.; MEYER, A. J. Glutathione peroxidase-like enzymes cover five distinct cell compartments and membrane surfaces in Arabidopsis thaliana. **Plant Cell and Environment**, *[s.l.]*, v. 40, n. 8, p. 1281–1295, 2017.

ATTIQUE, S. A.; HASSAN, M.; USMAN, M.; ATIF, R. M.; MAHBOOB, S.; AL-GHANIM, K. A.; BILAL, M.; NAWAZ, M. Z. A molecular docking approach to evaluate the pharmacological properties of natural and synthetic treatment candidates for use against hypertension. **International Journal of Environmental Research and Public Health**, *[s.l.]*, v. 16, n. 6, p. 1–17, 2019.

BAILLY, C. The signalling role of ROS in the regulation of seed germination and dormancy. **Biochemical Journal**, *[s.l.]*, v. 476, n. 20, p. 3019–3032, 2019.

BALMER, Y.; VENSEL, W. H.; TANAKA, C. K.; HURKMAN, W. J.; GELHAYE, E.; ROUHIER, N.; JACQUOT, J.-P.; MANIERI, W.; SCHURMANN, P.; DROUX, M.; BUCHANAN, B. B. Thioredoxin links redox to the regulation of fundamental processes of plant mitochondria. **Proceedings of the National Academy of Sciences**, *[s.l.]*, v. 101, n. 8, p. 2642–2647, 2004.

BASHANDY, T.; GUILLEMINOT, J.; VERNOUX, T.; CAPARROS-RUIZ, D.; LJUNG, K.; MEYER, Y.; REICHHELD, J.-P. Interplay between the NADP-Linked Thioredoxin and Glutathione Systems in Arabidopsis Auxin Signaling. **The Plant Cell**, *[s.l.]*, v. 22, n. 2, p. 376–391, 2010.

BASLER, G.; NIKOLOSKI, Z.; LARHLIMI, A.; BARABÁSI, A. L.; LIU, Y. Y. Control of fluxes in metabolic networks. **Genome Research**, *[s.l.]*, v. 26, n. 7, p. 956–968, 2016.

BAUWE, H.; KOLUKISAOGLU, Ü. Genetic manipulation of glycine decarboxylation. **Journal of Experimental Botany**, *[s.l.]*, v. 54, n. 387, p. 1523–1535, 2003.

BEERS, R. F.; SIZER, I. W. A spectrophotometric method for measuring the breakdown of hydrogen peroxide by catalase. **The Journal of biological chemistry**, *[s.l.]*, v. 195, n. 1, p. 133–140, 1952.

BELIN, C.; BASHANDY, T.; CELA, J.; DELORME-HINOUX, V.; RIONDET, C.; REICHHELD, J. P. A comprehensive study of thiol reduction gene expression under stress conditions in Arabidopsis thaliana. **Plant, Cell and Environment**, *[s.l.]*,v. 38, n. 2, p. 299–314, 2015.

BENITEZ-ALFONSO, Y.; CILIA, M.; SAN ROMAN, A.; THOMAS, C.; MAULE, A.; HEARN, S.; JACKSON, D. Control of Arabidopsis meristem development by thioredoxin-dependent regulation of intercellular transport. **Proceedings of the National Academy of Sciences of the United States of America, USA**, *[s.l.]*, v. 106, n. 9, p. 3615–3620, 2009.

BENKERT, P.; TOSATTO, S. C. E.; SCHOMBURG, D. QMEAN: A comprehensive scoring function for model quality assessment. **Proteins: Structure, Function, and Bioinformatics**, *[s.l.]*, v. 71, n. 1, p. 261–277, 2008.

BERKEMEYER, M.; SCHEIBE, R.; OCHERETINA, O. A Novel , Non-redox-regulated NAD-dependent Malate Dehydrogenase from Chloroplasts of Arabidopsis thaliana L .*. *[s.l.]*, v. 273, n. 43, p. 27927–27933, 1998.

BIDDAU, M. *et al.* Two essential Thioredoxins mediate apicoplast biogenesis, protein import, and gene expression in Toxoplasma gondii. **PLoS Pathogens**, *[s.l.]*, v. 14, n. 2, p. 1–27, 2018.

BLANC, G.; BARAKAT, A.; GUYOT, R.; COOKE, R.; DELSENY, M. Extensive duplication and reshuffling in the Arabidopsis genome. **Plant Cell**, *[s.l.]*, v. 12, n. 7, p. 1093–1101, 2000.

BOURGUIGNON, J.; NEUBURGER, M.; DOUCE, R. Resolution and characterization of the glycine-cleavage reaction in pea leaf mitochondria. Properties of the forward reaction catalysed by glycine decarboxylase and serine hydroxymethyltransferase. **The Biochemical journal**, *[s.l.]*, v. 255, p. 169–178, 1988.

BOWLES, A. M. C.; BECHTOLD, U.; PAPS, J. The Origin of Land Plants Is Rooted in Two Bursts of Genomic Novelty. **Current biology : CB**, *[s.l.]*, p. 1–7, 2019.

BRADFORD, M. M. A rapid and sensitive method for the quantitation of microgram quantities of protein utilizing the principle of protein-dye binding. **Analytical Biochemistry**, *[s.l.]*,v. 72, n. 1–2, p. 248–254, 1976.

BRESTIC, M.; ZIVCAK, M.; OLSOVSKA, K.; SHAO, H. B.; KALAJI, H. M.; ALLAKHVERDIEV, S. I. Reduced glutamine synthetase activity plays a role in control of photosynthetic responses to high light in barley leaves. **Plant Physiology and Biochemistry**, *[s.l.]*, v. 81, p. 74–83, 2014.

BUCHANAN, B. B. The birth of redox regulation. **Molecular Plant**, v. 7, n. 1, p. 1–3, 2014.

___. The Path to Thioredoxin and Redox Regulation in Chloroplasts. **Annual Review of Plant Biology**, *[s.l.]*, v. 67, n. 1, p. 1–24, 2016a.

The carbon (formerly dark) reactions of photosynthesis. **Photosynthesis Research**, *[s.l.]*, v. 128, n. 2, p. 215–217, 2016b.

The path to thioredoxin and redox regulation beyond chloroplasts. **Plant and Cell Physiology**, *[s.l.]*, v. 58, n. 11, p. 1826–1832, 2017a.

The Path to Thioredoxin and Redox Regulation beyond Chloroplasts. **Plant and Cell Physiology**, *[s.l.]*, v. 58, n. 11, p. 1826–1832, 2017b.

BUCHANAN, B. B.; BALMER, Y. Redox regulation: A broadening horizon. **Annual Review of Plant Biology**, *[s.l.]*, v. 56, n. 1, p. 187–220, 2005.

BUCHANAN, B. B.; GRUISSEM, W.; JONES, R. L. **Biochemistry & Molecular Biology of Plants**. [s.l: s.n.]. v. 53

BUCHANAN, B. B.; HOLMGREN, A.; JACQUOT, J. P.; SCHEIBE, R. Fifty years in the thioredoxin field and a bountiful harvest. **Biochimica et Biophysica Acta - General Subjects**, *[s.l.]*,v. 1820, n. 11, p. 1822–1829, 2012.

BUDDE, R. J.; RANDALL, D. D. Pea leaf mitochondrial pyruvate dehydrogenase complex is inactivated in vivo in a light-dependent manner. **Proceedings of the National Academy of Sciences**, *[s.l.]*, v. 87, n. 2, p. 673–676, jan. 1990.

BUSCH, A.; HIPPLER, M. The structure and function of eukaryotic photosystem i. **Biochimica et Biophysica Acta - Bioenergetics**, *[s.l.]*, v. 1807, n. 8, p. 864–877, 2011.

BYKOVA, N. V.; MØLLER, I. M.; GARDESTRÖM, P.; IGAMBERDIEV, A. U. The function of glycine decarboxylase complex is optimized to maintain high photorespiratory flux via buffering of its reaction products. **Mitochondrion**, *[s.l.]*,v. 19, n. PB, p. 357–364, 2014.

CALDERÓN, A.; SÁNCHEZ-GUERRERO, A.; ORTIZ-ESPÍN, A.; MARTÍNEZ-ALCALÁ, I.; CAMEJO, D.; JIMÉNEZ, A.; SEVILLA, F. Lack of mitochondrial thioredoxin o 1 is compensated by antioxidant components under salinity in Arabidopsis thaliana plants. **Physiologia Plantarum**, *[s.l.]*, v. 7418, p. 1–24, 2018a.

Lack of mitochondrial thioredoxin o 1 is compensated by antioxidant components under salinity in Arabidopsis thaliana plants. **Physiologia Plantarum**, *[s.l.]*, v. 7418, p. 1–24, fev. 2018b.

CALDERON, J.; MORA, J. Glutamine assimilation pathways in Neurospora crassa growing on glutamine as sole nitrogen and carbon source. **Journal of General Microbiology**, *[s.l.]*, v. 135, n. 10, p. 2699–2707, 1989.

CARR, P. D.; VERGER, D.; ASHTON, A. R.; OLLIS, D. L. Chloroplast NADP-malate dehydrogenase: Structural basis of light- dependent regulation of activity by thiol oxidation and reduction. **Structure**, *[s.l.]*, v. 7, n. 4, p. 461–475, 1999.

CEJUDO, F. J.; GONZÁLEZ, M.-C.; PÉREZ-RUIZ, J. M. Redox regulation of chloroplast metabolism. **Plant Physiology**, *[s.l.]*, v. 186, n. 1, p. 9–21, 2021.

CEJUDO, F. J.; MARÍA-CRUZ GONZÁLEZ; PÉREZ-RUIZ, J. M. Redox regulation of chloroplast metabolism. **Plant Physiology**, 2020 *[s.l.]*,*[s.n.]*.

CEJUDO, F. J.; MEYER, A. J.; REICHHELD, J.-P.; ROUHIER, N.; TRAVERSO, J. A. Thiol-based redox homeostasis and signaling. **Frontiers in Plant Science**, *[s.l.]*,v. 5, n. June, p. 2013–2015, 2014.

CERNUSAK, L. A.; HAVERD, V.; BRENDEL, O.; THIEC, D. LE; GUEHL, J.; CUNTZ, M. Robust Response of Terrestrial Plants to Rising CO2. **Trends in Plant Science**, *[s.l.]*, v. 24, n. 7, p. 578–586, jul. 2019.

CHENG, C. *et al.* Thioredoxin a is essential for motility and contributes to host infection of listeria monocytogenes via redox interactions. **Frontiers in Cellular and Infection Microbiology**, *[s.l.]*, v. 7, n. JUN, p. 1–19, 2017.

CHEW, O.; WHELAN, J.; MILLAR, A. H. Molecular Definition of the Ascorbate-Glutathione Cycle in Arabidopsis Mitochondria Reveals Dual Targeting of Antioxidant Defenses in Plants. **Journal of Biological Chemistry**, *[s.l.]*, v. 278, n. 47, p. 46869–46877, 2003.

CHOI, Y. A.; KIM, S. G.; KWON, Y. M. The plastidic glutamine synthetase activity is directly modulated by means of redox change at two unique cysteine residues. **Plant Science**, *[s.l.]*, v. 149, n. 2, p. 175–182, 1999.

CHONG, J.; WISHART, D. S.; XIA, J. Using MetaboAnalyst 4.0 for Comprehensive and Integrative Metabolomics Data Analysis. **Current Protocols in Bioinformatics**, *[s.l.]*, v. 68, n. 1, p. 1–128, 2019.

CONRAD, M.; JAKUPOGLU, CEMILE; *et al.* Essential Role for Mitochondrial Thioredoxin Reductase in Hematopoiesis, Heart Development, and Heart Function. **Molecular and Cellular Biology**, *[s.l.]*, v. 24, n. 21, p. 9414–9423, 2004.

CONRAD, M.; JAKUPOGLU, C; *et al.* Essential role for mitochondrial thioredoxin reductase in hematopoiesis, heart development, and heart function. **Molecular and**, *[s.l.]*, v. 24, n. 21, p. 9414, 2004.

COUSINS, A. B.; WALKER, B. J.; PRACHAROENWATTANA, I.; SMITH, S. M.; BADGER, M. R. Peroxisomal hydroxypyruvate reductase is not essential for photorespiration in Arabidopsis but its absence causes an increase in the stoichiometry of photorespiratory CO2 release. **Photosynthesis Research**, *[s.l.]*, v. 108, n. 2–3, p. 91–100, 2011.

DALOSO, DANILO M. *et al.* Thioredoxin, a master regulator of the tricarboxylic acid cycle in plant mitochondria. **Proceedings of the National Academy of Sciences**, *[s.l.]*, v. 112, n. 11, p. E1392–E1400, 2015.

DALOSO, DANILO M *et al.* Thioredoxin, a master regulator of the tricarboxylic acid cycle in plant mitochondria. **Proceedings of the National Academy of Sciences**, *[s.l.]*,v. 112, n. 11, p. E1392–E1400, 17 mar. 2015.

DEL-SAZ, N. F.; RIBAS-CARBO, M.; MCDONALD, A. E.; LAMBERS, H.; FERNIE, A. R.; FLOREZ-SARASA, I. An In Vivo Perspective of the Role(s) of the Alternative Oxidase Pathway. **Trends in Plant Science**, *[s.l.]*,v. 23, n. 3, p. 206–219, 2018.

DEMIRCAN, N.; CUCUN, G.; UZILDAY, B. Mitochondrial alternative oxidase (AOX1a) is required for the mitigation of arsenic - induced oxidative stress in Arabidopsis thaliana. **Plant Biotechnology Reports**, n. III, 2020, *[s.l.]*, *[s.n.]*.

DOUCE, R.; BOURGUIGNON, J.; NEUBURGER, M.; RÉBEILLÉ, F. The glycine decarboxylase system: A fascinating complex. **Trends in Plant Science**, *[s.l.]*, v. 6, n. 4, p. 167–176, 2001.

EISENHUT, M.; BAUWE, H.; HAGEMANN, M. Glycine accumulation is toxic for the cyanobacterium Synechocystis sp. strain PCC 6803, but can be compensated by supplementation with magnesium ions. **FEMS Microbiology Letters**, *[s.l.]*, v. 277, n. 2, p. 232–237, 2007.

EISENHUT, M.; ROELL, M. S.; WEBER, A. P. M. Mechanistic understanding of photorespiration paves the way to a new green revolution. **New Phytologist**, 2019 *[s.l.]*, *[s.n.]*.. ELSÄSSER, M. *et al.* Photosynthetic activity triggers pH and NAD redox signatures across different plant cell compartments. **bioRxiv**, *[s.l.]*, p. 2020.10.31.363051, 2020.

ENGEL, N.; DAELE, K. VAN DEN; KOLUKISAOGLU, Ü.; MORGENTHAL, K.; WECKWERTH, W.; PÄRNIK, T.; KEERBERG, O.; BAUWE, H. Deletion of glycine decarboxylase in Arabidopsis is lethal under nonphotorespiratory conditions. **Plant Physiology**, *[s.l.]*, v. 144, n. July, p. 1328–1335, 2007.

EPRINTSEV, A. T.; FEDORIN, D. N.; CHERKASSKIKH, M. V.; IGAMBERDIEV, A. U. Expression of succinate dehydrogenase and fumarase genes in maize leaves is mediated by cryptochrome. **Journal of Plant Physiology**, *[s.l.]*, v. 221, n. October 2017, p. 81–84, 2018.

Regulation of expression of the mitochondrial and cytosolic forms of aconitase in maize leaves via phytochrome. **Plant Physiology and Biochemistry**, *[s.l.]*, v. 146, n. November 2019, p. 157–162, 2020.

EPRINTSEV, A. T.; FEDORIN, D. N.; IGAMBERDIEV, A. U. Ca2+ is involved in phytochrome A-dependent regulation of the succinate dehydrogenase gene sdh1-2 in Arabidopsis. **Journal of Plant Physiology**, *[s.l.]*, v. 170, n. 15, p. 1349–1352, 2013.

EPRINTSEV, A. T.; FEDORIN, D. N.; SAZONOVA, O. V.; IGAMBERDIEV, A. U. Light inhibition of fumarase in Arabidopsis leaves is phytochrome A-dependent and mediated by calcium. **Plant Physiology and Biochemistry**, *[s.l.]*, v. 102, p. 161–166, 2016.

EVANS, J. R.; LAWSON, T. From green to gold: agricultural revolution for food security. **Journal of Experimental Botany**, *[s.l.]*, v. 71, n. 7, p. 2211–2215, 2020.

EVANS, M. C.; BUCHANAN, B. B.; ARNON, D. I. A new ferredoxin-dependent carbon reduction cycle in a photosynthetic bacterium. **Proceedings of the National Academy of Sciences of the United States of America**, *[s.l.]*, v. 55, n. 4, p. 928–934, 1966.

FERNIE, A. R.; MORGAN, J. A. Analysis of metabolic flux using dynamic labelling and metabolic modelling. **Plant, Cell and Environment**, v. 36, n. 9, p. 1738–1750, 2013.
FERRÈ, F.; CLOTE, P. DiANNA: A web server for disulfide connectivity prediction. **Nucleic Acids Research**, *[s.l.]*, v. 33, n. SUPPL. 2, p. 230–232, 2005.

FINKEMEIER, I.; FUCHS, P.; RUGEN, N.; CARRIE, C.; ELS, M.; GIESE, J.; KRISTINA, K.; MAURINO, V. G.; RUBERTI, C.; SCHALLENBERG-, M.; EUBEL, H. Single organelle function and organization as estimated from Arabidopsis mitochondrial proteomics. p. 420–441, 2020.

FINKEMEIER, I.; GOODMAN, M.; LAMKEMEYER, P.; KANDLBINDER, A.; SWEETLOVE, L. J.; DIETZ, K. J. The mitochondrial type II peroxiredoxin F is essential for redox homeostasis and root growth of Arabidopsis thaliana under stress. **Journal of Biological Chemistry**, *[s.l.]*, v. 280, n. 13, p. 12168–12180, 2005.

FINNEMANN, J.; SCHJOERRING, J. K. Post-translational regulation of cytosolic glutamine synthetase by reversible phosphorylation and 14-3-3 protein interaction. **Plant Journal**, *[s.l.]*, v. 24, n. 2, p. 171–181, 2000.

FLORENCIO, F. J.; GADAL, P.; BUCHANAN, B. B. Thioredoxin-linked activation of the chloroplast and cytosolic forms of Chlamydomonas reinhardtii glutamine synthetase. **Plant Physiology and Biochemistry**, *[s.l.]*, v. 31, p. 649–655, 1993.

FLOREZ-SARASA, I.; OBATA, T.; DEL-SAZ, NÉSTOR FERNÁNDEZ; REICHHELD, J.-P.; MEYER, E. H.; RODRIGUEZ-CONCEPCION, M.; RIBAS-CARBO, M.; FERNIE, A. R. The lack of mitochondrial thioredoxin TRXo1 affects in vivo alternative oxidase activity and carbon metabolism under different light conditions. **Plant & Cell Physiology**, *[s.l.]*, *[s.n.]*, 2019.

FLOREZ-SARASA, I.; OBATA, T.; DEL-SAZ, NÏ¿½STOR FERNÏ¿½NDEZ; REICHHELD, J.-P.; MEYER, E. H.; RODRIGUEZ-CONCEPCION, M.; RIBAS-CARBO, M.; FERNIE, A. R. The Lack of Mitochondrial Thioredoxin TRXo1 Affects In Vivo Alternative Oxidase Activity and Carbon Metabolism under Different Light Conditions. **Plant and Cell Physiology**, *[s.l.]*, v. 60, n. 11, p. 2369–2381, 1 nov. 2019.

FONSECA-PEREIRA, P. DA; DALOSO, D. M.; GAGO, J.; OLIVEIRA SILVA, F. M. DE; CONDORI-APFATA, J. A.; FLOREZ-SARASA, I.; TOHGE, T.; REICHHELD, J. P.; NUNES-NESI, A.; FERNIE, A. R.; ARAJO, W. L. The Mitochondrial Thioredoxin System Contributes to the Metabolic Responses under Drought Episodes in Arabidopsis. **Plant and Cell Physiology**, *[s.l.]*, v. 60, n. 1, p. 213–229, 2019.

FONSECA-PEREIRA, P. DA; SOUZA, P. V. L.; FERNIE, A. R.; TIMM, S.; DALOSO, D. M.; ARAÚJO, W. L. Thioredoxin-mediated regulation of (photo)respiration and central metabolism. **Journal of Experimental Botany**, *[s.l.]*, v. 72, n. 17, p. 5987–6002, 2 set. 2021.

FONSECA-PEREIRA, P. DA; SOUZA, P. V. L.; HOU, L. Y.; SCHWAB, S.; GEIGENBERGER, P.; NUNES-NESI, A.; TIMM, S.; FERNIE, A. R.; THORMÄHLEN, I.; ARAÚJO, W. L.; DALOSO, D. M. Thioredoxin h2 contributes to the redox regulation of mitochondrial photorespiratory metabolism. **Plant Cell and Environment**, *[s.l.]*, v. 43, n. 1, p. 188–208, 2020.

FONTAINE, J. X. *et al.* Characterization of a NADH-dependent glutamate dehydrogenase mutant of arabidopsis demonstrates the key role of this enzyme in root carbon and nitrogen metabolism. **Plant Cell**, *[s.l.]*, v. 24, n. 10, p. 4044–4065, 2012.

FOYER, C. H.; BAKER, A.; WRIGHT, M.; SPARKES, I. A.; MHAMDI, A.; SCHIPPERS, J. H. M.; BREUSEGEM, F. VAN. On the move: Redox-dependent protein relocation in plants. **Journal of Experimental Botany**, *[s.l.]*, v. 71, n. 2, p. 620–631, 2020.

FOYER, C. H.; NOCTOR, G. Oxidant and antioxidant signaling in plants: a re-evaluation of the concept of oxidative stress in a physiological context. **Plant, Cell and Environment**, *[s.l.]*, v. 28, p. 1056–1071, 2005.

FOYER, C. H.; NOCTOR, G. Redox regulation in photosynthetic organisms: signaling, acclimation, and practical implications. **Regulation**, *[s.l.]*, v. 11, n. 4, p. 861–905, 2009.

Redox Signaling in Plants. **Antioxidants & Redox Signaling**, *[s.l.]*, v. 18, n. 16, p. 2087–2090, 2013.

FOYER, C. H.; NOCTOR, G. **Redox Homeostasis and Signaling in a Higher-CO2 WorldAnnual Review of Plant Biology**, *[s.l.]*, *[s.n.]*, 2020.

FRISO, G.; WIJK, K. J. VAN. Update: Post-translational protein modifications in plant metabolism. **Plant Physiology**, *[s.l.]*, v. 169, n. November, p. pp.01378.2015, 3 set. 2015.

FUCHS, P. *et al.* Single organelle function and organization as estimated from Arabidopsis mitochondrial proteomics. **The Plant Journal**, *[s.l.]*, v. 101, n. 2, p. 420–441, 2020a.

Single organelle function and organization as estimated from Arabidopsis mitochondrial proteomics. **Plant Journal**, *[s.l.]*, v. 101, n. 2, p. 420–441, 2020b.

GALLAIS, A.; HIREL, B. An approach to the genetics of nitrogen use efficiency in maize. **Journal of Experimental Botany**, *[s.l.]*, v. 55, n. 396, p. 295–306, 2004.

GAUFICHON, L.; ROTHSTEIN, S. J.; SUZUKI, A. Asparagine metabolic pathways in arabidopsis. **Plant and Cell Physiology**, *[s.l.]*, v. 57, n. 4, p. 675–689, 2016.

GAUTHIER, PAUL P.G.; BLIGNY, R.; GOUT, E.; MAHÉ, A.; NOGUÉS, S.; HODGES, M.; TCHERKEZ, G. G. B. In folio isotopic tracing demonstrates that nitrogen assimilation into glutamate is mostly independent from current CO2 assimilation in illuminated leaves of Brassica napus. **New Phytologist**, *[s.l.]*, v. 185, n. 4, p. 988–999, 2010.

GAUTHIER, PAUL P G; BLIGNY, R.; GOUT, E.; MAHÉ, A.; NOGUÉS, S.; HODGES, M.; TCHERKEZ, G. G. B. In folio isotopic tracing demonstrates that nitrogen assimilation into glutamate is mostly independent from current CO2 assimilation in illuminated leaves of Brassica napus. **New Phytol.**, *[s.l.]*, v. 185, n. 4, p. 988–999, 2010.

GEIGENBERGER, P.; FERNIE, A. R. Metabolic Control of Redox and Redox Control of Metabolism in Plants. **Antioxidants & Redox Signaling**, v. 21, n. 9, p. 1389–1421, 2014.
GEIGENBERGER, P.; THORMÄHLEN, I.; DALOSO, DANILO M.; FERNIE, A. R. The Unprecedented Versatility of the Plant Thioredoxin System. **Trends in Plant Science**, *[s.l.]*, v. 22, n. 3, p. 249–262, 2017.

GEIGENBERGER, P.; THORMÄHLEN, I.; DALOSO, DANILO M; FERNIE, A. R. The Unprecedented Versatility of the Plants Thioredoxin System. **Trends in Plant Science**, *[s.l.]*, v. 22, n. 3, p. 249–262, 2017.

GELHAYE, E. *et al.* A specific form of thioredoxin h occurs in plant mitochondria and regulates the alternative oxidase. **Proceedings of the National Academy of Sciences of the United States of America**, *[s.l.]*, v. 101, n. 40, p. 14545–50, 2004.

GENTY, B.; BRIANTAIS, J. M.; BAKER, N. R. The relationship between the quantum yield of

photosynthetic electron transport and quenching of chlorophyll fluorescence. **Biochimica et Biophysica Acta - General Subjects**, *[s.l.]*, v. 990, n. 1, p. 87–92, 1989.

GERNA, D.; ROACH, T.; STÖGGL, W.; WAGNER, J.; VACCINO, P.; LIMONTA, M.; KRANNER, I. Changes in low-molecular-weight thiol-disulphide redox couples are part of bread wheat seed germination and early seedling growth. **Free Radical Research**, *[s.l.]*, v. 51, n. 6, p. 568–581, 2017.

GIANNOPOLITIS, C. N.; RIES, S. K. Superoxide Dismutases: II. Purification and Quantitative Relationship with Water-soluble Protein in Seedlings. **Plant physiology**, *[s.l.]*, v. 59, n. 2, p. 315–318, 1977.

GIOVAGNETTI, V.; RUBAN, A. V. Discerning the effects of photoinhibition and photoprotection on the rate of oxygen evolution in Arabidopsis leaves. **Journal of Photochemistry and Photobiology B: Biology**, *[s.l.]*, v. 152, n. October, p. 272–278, 2015.

GONZÁLEZ, M.; DELGADO-REQUEREY, V.; FERRÁNDEZ, J.; SERNA, A.; CEJUDO, F. J.; NOCTOR, G. Insights into the function of NADPH thioredoxin reductase C (NTRC) based on identification of NTRC-interacting proteins in vivo. **Journal of Experimental Botany**, *[s.l.]*, v. 70, n. 20, p. 5787–5798, 2019.

GOOD, A. G.; SHRAWAT, A. K.; MUENCH, D. G. Can less yield more? Is reducing nutrient input into the environment compatible with maintaining crop production? **Trends in Plant Science**, *[s.l.]*, v. 9, n. 12, p. 597–605, 2004.

GRAHAM, J. W. A.; WILLIAMS, T. C. R.; MORGAN, M.; FERNIE, A. R.; RATCLIFFE, R. G.; SWEETLOVE, L. J. Glycolytic enzymes associate dynamically with mitochondria in response to respiratory demand and support substrate channeling. **Tha Plant Cell**, *[s.l.]*, v. 19, n. 11, p. 3723–3738, 2007.

GRIFFITH, O. W. Determination of glutathione and glutathione disulfide using glutathione reductase and 2-vinylpyridine. **Analytical Biochemistry**, v. 106, n. 1, p. 207–212, jul. 1980.
GUAN, M.; MØLLER, I. S.; SCHJOERRING, J. K. Two cytosolic glutamine synthetase isoforms play specific roles for seed germination and seed yield structure in Arabidopsis. **Journal of Experimental Botany**, *[s.l.]*, v. 66, n. 1, p. 203–212, 2015.

GUILHERME, E. A.; CARVALHO, F. E. L.; DALOSO, D. M.; SILVEIRA, J. A. G. Increase in assimilatory nitrate reduction and photorespiration enhances CO2 assimilation under high light-induced photoinhibition in cotton. **Environmental and Experimental Botany**, *[s.l.]*, v. 159, n. October 2018, p. 66–74, 2019.

HABASH, D. Z.; BERNARD, S.; SCHONDELMAIER, J.; WEYEN, J.; QUARRIE, S. A. The genetics of nitrogen use in hexaploid wheat: N utilisation, development and yield. **Theoretical and Applied Genetics**, *[s.l.]*, v. 114, n. 3, p. 403–419, 2007.

HACHIYA, T. *et al.* Excessive ammonium assimilation by plastidic glutamine synthetase causes

ammonium toxicity in Arabidopsis thaliana. **Nature Communications**, v. 12, n. 1, 2021.
HÄGGLUND, P.; FINNIE, C.; YANO, H.; SHAHPIRI, A.; BUCHANAN, B. B.; HENRIKSEN, A.; SVENSSON, B. Seed thioredoxin h. **Biochimica et Biophysica Acta - Proteins and Proteomics**, *[s.l.]*, v. 1864, n. 8, p. 974–982, 2016.

HASHIDA, S. NOSUKE; MIYAGI, A.; NISHIYAMA, M.; YOSHIDA, K.; HISABORI, T.; KAWAI-YAMADA, M. Ferredoxin/thioredoxin system plays an important role in the chloroplastic NADP status of Arabidopsis. **Plant Journal**, *[s.l.]*, *[s.n.]*, p. 947–960, 2018.

HASSE, D.; ANDERSSON, E.; CARLSSON, G.; MASLOBOY, A.; HAGEMANN, M.; BAUWE, H.; ANDERSSON, I. Structure of the homodimeric glycine decarboxylase P-protein from synechocystis sp. PCC 6803 suggests a mechanism for redox regulation. **Journal of Biological Chemistry**, *[s.l.]*, v. 288, n. 49, p. 35333–35345, 2013.

HAVIR, E. A; MCHALE, N. A. Biochemical and developmental characterization of multiple forms of catalase in tobacco leaves. **Plant physiology**, *[s.l.]*, v. 84, n. 2, p. 450–455, 1987.

HERBETTE, S.; LENNE, C.; LEBLANC, N.; JULIEN, J. L.; DREVET, J. R.; ROECKEL-DREVET, P. Two GPX-like proteins from Lycopersicon esculentum and Helianthus annuus are antioxidant enzymes with phospholipid hydroperoxide glutathione peroxidase and thioredoxin peroxidase activities. **European Journal of Biochemistry**, *[s.l.]*, v. 269, n. 9, p. 2414–2420, 2002.

HILDEBRANDT, T. M.; NUNES NESI, A.; ARAÚJO, W. L.; BRAUN, H. P. Amino Acid Catabolism in Plants. **Molecular Plant**, *[s.l.]*, v. 8, n. 11, p. 1563–1579, 2015.

HIREL, B.; GADAL, P. Glutamine Synthetase in Rice. **Plant physiology**, *[s.l.]*, v. 66, n. 4, p. 619–623, 1980.

HIRT, H. *et al.* PlantACT ! – how to tackle the climate crisis. **Trends in Plant Science**, *[s.l.]*, *[s.n]*, p. 1–7, 2023.

HODGES, M.; JOSSIER, M.; BOEX-FONTVIEILLE, E.; TCHERKEZ, G. Protein phosphorylation and photorespiration. **Plant Biology**, *[s.l.]*, v. 15, n. 4, p. 694–706, 2013.

HOFFMANN, C.; PLOCHARSKI, B.; HAFERKAMP, I.; LEROCH, M.; EWALD, R.; BAUWE, H.; RIEMER, J.; HERRMANN, J. M.; EKKEHARD NEUHAUS, H. From endoplasmic reticulum to mitochondria: absence of the arabidopsis ATP antiporter endoplasmic reticulum adenylate transporter1 perturbs photorespiration. **The Plant Cell**, *[s.l.]*, v. 25, n. 7, p. 2647–2660, 2013.

HOLZEROVA, E. *et al.* Human thioredoxin 2 deficiency impairs mitochondrial redox homeostasis and causes early-onset neurodegeneration. **Brain**, v. 139, n. 2, p. 346–354, 2016.
HOTTA, C. T. From crops to shops: how agriculture can use circadian clocks. **Journal of Experimental Botany**, *[s.l.]*, *[s.n]* ago. 2021.

HOU, L.; LEHMANN, M.; GEIGENBERGER, P. Thioredoxin h 2 and o 1 Show Different Subcellular Localizations and Redox-Active Functions , and Are Extrachloroplastic Factors Influencing Photosynthetic Performance in Fluctuating Light, *[s.l.], [s.n]* 2021.

HUANG, J. *et al.* Self-protection of cytosolic malate dehydrogenase against oxidative stress in Arabidopsis. **Journal of Experimental Botany**, *[s.l.]*, v. 69, n. 14, p. 3491–3505, 2018.

HUANG, S.; AKEN, O. VAN; SCHWARZLÄNDER, M.; BELT, K.; MILLAR, A. H. The Roles of Mitochondrial Reactive Oxygen Species in Cellular Signaling and Stress Response in Plants. **Plant Physiology**, *[s.l.]*, v. 171, n. 3, p. 1551–1559, 2016.

HYUN, A. W.; JEONG, W.; CHANG, T. S.; KWANG, J. P.; SUNG, J. P.; JEONG, S. Y.; SUE, G. R. Reduction of cysteine sulfinic acid by sulfiredoxin is specific to 2-Cys peroxiredoxins. **Journal of Biological Chemistry**, *[s.l.]*, v. 280, n. 5, p. 3125–3128, 2005.

IGAMBERDIEV, A. U. Citrate valve integrates mitochondria into photosynthetic metabolism. **Mitochondrion**, *[s.l.]*, v. 52, p. 218–230, 2020.

IGAMBERDIEV, A. U.; BYKOVA, N. V.; LEA, P. J.; GARDESTRÖM, P. The role of photorespiration in redox and energy balance of photosynthetic plant cells: A study with a barley mutant deficient in glycine decarboxylase. **Physiologia Plantarum**, *[s.l.]*, v. 111, n. 4, p. 427–438, 2001.

IGAMBERDIEV, A. U.; EPRINTSEV, A. T. Organic Acids: The Pools of Fixed Carbon Involved in Redox Regulation and Energy Balance in Higher Plants. **Frontiers in Plant Science**, *[s.l.]*, v. 7, n. July, p. 1–15, 2016.

IGAMBERDIEV, A. U.; EPRINTSEV, A. T.; FEDORIN, D. N.; POPOV, V. N. Phytochrome-mediated regulation of plant respiration and photorespiration. **Plant, Cell and Environment**, *[s.l.]*, v. 37, n. 2, p. 290–299, 2014.

IGAMBERDIEV, A. U.; GARDESTRÖM, P. Regulation of NAD- and NADP-dependent isocitrate dehydrogenases by reduction levels of pyridine nucleotides in mitochondria and cytosol of pea leaves. **Biochimica et Biophysica Acta - Bioenergetics**, *[s.l.]*, v. 1606, n. 1–3, p. 117–125, 2003.

IGAMBERDIEV, A. U.; GARDESTRÖM, P. Mitochondrion Activity of the mitochondrial pyruvate dehydrogenase complex in plants is stimulated in the presence of malate. *[s.l.]*, v. 19, p. 184–190, 2014.

IQBAL, A.; YABUTA, Y.; TAKEDA, T.; NAKANO, Y.; SHIGEOKA, S. Hydroperoxide reduction by thioredoxin-specific glutathione peroxidase isoenzymes of Arabidopsis thaliana. **FEBS Journal**, *[s.l.]*, v. 273, n. 24, p. 5589–5597, 2006.

ISHIYAMA, K.; INOUE, E.; TABUCHI, M.; YAMAYA, T.; TAKAHASHI, H. Biochemical Background and Compartmentalized Functions of Cytosolic Glutamine Synthetase for Active

Ammonium Assimilation in Rice Roots. **Plant and Cell Physiology**, *[s.l.]*, v. 45, n. 11, p. 1640–1647, 2004.

JAKUPOGLU, C.; PRZEMECK, G. K. H.; SCHNEIDER, M.; MORENO, S. G.; MAYR, N.; HATZOPOULOS, A. K.; ANGELIS, M. H. DE; WURST, W.; BORNKAMM, G. W.; BRIELMEIER, M.; CONRAD, M. Cytoplasmic Thioredoxin Reductase Is Essential for Embryogenesis but Dispensable for Cardiac Development. **Molecular and Cellular Biology**, *[s.l.]*, v. 25, n. 5, p. 1980–1988, 2005.

JOHNSON, M. P.; RUBAN, A. V. Restoration of rapidly reversible photoprotective energy dissipation in the absence of PsbS protein by enhanced ΔpH. **Journal of Biological Chemistry**, *[s.l.]*, v. 286, n. 22, p. 19973–19981, 2011.

JONES, D. L.; HEALEY, J. R.; WILLETT, V. B.; FARRAR, J. F.; HODGE, A. Dissolved organic nitrogen uptake by plants - An important N uptake pathway? **Soil Biology and Biochemistry**, *[s.l.]*, v. 37, n. 3, p. 413–423, 2005.

JUNG, B. G. *et al.* A Chinese cabbage cDNA with high sequence identity to phospholipid hydroperoxide glutathione peroxidases encodes a novel isoform of thioredoxin-dependent peroxidase. **Journal of Biological Chemistry**, *[s.l.]*, v. 277, n. 15, p. 12572–12578, 2002.

KAMPFENKEL, K.; MONTAGU, M. VAN; INZÉ, D. **Extraction and determination of ascorbate and dehydroascorbate from plant tissueAnalytical Biochemistry**, 1995.
KEECH, O.; GARDESTRÖM, P.; KLECZKOWSKI, L. A.; ROUHIER, N. The redox control of photorespiration: from biochemical and physiological aspects to biotechnological considerations. **Plant Cell and Environment**, *[s.l.]*, v. 40, n. 4, p. 553–569, 2017.

KHUSH, G. S. What it will take to Feed 5.0 Billion Rice consumers in 2030. **Plant Molecular Biology**, *[s.l.]*, v. 59, n. 1, p. 1–6, 2005.

KIM, Y.; INGRAM, L. O.; SHANMUGAM, K. T. Dihydrolipoamide dehydrogenase mutation alters the NADH sensitivity of pyruvate dehydrogenase complex of Escherichia coli K-12. **Journal of Bacteriology**, *[s.l.]*, v. 190, n. 11, p. 3851–3858, 2008.

KNUESTING, J.; SCHEIBE, R. Small Molecules Govern Thiol Redox Switches. *[s.l.]*, v. xx, p. 1–14, 2018.

KOLLA, V. A.; VAVASSEUR, A.; RAGHAVENDRA, A. S. Hydrogen peroxide production is an early event during bicarbonate induced stomatal closure in abaxial epidermis of Arabidopsis. **Planta**, *[s.l.]*, v. 225, n. 6, p. 1421–1429, 2007.

KOPKA, J. *et al.* GMD@CSB.DB: The Golm metabolome database. **Bioinformatics**, *[s.l.]*, v. 21, n. 8, p. 1635–1638, 2005.

KOZAKOV, D.; BEGLOV, D.; BOHNUUD, T.; MOTTARELLA, S. E.; XIA, B.; HALL, D. R.; VAJDA, S. How good is automated protein docking? **Proteins: Structure, Function, and**

Bioinformatics, *[s.l.]*, v. 81, n. 12, p. 2159–2166, dez. 2013.

KROMER, S. Respiration During, *[s.l.]*, *[s.n.]* p. 45–70, 1995.

KURKCUOGLU, Z. *et al.* Performance of HADDOCK and a simple contact-based protein–ligand binding affinity predictor in the D3R Grand Challenge 2. **Journal of Computer-Aided Molecular Design**, *[s.l.]*, v. 32, n. 1, p. 175–185, 2018.

KWINTA, J.; BIELAWSKI, W. Glutamate dehydrogenase in higher plants. **Acta Physiologiae Plantarum**, *[s.l.]*, v. 20, n. 4, p. 453–463, 1998.

LALOI, C.; RAYAPURAM, N.; CHARTIER, Y.; GRIENENBERGER, J.-M.; BONNARD, G.; MEYER, Y. Identification and characterization of a mitochondrial thioredoxin system in plants. **Proceedings of the National Academy of Sciences**, *[s.l.]*, v. 98, n. 24, p. 14144–14149, 2001.

LE, X. H.; LEE, C.-P.; MILLAR, A. H. The mitochondrial pyruvate carrier (MPC) complex mediates one of three pyruvate-supplying pathways that sustain Arabidopsis respiratory metabolism. **The Plant Cell**, *[s.l.]*, v. 33, n. 8, p. 2776–2793, ago. 2021.

LE, X. H.; LEE, C. P.; MONACHELLO, D.; MILLAR, A. H. Metabolic evidence for distinct pyruvate pools inside plant mitochondria. **Nature Plants**, v. 8, n. 6, p. 694–705, 2022.
LE, X. H.; MILLAR, A. H. The diversity of substrates for plant respiration and how to optimize their use. **Plant Physiology**, *[s.l.]*, p. 1–17, 2022.

LEA, P. J.; BLACKWELL, R. D.; CHEN, F.-L.; HECHT, U. **Enzymes of Ammonia Assimilation**. [s.l.] ACADEMIC PRESS LIMITED, 1990. v. 3
LEAKEY, A. D. B.; AINSWORTH, E. A.; BERNACCHI, C. J.; ROGERS, A.; LONG, S. P.; ORT, D. R. Elevated CO2 effects on plant carbon, nitrogen, and water relations: six important lessons from FACE. **Journal of Experimental Botany**, *[s.l.]*, v. 60, n. 10, p. 2859–2876, 2009.

LEHMANN, M. M.; RINNE, K. T.; BLESSING, C.; SIEGWOLF, R. T. W.; BUCHMANN, N.; WERNER, R. A. Malate as a key carbon source of leaf dark-respired CO<inf>2</inf> across different environmental conditions in potato plants. **Journal of Experimental Botany**, *[s.l.]*, v. 66, n. 19, p. 5769–5781, 2015.

LEROCH, M.; NEUHAUS, H. E.; KIRCHBERGER, S.; ZIMMERMANN, S.; MELZER, M.; GERHOLD, J.; TJADEN, J. Identification of a novel adenine nucleotide transporter in the endoplasmic reticulum of Arabidopsis. **The Plant Cell**, v. 20, n. 2, p. 438–451, 2008.
LI, S. *et al.* Modulating plant growth–metabolism coordination for sustainable agriculture. **Nature**, *[s.l.]*, v. 560, n. 7720, p. 595–600, 15 ago. 2018.

LIMA, V. F. *et al.* Establishment of a GC-MS-based 13 C-positional isotopomer approach suitable for investigating metabolic fluxes in plant primary metabolism. **The Plant Journal**, *[s.l.]*, v. 108, n. 4, p. 1213–1233, nov. 2021.

LIMA, V. F.; SOUZA, L. P. DE; WILLIAMS, T. C. R.; FERNIE, A. R.; DALOSO, D. M. Gas

Chromatography–Mass Spectrometry-Based 13C-Labeling Studies in Plant Metabolomics. *In*: **Plant Metabolomics**. [s.l: s.n.]. v. 1778p. 47–58.

LINDÉN, P.; KEECH, O.; STENLUND, H.; GARDESTRÖM, P.; MORITZ, T. Reduced mitochondrial malate dehydrogenase activity has a strong effect on photorespiratory metabolism as revealed by13C labelling. **Journal of Experimental Botany**, *[s.l.]*, v. 67, n. 10, p. 3123–3135, 2016.

LISEC, J.; SCHAUER, N.; KOPKA, J.; WILLMITZER, L.; FERNIE, A. R. Gas chromatography mass spectrometry-based metabolite profiling in plants. **Nature Protocols**, *[s.l.]*, v. 1, n. 1, p. 387–396, 2006.

LISEC, J.; SCHAUER, N.; KOPKA, J.; WILLMITZER, L.; FERNIE, A. R. Gas chromatography mass spectrometry – based metabolite profiling in plants. *[s.l.]*, v. 1, n. 1, 2015.

LIU, X.; HU, B.; CHU, C. Nitrogen assimilation in plants: current status and future prospects. **Journal of Genetics and Genomics**, *[s.l.]*, v. 49, n. 5, p. 394–404, 2022.

LÓPEZ-CALCAGNO, P. E.; FISK, S.; BROWN, K. L.; BULL, S. E.; SOUTH, P. F.; RAINES, C. A. Overexpressing the H-protein of the glycine cleavage system increases biomass yield in glasshouse and field-grown transgenic tobacco plants. **Plant Biotechnology Journal**, *[s.l.]*, v. 17, n. 1, p. 141–151, 2018.

LÓPEZ-GRUESO, M. J.; GONZÁLEZ-OJEDA, R.; REQUEJO-AGUILAR, R.; MCDONAGH, B.; FUENTES-ALMAGRO, C. A.; MUNTANÉ, J.; BÁRCENA, J. A.; PADILLA, C. A. Thioredoxin and glutaredoxin regulate metabolism through different multiplex thiol switches. **Redox Biology**, *[s.l.]*, v. 21, n. November 2018, p. 101049, 2019.

LUEDEMANN, A.; STRASSBURG, K.; ERBAN, A.; KOPKA, J. TagFinder for the quantitative analysis of gas metabolite profiling experiments. **Bioinformatics**, *[s.l.]*, v. 24, n. 5, p. 732–737, 2008.

LUTZIGER, I.; OLIVER, D. J. Characterization of two cDNAs encoding mitochondrial lipoamide dehydrogenase from Arabidopsis. **Plant Physiology**, *[s.l.]*, v. 127, n. 2, p. 615–623, 2001.

MA, J.; WANG, S.; ZHU, X.; SUN, G.; CHANG, G.; LI, L.; HU, X.; ZHANG, S.; ZHOU, Y.; SONG, C.-P.; HUANG, J. Major episodes of horizontal gene transfer drove the evolution of land plants. **Molecular Plant**, *[s.l.]*, v. 15, n. 5, p. 857–871, 2022.

MARCHAL, C.; DELORME-HINOUX, V.; BARIAT, L.; SIALA, W.; BELIN, C.; SAEZ-VASQUEZ, J.; RIONDET, C.; REICHHELD, J. P. NTR/NRX define a new thioredoxin system in the nucleus of arabidopsis thaliana cells. **Molecular Plant**, *[s.l.]*, v. 7, n. 1, p. 30–44, 2014.

MARCUS, F.; CHAMBERLAIN, S. H.; CHU, C.; MASIARZ, F. R.; SHIN, S.; YEE, B. C.; BUCHANAN, B. B. Plant thioredoxin h: an animal-like thioredoxin occurring in multiple cell

compartments. **Archives of Biochemistry and Biophysics**, *[s.l.]*, v. 287, n. 1, p. 195–198, 1991.
MARTÍ, M. C.; JIMÉNEZ, A.; SEVILLA, F. Thioredoxin Network in Plant Mitochondria

Cysteine S-Posttranslational Modifications and Stress Conditions. **Frontiers in Plant Science**, v. 11, n. September, *[s.l.]*,p. 1–20, 2020.

MARTINELLI, T.; WHITTAKER, A.; BOCHICCHIO, A.; VAZZANA, C.; SUZUKI, A.; MASCLAUX-DAUBRESSE, C. Amino acid pattern and glutamate metabolism during dehydration stress in the "resurrection" plant Sporobolus stapfianus: A comparison between desiccation-sensitive and desiccation-tolerant leaves. **Journal of Experimental Botany**, *[s.l.]*, v. 58, n. 11, p. 3037–3046, 2007.

MARTY, L.; BAUSEWEIN, D.; MÜLLER, C.; BANGASH, S. A. K.; MOSELER, A.; SCHWARZLÄNDER, M.; MÜLLER-SCHÜSSELE, S. J.; *et al.* Arabidopsis glutathione reductase 2 is indispensable in plastids, while mitochondrial glutathione is safeguarded by additional reduction and transport systems. **New Phytologist**, *[s.l.]*, v. 224, n. 4, p. 1569–1584, 2019.

MARTY, L.; BAUSEWEIN, D.; MÜLLER, C.; BANGASH, S. A. K.; MOSELER, A.; SCHWARZLÄNDER, M.; MÜLLER-SCHÜSSELE, S. J.; *et al.* Arabidopsis glutathione reductase 2 is indispensable in plastids, while mitochondrial glutathione is safeguarded by additional reduction and transport systems. **New Phytologist**, *[s.l.]*, v. 224, n. 4, p. 1569–1584, 28 dez. 2019.

MARTY, L.; SIALA, W.; SCHWARZLANDER, M.; FRICKER, M. D.; WIRTZ, M.; SWEETLOVE, L. J.; MEYER, Y.; MEYER, A. J.; REICHHELD, J.-P.; HELL, R. The NADPH-dependent thioredoxin system constitutes a functional backup for cytosolic glutathione reductase in Arabidopsis. **Proceedings of the National Academy of Sciences**, *[s.l.]*, v. 106, n. 22, p. 9109–9114, 2009.

MARTY, LAURENT; SIALA, W.; SCHWARZLÄNDER, M.; FRICKER, M. D.; WIRTZ, M.; SWEETLOVE, L. J.; MEYER, Y.; MEYER, A. J.; REICHHELD, J.-P.; HELL, R. The NADPH-dependent thioredoxin system constitutes a functional backup for cytosolic glutathione reductase in Arabidopsis. **Proceedings of the National Academy of Sciences of the United States of America**, *[s.l.]*, v. 106, n. 22, p. 9109–9114, 2009.

MASCLAUX-DAUBRESSE, C.; DANIEL-VEDELE, F.; DECHORGNAT, J.; CHARDON, F.; GAUFICHON, L.; SUZUKI, A. Nitrogen uptake, assimilation and remobilization in plants: Challenges for sustainable and productive agriculture. **Annals of Botany**, *[s.l.]*, v. 105, n. 7, p. 1141–1157, 2010.

MATOH, T.; IDA, S.; TAKAHASHI, E. (Pisum sativum. v. 21, n. 8, p. 1461–1474, 1980.
MAURICE CHEUNG, C. Y.; POOLMAN, M. G.; FELL, D. A.; GEORGE RATCLIFFE, R.; SWEETLOVE, L. J. A diel flux balance model captures interactions between light and dark metabolism during day-night cycles in C3 and crassulacean acid metabolism leaves. **Plant Physiology**, *[s.l.]*, v. 165, n. 2, p. 917–929, 2014.

MAX, I.; IGAMBERDIEV, A. U.; BYKOVA, N. V; FINKEMEIER, I.; ALLAN, G. Matrix Redox Physiology Governs the Regulation of Plant Mitochondrial Metabolism through Post-Translational Protein Modifications. *[s.l.]*, *[s.n.]*, 2020.

MCNALLY, S. F.; HIREL, B.; GADAL, P.; MANN, A F.; STEWART, G. R. Glutamine Synthetases of Higher Plants : Evidence for a Specific Isoform Content Related to Their Possible Physiological Role and Their Compartmentation within the Leaf. **Plant physiology**, *[s.l.]*, v. 72, n. 1, p. 22–25, 1983.

MEDEIROS, D. B. *et al.* Impaired Malate and Fumarate Accumulation Due to the Mutation of the Tonoplast Dicarboxylate Transporter Has Little Effects on Stomatal Behavior. **Plant Physiology**, *[s.l.]*, v. 175, n. 3, p. 1068–1081, nov. 2017.

MEDEIROS, D. B.; MARTINS, S. C. V.; CAVALCANTI, J. H. F.; DALOSO, D. M.; MARTINOIA, E.; NUNES-NESI, A.; DAMATTA, F. M.; FERNIE, A. R.; ARAÚJO, W. L. Enhanced Photosynthesis and Growth in *atquac1* Knockout Mutants Are Due to Altered Organic Acid Accumulation and an Increase in Both Stomatal and Mesophyll Conductance. **Plant Physiology**, *[s.l.]*, v. 170, n. 1, p. 86–101, 2016.

MELO, P. M.; SILVA, L. S.; RIBEIRO, I.; SEABRA, A. R.; CARVALHO, H. G. Glutamine synthetase is a molecular target of nitric oxide in root nodules of Medicago truncatula and is regulated by tyrosine nitration. **Plant Physiology**, *[s.l.]*, v. 157, n. 3, p. 1505–1517, 2011.

MENG, LING; WONG, J. H.; FELDMAN, L. J.; LEMAUX, P. G.; BUCHANAN, B. B. A membrane-associated thioredoxin required for plant growth moves from cell to cell, suggestive of a role in intercellular communication. **Proceedings of the National Academy of Sciences of the United States of America**, *[s.l.]*, v. 107, n. 8, p. 3900–3905, 2010.

MENG, L.; WONG, J. H.; FELDMAN, L. J.; LEMAUX, P. G.; BUCHANAN, B. B. A membrane-associated thioredoxin required for plant growth moves from cell to cell, suggestive of a role in intercellular communication. **Proceedings of the National Academy of Sciences**, *[s.l.]*, v. 107, n. 8, p. 3900–3905, 2010.

MEYER, A. J.; DREYER, A.; UGALDE, J. M.; FEITOSA-ARAUJO, E.; DIETZ, K. J.; SCHWARZLÄNDER, M. Shifting paradigms and novel players in Cys-based redox regulation and ROS signaling in plants - And where to go next. **Biological Chemistry**, *[s.l.]*, v. 402, n. 3, p. 399–423, 2021a.

Shifting paradigms and novel players in Cys-based redox regulation and ROS signaling in plants - And where to go next. **Biological Chemistry**, *[s.l.]*, v. 402, n. 3, p. 399–423, 2021b.

MEYER, Y.; BELIN, C.; DELORME-HINOUX, V.; REICHHELD, J.-P.; RIONDET, C. Thioredoxin and Glutaredoxin Systems in Plants: Molecular Mechanisms, Crosstalks, and Functional Significance. **Antioxidants & Redox Signaling**, *[s.l.]*, v. 17, n. 8, p. 1124–1160, 2012.

MEYER, Y.; BUCHANAN, B. B.; VIGNOLS, F.; REICHHELD, J.-P. Thioredoxins and Glutaredoxins: Unifying Elements in Redox Biology. **Annual Review of Genetics**, *[s.l.]*, v. 43, n. 1, p. 335–367, 2009.

MEYER, Y.; SIALA, W.; BASHANDY, T.; RIONDET, C.; VIGNOLS, F.; REICHHELD, J. P. Glutaredoxins and thioredoxins in plants. **Biochimica et Biophysica Acta - Molecular Cell Research**, *[s.l.]*, v. 1783, n. 4, p. 589–600, 2008.

MICHELET, L.; ZAFFAGNINI, M.; MORISSE, S.; SPARLA, F.; PÉREZ-PÉREZ, M. E.; FRANCIA, F.; DANON, A.; MARCHAND, C. H.; FERMANI, S.; TROST, P.; LEMAIRE, S. D. Redox regulation of the Calvin-Benson cycle: something old, something new. **Frontiers in plant science**, *[s.l.]*, v. 4, n. November, p. 470, 2013.

MITTLER, R.; VANDERAUWERA, S.; GOLLERY, M.; BREUSEGEM, F. VAN. Reactive oxygen gene network of plants. **Trends in Plant Science**, *[s.l.]*, v. 9, n. 10, p. 490–498, 2004.

MITTLER, R.; VANDERAUWERA, S.; SUZUKI, N.; MILLER, G.; TOGNETTI, V. B.; VANDEPOELE, K.; GOLLERY, M.; SHULAEV, V.; BREUSEGEM, F. VAN. ROS signaling: The new wave? **Trends in Plant Science**, *[s.l.]*, v. 16, n. 6, p. 300–309, 2011.

MOCK, H. P.; DIETZ, K. J. Redox proteomics for the assessmMock, H.P., Dietz, K.J., 2016. Redox proteomics for the assessment of redox-related posttranslational regulation in plants. Biochim. Biophys. Acta - Proteins Proteomics 1864, 967–973.

https://doi.org/10.1016/j.bbapap.2016.0. **Biochimica et Biophysica Acta - Proteins and Proteomics**, *[s.l.]*, v. 1864, n. 8, p. 967–973, 2016.

MØLLER, I. M.; RASMUSSON, A. G. The role of NADP in the mitochondrial matrix. **Trends in Plant Science**, *[s.l.]*, v. 3, n. 1, p. 21–27, 1998.

MONROE, J. G. *et al.* Mutation bias reflects natural selection in Arabidopsis thaliana. **Nature**, *[s.l.]*, v. 602, n. 7895, p. 101–105, 2022.

MONTRICHARD, F.; ALKHALFIOUI, F.; YANO, H.; VENSEL, W. H.; HURKMAN, W. J.; BUCHANAN, B. B. Thioredoxin targets in plants: The first 30 years. **Journal of Proteomics**, *[s.l.]*, v. 72, n. 3, p. 452–474, 2009.

MOONEY, B. P.; MIERNYK, J. A.; RANDALL, D. D. The complex fate of A-Ketoacids. **Annual Review of Plant Biology**, *[s.l.]*, v. 53, n. 1, p. 357–375, 2002.

MOSELER, A.; ALLER, I.; WAGNER, S.; NIETZEL, T.; PRZYBYLA-TOSCANO, J.; MÜHLENHOFF, U. The mitochondrial monothiol glutaredoxin S15 is essential for iron-sulfur protein maturation in Arabidopsis thaliana. *[s.l.]*, *[s.n.]*, 2015.

MOTOHASHI, K.; KONDOH, A.; STUMPP, M. T.; HISABORI, T. Comprehensive survey of proteins targeted by chloroplast thioredoxin. **Proceedings of the National Academy of Sciences**

of the United States of America, *[s.l.]*, v. 98, n. 20, p. 11224–11229, 2001.

MURI, J.; HEER, S.; MATSUSHITA, M.; POHLMEIER, L.; TORTOLA, L.; FUHRER, T.; CONRAD, M.; ZAMBONI, N.; KISIELOW, J.; KOPF, M. The thioredoxin-1 system is essential for fueling DNA synthesis during T-cell metabolic reprogramming and proliferation. **Nature Communications**, *[s.l.]*, v. 9, n. 1, p. 1–16, 2018.

NAKANO, Y.; ASADA, K. Hydrogen peroxide is scavenged by ascorbate-specific peroxidase in spinach chloroplasts. **Plant Cell Physiology**, *[s.l.]*, v. 22, n. 5, p. 867–880, 1981.

NAPOLITANO, S.; REBER, R. J.; RUBINI, M.; GLOCKSHUBER, R. Functional analyses of ancestral thioredoxins provide insights into their evolutionary history. **Journal of Biological Chemistry**, *[s.l.]*, v. 294, n. 38, p. 14105–14118, 2019.

NARANJO, B.; MIGNÉE, C.; KRIEGER-LISZKAY, A.; HORNERO-MÉNDEZ, D.; GALLARDO-GUERRERO, L.; CEJUDO, F. J.; LINDAHL, M. The chloroplast NADPH thioredoxin reductase C, NTRC, controls non-photochemical quenching of light energy and photosynthetic electron transport in Arabidopsis. **Plant Cell and Environment**, *[s.l.]*, v. 39, n. 4, p. 804–822, 2016.

NIETZEL, T.; MOSTERTZ, J.; HOCHGRÄFE, F.; SCHWARZLÄNDER, M. Redox regulation of mitochondrial proteins and proteomes by cysteine thiol switches. **Mitochondrion**, *[s.l.]*, v. 33, p. 72–83, 2017.

NIKKANEN, L.; TOIVOLA, J.; RINTAMÄKI, E. Crosstalk between chloroplast thioredoxin systems in regulation of photosynthesis. **Plant Cell and Environment**, *[s.l.]*, v. 39, n. 8, p. 1691–1705, 2016.

NOGUCHI, K.; YOSHIDA, K. Interaction between photosynthesis and respiration in illuminated leaves. **Mitochondrion**, *[s.l.]*, v. 8, n. 1, p. 87–99, 2008.

NUNES-NESI, A.; ARAÚJO, W. L.; OBATA, T.; FERNIE, A. R. Regulation of the mitochondrial tricarboxylic acid cycle. **Current Opinion in Plant Biology**, *[s.l.]*, v. 16, n. 3, p. 335–343, 2013.

NUNES-NESI, A.; CARRARI, F.; GIBON, Y.; SULPICE, R.; LYTOVCHENKO, A.; FISAHN, J.; GRAHAM, J.; RATCLIFFE, R. G.; SWEETLOVE, L. J.; FERNIE, A. R. Deficiency of mitochondrial fumarase activity in tomato plants impairs photosynthesis via an effect on stomatal function. **Plant Journal**, *[s.l.]*, v. 50, n. 6, p. 1093–1106, 2007.

O'NEAL, D.; JOY, K. W. Glutamine Synthetase of Pea Leaves. **Plant physiology**, *[s.l.]*, v. 54, n. 5, p. 773–779, 1974.

OA, G. W.; PALMIERI, M. C.; LINDERMAYR, C.; BAUWE, H.; STEINHAUSER, C.; DURNER, J. Regulation of Plant Glycine Decarboxylase by. *[s.l.]*, v. 152, n. March, p. 1514–1528, 2010.

OBATA, T. Toward an evaluation of metabolite channeling in vivo. **Current Opinion in Biotechnology**, *[s.l.]*, v. 64, n. Figure 2, p. 55–61, 2020.

OBATA, T.; FLORIAN, A.; TIMM, S.; BAUWE, H.; FERNIE, A. R. On the metabolic interactions of (photo)respiration. **Journal of Experimental Botany**, *[s.l.]*, v. 67, n. 10, p. erw128, 2016.

OBATA, T.; MATTHES, A.; KOSZIOR, S.; LEHMANN, M.; ARAÚJO, W. L.; BOCK, R.; SWEETLOVE, L. J.; FERNIE, A. R. Phytochemistry Alteration of mitochondrial protein complexes in relation to metabolic regulation under short-term oxidative stress in Arabidopsis seedlings. **Phytochemistry**, *[s.l.]*, v. 72, n. 10, p. 1081–1091, 2011.

OJEDA, V.; PÉREZ-RUIZ, J. M.; CEJUDO, F. J. 2-Cys peroxiredoxins participate in the oxidation of chloroplast enzymes in the dark. **Molecular Plant**, *[s.l.]*, *[s.n.]*, 2018.

OJEDA, V.; PÉREZ-RUIZ, J. M.; GONZÁLEZ, M.; NÁJERA, V. A.; SAHRAWY, M.; SERRATO, A. J.; GEIGENBERGER, P.; CEJUDO, F. J. NADPH Thioredoxin Reductase C and Thioredoxins Act Concertedly in Seedling Development. **Plant Physiology**, *[s.l.]*, v. 174, n. 3, p. 1436–1448, 2017.

OLIVEIRA, I. C.; CORUZZI, G. M. Carbon and amino acids reciprocally modulate the expression of glutamine synthetase in Arabidopsis. **Plant Physiology**, *[s.l.]*, v. 121, n. 1, p. 301–309, 1999.

OLIVER, D. J. The Glycine Decarboxylase Complex from Plant Mitochondria. **Annual Review of Plant Physiology and Plant Molecular Biology**, *[s.l.]*, v. 45, n. 1, p. 323–337, jun. 1994.

OPEN, O. I.; SELINSKI, J.; HARTMANN, A.; KORDES, A.; DECKERS-HEBESTREIT, G.; WHELAN, J. Analysis of Posttranslational Activation of Alternative, *[s.l.]*, v. 174, n. August, p. 2113–2127, 2017.

ORTEGA, J. L.; ROCHE, D.; SENGUPTA-GOPALAN, C. Oxidative turnover of soybean root glutamine synthetase. In vitro and in vivo studies. **Plant Physiology**, *[s.l.]*, v. 119, n. 4, p. 1483–1495, 1999.

OZYIGIT, I. I.; FILIZ, E.; VATANSEVER, R.; KURTOGLU, K. Y.; KOC, I.; ÖZTÜRK, M. X.; ANJUM, N. A. Identification and Comparative Analysis of H2O2-Scavenging Enzymes (Ascorbate Peroxidase and Glutathione Peroxidase) in Selected Plants Employing Bioinformatics Approaches. **Frontiers in Plant Science**, *[s.l.]*, v. 7, n. March, p. 1–23, 2016.

PANG, Z.; CHONG, J.; ZHOU, G.; LIMA MORAIS, D. A. DE; CHANG, L.; BARRETTE, M.; GAUTHIER, C.; JACQUES, P. É.; LI, S.; XIA, J. MetaboAnalyst 5.0: Narrowing the gap between raw spectra and functional insights. **Nucleic Acids Research**, *[s.l.]*, v. 49, n. W1, p. W388–W396, 2021.

PÉREZ-RUIZ, J. M.; NARANJO, B.; OJEDA, V.; GUINEA, M.; CEJUDO, F. J. NTRC-

dependent redox balance of 2-Cys peroxiredoxins is needed for optimal function of the photosynthetic apparatus. **Proceedings of the National Academy of Sciences**, *[s.l.]*, v. 114, n. 45, p. 12069–12074, 2017.

PINTÓ-MARIJUAN, M.; MUNNÉ-BOSCH, S. Photo-oxidative stress markers as a measure of abiotic stress-induced leaf senescence: Advantages and limitations. **Journal of Experimental Botany**, *[s.l.]*, v. 65, n. 14, p. 3845–3857, 2014.

PLAXTON, W. C.; PODESTÁ, F. E. The functional organization and control of plant respiration. **Critical Reviews in Plant Sciences**, *[s.l.]*, v. 25, n. 2, p. 159–198, 2006.

POPOV, V. N.; EPRINTSEV, A. T.; FEDORIN, D. N.; IGAMBERDIEV, A. U. Succinate dehydrogenase in Arabidopsis thaliana is regulated by light via phytochrome A. **FEBS Letters**, *[s.l.]*, v. 584, n. 1, p. 199–202, 2010.

PORTO, N. P.; BRET, R. S. C.; SOUZA, P. V. L.; SILVIO, A. C.; MEDEIROS, D. B.; FERNIE, A. R.; DALOSO, D. M. Plant Physiology and Biochemistry Thioredoxins regulate the metabolic fluxes throughout the tricarboxylic acid cycle and associated pathways in a light-independent manner. *[s.l.]*, v. 193, n. July, p. 36–49, 2022.

PRACHAROENWATTANA, I.; ZHOU, W.; KEECH, O.; FRANCISCO, P. B.; UDOMCHALOTHORN, T.; TSCHOEP, H.; STITT, M.; GIBON, Y.; SMITH, S. M. Arabidopsis has a cytosolic fumarase required for the massive allocation of photosynthate into fumaric acid and for rapid plant growth on high nitrogen. **Plant Journal**, *[s.l.]*, v. 62, n. 5, p. 785–795, 2010.

RASMUSSON, A. G.; ESCOBAR, M. A. Light and diurnal regulation of plant respiratory gene expression. **Physiologia Plantarum**, *[s.l.]*, v. 129, n. 1, p. 57–67, 2007.

REICHHELD, J.-P.; KHAFIF, M.; RIONDET, C.; DROUX, M.; BONNARD, G.; MEYER, Y. Inactivation of thioredoxin reductases reveals a complex interplay between thioredoxin and glutathione pathways in Arabidopsis development. **The Plant cell**, *[s.l.]*, v. 19, n. 6, p. 1851–1865, 2007.

REICHHELD, J. P.; MEYER, E.; KHAFIF, M.; BONNARD, G.; MEYER, Y. AtNTRB is the major mitochondrial thioredoxin reductase in Arabidopsis thaliana. **FEBS Letters**, *[s.l.]*, v. 579, n. 2, p. 337–342, 2005.

REINHOLDT, O.; BAUWE, H.; HAGEMANN, M.; TIMM, S. Redox-regulation of mitochondrial metabolism through thioredoxin o1 facilitates light induction of photosynthesis. **Plant Signaling and Behavior**, *[s.l.]*, v. 14, n. 12, 2019.

REINHOLDT, O.; SCHWAB, S.; ZHANG, Y.; REICHHELD, J.; FERNIE, A. R.; HAGEMANN, M.; TIMM, S. Redox-Regulation of Photorespiration through Mitochondrial Thioredoxin o1. **Plant Physiology**, *[s.l.]*, v. 181, n. 2, p. 442–457, out. 2019.

REINHOLDT, O.; SCHWAB, S.; ZHANG, Y.; REICHHELD, J. P.; FERNIE, A. R.; HAGEMANN, M.; TIMM, S. Redox-regulation of photorespiration through mitochondrial thioredoxin O1. **Plant Physiology**, *[s.l.]*, v. 181, n. 2, p. 442–457, 2019.

REN, R.; WANG, H.; GUO, C.; ZHANG, N.; ZENG, L.; CHEN, Y.; MA, H.; QI, J. Widespread Whole Genome Duplications Contribute to Genome Complexity and Species Diversity in Angiosperms. **Molecular Plant**, *[s.l.]*, v. 11, n. 3, p. 414–428, 2018.

RHEE, S. G.; CHOCK, P. B.; STADTMAN, E. R. Regulation of Escherichia coli glutamine synthetase. **Advances in enzymology and related areas of molecular biology**, *[s.l.]*, v. 62, p. 37–92, 1989.

RHOADS, D. M.; UMBACH, A. L.; SWEET, C. R.; LENNON, A. M.; RAUCH, G. S.; SIEDOW, J. N. Regulation of the cyanide-resistant alternative oxidase of plant mitochondria. **Journal of Biological Chemistry**, *[s.l.]*, v. 273, n. 46, p. 30750–30756, 1998.

ROUHIER, N.; GELHAYE, E.; JACQUOT, J. P. Plant glutaredoxins: Still mysterious reducing systems. **Cellular and Molecular Life Sciences**, *[s.l.]*, v. 61, n. 11, p. 1266–1277, 2004.

ROWLEY, J. A.; TAYLOR, A. O. Plants Under Climatic Stress. **New Phytologist**, *[s.l.]*, v. 71, n. 3, p. 477–481, 1972.

RUBAN, A. V. Evolution under the sun: Optimizing light harvesting in photosynthesis. **Journal of Experimental Botany**, *[s.l.]*, v. 66, n. 1, p. 7–23, 2015.

SCHMIDTMANN, E.; KÖNIG, A.-C.; ORWAT, A.; LEISTER, D.; HARTL, M.; FINKEMEIER, I. Redox regulation of Arabidopsis mitochondrial citrate synthase. **Molecular plant**, *[s.l.]*, v. 7, n. 1, p. 156–69, 2014.

SCHÜRMANN, P.; BUCHANAN, B. B. The ferredoxin/thioredoxin system of oxygenic photosynthesis. **Antioxidants & redox signaling**, *[s.l.]*, v. 10, n. 7, p. 1235–74, 2008.

SCHWARZLÄNDER, M.; FUCHS, P. Keeping mitochondrial Alternative Oxidase reduced and active in vivo does not require Thioredoxin o1. **Plant and Cell Physiology**, *[s.l.]*, *[s.n.]*, 2019.

SEGER, M.; ORTEGA, J. L.; BAGGA, S.; GOPALAN, C.-S. Repercussion of mesophyll-specific overexpression of a soybean cytosolic glutamine synthetase gene in alfalfa (Medicago sativa L.) and tobacco (Nicotiana tabaccum L.). **Plant Science**, *[s.l.]*, v. 176, n. 1, p. 119–129, jan. 2009.

SELINSKI, J.; HARTMANN, A.; KORDES, A.; DECKERS-HEBESTREIT, G.; WHELAN, J.; SCHEIBE, R. Analysis of Posttranslational Activation of Alternative Oxidase Isoforms. **Plant Physiology**, *[s.l.]*, v. 174, n. 4, p. 2113–2127, 2017.

SELINSKI, J.; SCHEIBE, R. Malate valves: old shuttles with new perspectives. **Plant Biology**, *[s.l.]*, v. 21, p. 21–30, 2019.

SELINSKI, J.; SCHEIBE, R.; DAY, D. A.; WHELAN, J. Alternative oxidase is positive for plant performance. **Trends in Plant Science**, *[s.l.]*, v. 23, n. 7, p. 588–597, 2018.

SERRATO, A. J.; PÉREZ-RUIZ, J. M.; SPÍNOLA, M. C.; CEJUDO, F. J. A novel NADPH thioredoxin reductase, localised in the chloroplast, which deficiency causes hypersensitivity to abiotic stress in Arabidopsis thaliana. **Journal of Biological Chemistry**, *[s.l.]*, v. 279, n. 42, p. 43821–43827, 2004.

SIEDOW, J. N. Covalent and Noncovalent Dimers of the Cyanide-Resistant Alternative Oxidase Protein in Higher Plant Mitochondria and Their Relationship to Enzyme Activity '. *[s.l.]*, *[s.n.]*, p. 845–854, 1993.

SIEDOW, J. N.; UMBACH, A. L. The mitochondrial cyanide-resistant oxidase: Structural conservation amid regulatory diversity. **Biochimica et Biophysica Acta - Bioenergetics**, *[s.l.]*, v. 1459, n. 2–3, p. 432–439, 2000.

SMIRNOFF, N.; ARNAUD, D. Hydrogen peroxide metabolism and functions in plants. **New Phytologist**, *[s.l.]*, v. 221, n. 3, p. 1197–1214, 2019.

SONI, N.; MADHUSUDHAN, M. S. Computational modeling of protein assemblies. **Current Opinion in Structural Biology**, *[s.l.]*, v. 44, p. 179–189, 2017.

SOUSA, R. H. V.; CARVALHO, F. E. L.; LIMA-MELO, Y.; ALENCAR, V. T. C. B.; DALOSO, D. M.; MARGIS-PINHEIRO, M.; KOMATSU, S.; SILVEIRA, J. A. G. Impairment of peroxisomal APX and CAT activities increases protection of photosynthesis under oxidative stress. **Journal of Experimental Botany**, *[s.l.]*, v. 70, n. 2, p. 627–639, 2019.

SOUSA, R. H. V.; CARVALHO, F. E. L.; RIBEIRO, C. W.; PASSAIA, G.; CUNHA, J. R.; LIMA-MELO, Y.; MARGIS-PINHEIRO, M.; SILVEIRA, J. A. G. Peroxisomal APX knockdown triggers antioxidant mechanisms favourable for coping with high photorespiratory H2O2 induced by CAT deficiency in rice. **Plant Cell and Environment**, *[s.l.]*, v. 38, n. 3, p. 499–513, mar. 2015.

SOUZA, L. P. DE; GARBOWICZ, K.; BROTMAN, Y.; TOHGE, T.; FERNIE, A. R. The acetate pathway supports flavonoid and lipid biosynthesis in Arabidopsis1[open]. **Plant Physiology**, *[s.l.]*, v. 182, n. 2, p. 857–869, 2020.

SOUZA, PAULO V.L.; LIMA-MELO, Y.; CARVALHO, F. E.; REICHHELD, J. P.; FERNIE, A. R.; SILVEIRA, J. A. G.; DALOSO, D. M. Function and compensatory mechanisms among the components of the chloroplastic redox network. **Critical Reviews in Plant Sciences**, *[s.l.]*, v. 0, n. 0, p. 1–28, 2018.

Not just a circle: Flux modes in the plant TCA cycle. **Trends in Plant Science**, *[s.l.]*, v. 15, n. 8, p. 462–470, 2010.

SWEETLOVE, L. J.; FERNIE, A. R. The role of dynamic enzyme assemblies and substrate

channelling in metabolic regulation. **Nature Communications**, *[s.l.]*, v. 9, n. 1, 2018.

SWEETLOVE, L. J.; NIELSEN, J.; FERNIE, A. R. Engineering central metabolism – a grand challenge for plant biologists. **Plant Journal**, *[s.l.]*, v. 90, n. 4, p. 749–763, 2017.

SZAL, E. N. A.; PODGÓRSKA, A. The role of mitochondria in leaf nitrogen metabolism OF N. *[s.l.]*, *[s.n.]*, p. 1756–1768, 2012.

SZECOWKA, M. *et al.* Metabolic Fluxes in an Illuminated Arabidopsis Rosette. **The Plant Cell**, *[s.l.]*, v. 25, n. 2, p. 694–714, 2013.

TAIRA, M.; VALTERSSON, U.; BURKHARDT, B.; LUDWIG, R. A. Arabidopsis thaliana GLN2-encoded glutamine synthetase is dual targeted to leaf mitochondria and chloroplasts. **Plant Cell**, *[s.l.]*, v. 16, n. 8, p. 2048–2058, 2004.

TAKAHASHI, S.; MILWARD, S. E.; YAMORI, W.; EVANS, J. R.; HILLIER, W.; BADGER, M. R. The Solar Action Spectrum of Photosystem II Damage. **Plant Physiology**, *[s.l.]*, v. 153, n. 3, p. 988–993, 2010.

TCHERKEZ, G.; BOEX-FONTVIEILLE, E.; MAHÉ, A.; HODGES, M. Respiratory carbon fluxes in leaves. **Current Opinion in Plant Biology**, *[s.l.]*, v. 15, n. 3, p. 308–314, 2012.

TCHERKEZ, G.; CORNIC, G.; BLIGNY, R.; GOUT, E.; GHASHGHAIE, J. In vivo respiratory metabolism of illuminated leaves. **Plant Physiology**, *[s.l.]*, v. 138, n. 3, p. 1596–1606, 2005.

TCHERKEZ, G.; MAHÉ, A.; GAUTHIER, P.; MAUVE, C.; GOUT, E.; BLIGNY, R.; CORNIC, G.; HODGES, M. In folio respiratory fluxomics revealed by 13C isotopic labeling and H/D isotope effects highlight the noncyclic nature of the tricarboxylic acid "cycle" in illuminated leaves. **Plant Physiology**, *[s.l.]*, v. 151, n. 2, p. 620–630, 2009.

TEPPERMAN, J. M.; HUDSON, M. E.; KHANNA, R.; ZHU, T.; CHANG, S. H.; WANG, X.; QUAIL, P. H. Expression profiling of phyB mutant demonstrates substantial contribution of other phytochromes to red-light-regulated gene expression during seedling de-etiolation. **The Plant Journal**, *[s.l.]*, v. 38, n. 5, p. 725–739, 2004.

THOMSEN, H. C.; ERIKSSON, D.; MØLLER, I. S.; SCHJOERRING, J. K. Cytosolic glutamine synthetase: A target for improvement of crop nitrogen use efficiency? **Trends in Plant Science**, *[s.l.]*, v. 19, n. 10, p. 656–663, 2014.

THORMÄHLEN, I.; MEITZEL, T.; GROYSMAN, J.; ÖCHSNER, A. B.; ROEPENACK-LAHAYE, E. VON; NARANJO, B.; CEJUDO, F. J.; GEIGENBERGER, P. Thioredoxin f1 and NADPH-dependent thioredoxin reductase C have overlapping functions in regulating photosynthetic metabolism and plant growth in response to varying light conditions. **Plant Physiology**, *[s.l.]*, v. 169, n. November, p. pp.01122.2015, 2015a.

Thioredoxin f1 and NADPH-dependent thioredoxin reductase C have overlapping functions in

regulating photosynthetic metabolism and plant growth in response to varying light conditions. **Plant Physiology**, *[s.l.]*, v. 169, n. November, p. pp.01122.2015, 2015b.

THORMÄHLEN, I.; ZUPOK, A.; RESCHER, J.; LEGER, J.; WEISSENBERGER, S.; GROYSMAN, J.; ORWAT, A.; CHATEL-INNOCENTI, G.; ISSAKIDIS-BOURGUET, E.; ARMBRUSTER, U.; GEIGENBERGER, P. Thioredoxins Play a Crucial Role in Dynamic Acclimation of Photosynthesis in Fluctuating Light. **Molecular Plant**, *[s.l.]*, v. 10, n. 1, p. 168–182, 2017.

TIMM, S.; FLORIAN, A.; ARRIVAULT, S.; STITT, M.; FERNIE, A. R.; BAUWE, H. Glycine decarboxylase controls photosynthesis and plant growth. **FEBS Letters**, *[s.l.]*, v. 586, n. 20, p. 3692–3697, 2012.

TIMM, S.; FLORIAN, A.; FERNIE, A. R.; BAUWE, H. The regulatory interplay between photorespiration and photosynthesis. **Journal of Experimental Botany**, *[s.l.]*, v. 67, n. 10, p. erw083, 2016.

TIMM, S.; FLORIAN, A.; JAHNKE, K.; NUNES-NESI, A.; FERNIE, A. R.; BAUWE, H. The hydroxypyruvate-reducing system in Arabidopsis: multiple enzymes for the same end. **Plant Physiology**, *[s.l.]*, v. 155, n. 2, p. 694–705, 2011.

TIMM, S.; GIESE, J.; ENGEL, N.; WITTMISS, M.; FLORIAN, A.; FERNIE, A. R.; BAUWE, H. T-protein is present in large excess over the other proteins of the glycine cleavage system in leaves of Arabidopsis. **Planta**, *[s.l.]*, v. 247, n. 1, p. 41–51, 2018.

TIMM, S.; HAGEMANN, M. Photorespiration – how is it regulated and regulates overall plant metabolism ?*[s.l.]*,*[s.n.]*, 2021.

TIMM, S.; WITTMISS, M.; GAMLIEN, S.; EWALD, R.; FLORIAN, A.; FRANK, M.; WIRTZ, M.; HELL, R.; FERNIE, A. R.; BAUWE, H. Mitochondrial Dihydrolipoyl Dehydrogenase Activity Shapes Photosynthesis and Photorespiration of *Arabidopsis thaliana*. **The Plant Cell**, *[s.l.]*, v. 27, n. 7, p. 1968–1984, 2015.

TISCHNER, R.; SCHMIDT, A. A Thioredoxin-Mediated Activation of Glutamine Synthetase and Glutamate Synthase in Synchronous Chlorella sorokiniana . **Plant Physiology**, *[s.l.]*, v. 70, n. 1, p. 113–116, 1982.

TOMAZ, T.; BAGARD, M.; PRACHAROENWATTANA, I.; LINDÉN, P.; LEE, C. P.; CARROLL, A. J.; STRÖHER, E.; SMITH, S. M.; GARDESTRÖM, P.; MILLAR, A. H. Mitochondrial malate dehydrogenase lowers leaf respiration and alters photorespiration and plant growth in Arabidopsis. **Plant Physiology**, *[s.l.]*, v. 154, n. 3, p. 1143–1157, 2010.

TOVAR-MÉNDEZ, A.; MIERNYK, J. A.; RANDALL, D. D. Regulation of pyruvate dehydrogenase complex activity in plant cells. **European Journal of Biochemistry**, *[s.l.]*, v. 270, n. 6, p. 1043–1049, 2003.

TOWBIN, H.; STAEHELINT, T.; GORDON, J. Electrophoretic transfer of proteins from polyacrylamide gels to nitrocellulose sheets : Procedure and some applications. *[s.l.]*, v. 76, n. 9, p. 4350–4354, 1979.

TRAVERSO, J. A.; MICALELLA, C.; MARTINEZ, A.; BROWN, S. C.; SATIAT-JEUNEMAÎTRE, B.; MEINNEL, T.; GIGLIONE, C. Roles of N-Terminal Fatty Acid Acylations in Membrane Compartment Partitioning: Arabidopsis h-Type Thioredoxins as a Case Study. **The Plant cell**, *[s.l.]*, v. 25, n. 3, p. 1056–1077, 2013.

UGALDE, J. M.; FUCHS, P.; NIETZEL, T.; CUTOLO, E. A.; HOMAGK, M.; VOTHKNECHT, U. C.; HOLUIGUE, L.; SCHWARZLÄNDER, M.; MÜLLER-SCHÜSSELE, S. J.; MEYER, A. J. Chloroplast-derived photo-oxidative stress causes changes in H2O2 and E GSH in other subcellular compartments . **Plant Physiology**, *[s.l.]*, v. 186, n. 1, p. 125–141, 2021.

UMBACH, A. L.; JOSEPH T. WISKICH; SIEDOW, J. N. Regulation of alternative oxidase kinetics by pyruvate and intermolecular disulfide bond redox status in soybean seedling mitochondria. **Plant Physiology**, *[s.l.]*, v. 348, n. 2, p. 181–184, 1994.

UMEKAWA, Y.; ITO, K. Thioredoxin o -mediated reduction of mitochondrial alternative oxidase in the thermogenic skunk cabbage Symplocarpus renifolius. v. 165, n. 1, p. 57–65, 2019. VAJDA, S.; YUEH, C.; BEGLOV, D.; BOHNUUD, T.; MOTTARELLA, S. E.; XIA, B.; HALL, D. R.; KOZAKOV, D. New additions to the <scp>C</scp> lus <scp>P</scp> ro server motivated by <scp>CAPRI</scp>. **Proteins: Structure, Function, and Bioinformatics**, *[s.l.]*, v. 85, n. 3, p. 435–444, 5 mar. 2017.

WALLSGROVE, R. M.; TURNER, J. C.; HALL, N. P.; KENDALL, A. C.; BRIGHT, S. W. J. Barley Mutants Lacking Chloroplast Glutamine Synthetase—Biochemical and Genetic Analysis. **Plant Physiology**, *[s.l.]*, v. 83, n. 1, p. 155–158, 1987.

WAQAS, M.; HAWKESFORD, M. J.; GEILFUS, C.-M. Feeding the world sustainably: efficient nitrogen use. **Trends in Plant Science**, *[s.l.]*, *[s.n.]*, p. 1–4, mar. 2023.

WILLIAMS, T. C. R.; MIGUET, L.; MASAKAPALLI, S. K.; KRUGER, N. J.; SWEETLOVE, L. J.; RATCLIFFE, R. G. Metabolic network fluxes in heterotrophic arabidopsis cells: Stability of the flux distribution under different oxygenation conditions. **Plant Physiology**, *[s.l.]*, v. 148, n. 2, p. 704–718, 2008.

WU, K. *et al.* Enhanced sustainable green revolution yield via nitrogen-responsive chromatin modulation in rice. **Science**, *[s.l.]*, v. 367, n. 6478, 2020.

YOSHIDA, K.; HARA, A.; SUGIURA, K.; FUKAYA, Y.; HISABORI, T. Thioredoxin-like2/2-Cys peroxiredoxin redox cascade supports oxidative thiol modulation in chloroplasts. **Proceedings of the National Academy of Sciences**, *[s.l.]*, *[s.n.]*, p. 201808284, 2018.

YOSHIDA, K.; HARA, S.; HISABORI, T. Thioredoxin Selectivity for Thiol-based Redox Regulation of Target Proteins in Chloroplasts *. *[s.l.]*, v. 290, n. 23, p. 14278–14288, 2015.

YOSHIDA, K.; HISABORI, T. Mitochondrial isocitrate dehydrogenase is inactivated upon oxidation and reactivated by thioredoxin-dependent reduction in Arabidopsis. **Frontiers in Environmental Science**, *[s.l.]*, v. 2, n. September, p. 1–7, 2014.

Two distinct redox cascades cooperatively regulate chloroplast functions and sustain plant viability. **Proceedings of the National Academy of Sciences**, *[s.l.]*, v. 113, n. 27, p. E3967–E3976, 2016a.

Adenine nucleotide-dependent and redox-independent control of mitochondrial malate dehydrogenase activity in Arabidopsis thaliana. **Biochimica et biophysica acta**, *[s.l.]*, v. 1857, n. 6, p. 810–818, 2016b.

Biochemical Basis for Redox Regulation of Chloroplast-Localized Phosphofructokinase from Arabidopsis thaliana. **cccc**, *[s.l.]*, v. 62, n. January, p. 401–410, 2021.

YOSHIDA, K.; MATSUOKA, Y.; HARA, S.; KONNO, H.; HISABORI, T. Distinct redox behaviors of chloroplast thiol enzymes and their relationships with photosynthetic electron transport in arabidopsis thaliana. **Plant and Cell Physiology**, *[s.l.]*, v. 55, n. 8, p. 1415–1425, 2014.

YOSHIDA, K.; NOGUCHI, K.; MOTOHASHI, K.; HISABORI, T. Systematic exploration of thioredoxin target proteins in plant mitochondria. **Plant and Cell Physiology**, *[s.l.]*, v. 54, n. 6, p. 875–892, 2013.

ZAFFAGNINI, M.; FERMANI, S.; MARCHAND, C. H.; COSTA, A.; SPARLA, F.; ROUHIER, N.; GEIGENBERGER, P.; LEMAIRE, S. D.; TROST, P. Redox homeostasis in photosynthetic organisms: novel and established thiol-based molecular mechanisms. **Antioxidants and Redox Signaling**, *[s.l.]*, v. 31, n. 3, p. 155–210, 2019.

ZHANG, Y. *et al.* Two mitochondrial phosphatases, PP2c63 and Sal2, are required for posttranslational regulation of the TCA cycle in Arabidopsis. **Molecular Plant**, *[s.l.]*, v. 14, n. 7, p. 1104–1118, jul. 2021.

ZHANG, Y.; BEARD, K. F. M.; SWART, C.; BERGMANN, S.; KRAHNERT, I.; NIKOLOSKI, Z.; GRAF, A.; GEORGE RATCLIFFE, R.; SWEETLOVE, L. J.; FERNIE, A. R.; OBATA, T. Protein-protein interactions and metabolite channelling in the plant tricarboxylic acid cycle. **Nature Communications**, *[s.l.]*, v. 8, n. May, 2017.

ZHANG, Y.; SWART, C.; ALSEEKH, S.; SCOSSA, F.; JIANG, L.; OBATA, T.; GRAF, A.; FERNIE, A. R. The Extra-Pathway Interactome of the TCA Cycle: Expected and Unexpected Metabolic Interactions. **Plant Physiology**, *[s.l.]*, v. 177, n. 3, p. 966–979, 2018.

ZHAO, Y.; YU, H.; ZHOU, J. M.; SMITH, S. M.; LI, J. Malate Circulation: Linking Chloroplast Metabolism to Mitochondrial ROS. **Trends in Plant Science**, *[s.l.]*, v. 25, n. 5, p. 446–454, 2020.

ZHOU, M.; DIWU, Z.; PANCHUK-VOLOSHINA, N.; HAUGLAND, R. P. A Stable Nonfluorescent Derivative of Resorufin for the Fluorometric Determination of Trace Hydrogen Peroxide : Applications in Detecting the Activity of Phagocyte NADPH Oxidase and Other Oxidases. *[s.l.]*, v. 168, n. 253, p. 162–168, 1997.

ZUBIMENDI, J. P.; MARTINATTO, A.; VALACCO, M. P.; MORENO, S.; ANDREO, C. S.; DRINCOVICH, M. F.; TRONCONI, M. A. The complex allosteric and redox regulation of the fumarate hydratase and malate dehydratase reactions of Arabidopsis thaliana Fumarase 1 and 2 gives clues for understanding the massive accumulation of fumarate. **FEBS Journal**, *[s.l.]*, v. 285, n. 12, p. 2205–2224, 2018.

ZUNDERT, G. C. P. VAN; RODRIGUES, J. P. G. L. M.; TRELLET, M.; SCHMITZ, C.; KASTRITIS, P. L.; KARACA, E.; MELQUIOND, A. S. J.; DIJK, M. VAN; VRIES, S. J. DE; BONVIN, A. M. J. J. The HADDOCK2.2 Web Server: User-Friendly Integrative Modeling of Biomolecular Complexes. **Journal of Molecular Biology**, *[s.l.]*, v. 428, n. 4, p. 720–725, fev. 2016.